

# **Shear-Associative Polymers for Ophthalmic Applications**

# **Shear-Associative Polymers for Ophthalmic Applications**

By  
Sahar Mokhtari, B. Sc.

A Thesis Submitted to the School of Graduate Studies in Partial Fulfillment of the  
Requirements for the Degree Master of Applied Science

MASTER OF APPLIED SCIENCE (2014)

(Chemical Engineering)

McMaster University

Hamilton, Ontario

TITLE: Shear-Associative Polymers for Ophthalmic Applications

AUTHOR: Sahar Mokhtari

SUPERVISOR: Dr. Todd Hoare

NUMBER OF PAGES: xi, 122

## Abstract

Most existing eyedrop formulations consist primarily of dilute solutions of water-soluble polymers. While these solutions provide temporary relief of dry eye or a means to transport a drug to the cornea, dilute solutions are quickly cleared from the eye via blinking, resulting in low drug uptake and the need for multiple treatments per day. In contrast, more viscous polymer solutions can cause discomfort or irritation of the ocular surface. Highly shear-thinning polymer solutions that can flow upon the application of shear but form gels at rest and (even more ideally) act to stabilize the tear film would instead be ideal for eyedrop formulations.

Poly(oligoethylene glycol methacrylate)-based hyperbranched polymers (prepared by the Strathclyde methodology using dodecanethiol as a chain transfer agent to graft hydrophobes on chain ends in a single step) represent a unique polymer building block intermediate between a nanoparticle and a linear polymer. These hyperbranched polymers exhibit shear thinning properties over at least 4 orders of magnitude in addition to a distinct internal domain with potential for drug delivery. Mixing linear, hydrophobically-modified polymers with cyclodextrin-functionalized hydrophobic-grafted hyperbranched polymers results in the formation of inclusion complexes between the hydrophobic cavity of cyclodextrin and the hydrophobic groups, introducing additional benefits in terms of generating extremely stiff gels at zero shear while maintaining the lubricity in the eye at high shear rates.

In addition, dual hydrophobe-boronic acid grafted copolymers based on a poly(vinylpyrrolidone-co-vinylformamide) graft platform polymer offer significant potential as artificial tear additives. The mucoadhesive properties of phenylboronic acids (PBA) improves the bioavailability of the drugs delivered to the front of the eye with eye drops while the hydrophobic grafts on the polymer provides shear-induced lubrication for these materials.

## Acknowledgement

First I would like to thank my supervisor Dr. Todd Hoare for his constant support and guidance throughout my graduate studies. He was always available for my questions and gave generously of his time and vast knowledge. It was an honor to work with him.

I would like to acknowledge the help and support I received from my friends and lab mates at McMaster. Special thanks to Mayra Tzoc and Paniz Sheikholeslami, who gave me the opportunity to start my work in the lab. Thank you to Niels Smeets, Rabia Mateen and Roozbeh Mafi for their help and research discussions.

I would like to thank my summer student Jacqueline Chau for all the time and effort she put in this project during the summer. Thank you to Samuel Suntharalingham for his help with designing and performing the cell culture experiments.

Most importantly, thank you to my family for their endless encouragements and love. To my mom for always supporting me and allowing me to follow my dreams. To my dad for the opportunities he provided me and everything he did for me over the years. To my brother Hajir who is always by my side. To Ghazal and Moein for making everything better in my life and making me smile all the time. To Ardavan for giving me the motivation to finish my work as soon as I can.

## Table of contents

|  |     |
|--|-----|
| Abstract.....  | iii |
| Acknowledgments.....                                     | iv  |
| Table of Contents.....                                   | v   |
| List of Figures.....                                     | ix  |
| List of Tables.....                                      | xii |
| 1 Literature review.....                                 | 1   |
| 1.1 Drug delivery.....                                   | 2   |
| 1.2 Barriers to ocular drug delivery .....               | 3   |
| 1.2.1 Eye structure and anatomy.....                     | 3   |
| 1.2.2 Tear film.....                                     | 5   |
| 1.2.3 Cornea.....  | 6   |
| 1.2.4 Conjunctival and sclera.....                       | 7   |
| 1.3 Ocular drug delivery systems.....                    | 8   |
| 1.3.1 Inserts.....                                       | 8   |
| 1.3.2 Ointments.....                                     | 8   |
| 1.3.3 Eyedrops .....                                     | 9   |
| 1.4 Eyedrop delivery improvement strategies.....         | 9   |
| 1.4.1 Viscosity and permeation enhancers.....            | 9   |
| 1.4.2 Mucoadhesion.....                                  | 10  |
| 1.4.2.1 Structure and function of mucosal membranes..... | 11  |
| 1.4.2.2 Factors affecting mucoadhesion.....              | 13  |
| 1.4.2.3 Mucoadhesive polymers.....                       | 16  |

|         |   |    |
|---------|---|----|
| 1.4.2.4 | Boronic acid copolymers as a mucoadhesive polymer .....   | 18 |
| 1.4.3   | Hyperbranched polymers .....  | 19 |
| 1.4.3.1 | Nanoparticles as ocular delivery systems.....   | 22 |
| 1.4.4   | Hydrophobic modified water soluble polymers.....  | 26 |
| 1.5     | Objectives.....   | 28 |
| 2       | -Manipulating Shear Thinning Properties of Ophthalmic Polymer Solutions as a Function of Polymer Morphology and Functionalization ..... | 30 |
| 2.1     | Introduction .....  | 31 |
| 2.2     | Experimental .....  | 34 |
| 2.2.1   | Materials .....   | 34 |
| 2.2.2   | Synthesis .....   | 35 |
| 2.2.2.1 | Hyperbranched POEGMA-co-AA .....  | 35 |
| 2.2.2.2 | Preparation of $\beta$ CD hyperbranched polymer derivatives .....   | 35 |
| 2.2.3   | Characterization .....  | 37 |
| 2.2.3.1 | Nuclear magnetic resonance.....   | 37 |
| 2.2.3.2 | Potentiometric-conductometric titrations .....  | 37 |
| 2.2.3.3 | Gel permeation chromatography.....  | 38 |
| 2.2.3.4 | Transmittance by UV-vis spectroscopy .....  | 38 |
| 2.2.3.5 | Particle size measurements by dynamic light scattering .....  | 38 |
| 2.2.3.6 | Rheological measurements.....   | 39 |
| 2.3     | Results and discussion.....   | 39 |
| 2.3.1   | Characterization .....  | 39 |
| 2.3.1.1 | POEGMA-co-AA characterization .....   | 39 |
| 2.3.1.2 | Optimization.....   | 41 |

|         |  |    |
|---------|--|----|
| 2.3.1.3 | Molecular weight optimization .....  | 43 |
| 2.3.1.4 | Transparency .....   | 47 |
| 2.3.1.5 | Size .....   | 48 |
| 2.3.1.6 | Viscosity optimization.....  | 50 |
| 2.3.2   | Cyclodextrin complex inclusion .....   | 57 |
| 2.3.2.1 | POEGMA-co-AA-g-CD characterization .....   | 57 |
| 2.3.2.2 | Rheology of POEGMA-co-AA-g-CD.....   | 58 |
| 2.4     | Conclusions .....  | 61 |
| 3       | -Mucoadhesive, Shear-Associative Polymers based on Dual Hydrophobe-Phenylboronic Acid Grafted Poly(vinyl pyrrolidone)..... | 63 |
| 3.1     | Introduction .....   | 64 |
| 3.2     | Experimental .....   | 66 |
| 3.2.1   | Materials .....  | 66 |
| 3.2.2   | Synthesis .....  | 67 |
| 3.2.2.1 | P (VP-co-VF) .....   | 67 |
| 3.2.2.2 | P (VP-co-VA).....  | 67 |
| 3.2.2.3 | P (VP-co-VA)- C <sub>x</sub> .....   | 68 |
| 3.2.2.4 | P(VP-co-VA)-C <sub>x</sub> -PBA .....  | 68 |
| 3.2.3   | Characterization .....   | 69 |
| 3.2.3.1 | Nuclear magnetic resonance.....  | 69 |
| 3.2.3.2 | Potentiometric-conductometric titration .....  | 69 |
| 3.2.3.3 | Gel permeation chromatography.....   | 69 |
| 3.2.3.4 | Transmittance by UV/visible spectroscopy.....  | 70 |
| 3.2.3.5 | Refractive index .....   | 70 |

|         |  |     |
|---------|--|-----|
| 3.2.3.6 | Rheology .....                               | 70  |
| 3.2.3.7 | Mucoadhesion via Rheological Synergism ..... | 71  |
| 3.2.3.8 | In vitro cytotoxicity assay .....            | 72  |
| 3.3     | Results and discussion.....                  | 73  |
| 3.3.1   | Characterization .....                       | 73  |
| 3.3.1.1 | P (VP-VF) .....                              | 73  |
| 3.3.1.2 | P (VP-VA).....                               | 74  |
| 3.3.1.3 | P(VP-VA)-C <sub>x</sub> .....                | 77  |
| 3.3.1.4 | P(VP-VA)-C-PBA.....                          | 78  |
| 3.3.2   | Transmittance.....                           | 80  |
| 3.3.3   | Refractive index .....                       | 82  |
| 3.3.4   | In vitro cytotoxicity assay.....             | 83  |
| 3.3.5   | Rheology .....                               | 84  |
| 3.3.6   | Mucoadhesion .....                           | 88  |
| 3.4     | Conclusion.....                              | 96  |
| 4       | -Conclusions and Recommendations.....        | 98  |
| 4.1     | Part I.....                                  | 99  |
| 4.1.1   | Conclusions.....                             | 99  |
| 4.1.2   | Recommendation .....                         | 100 |
| 4.2     | Part II.....                                 | 100 |
| 4.2.1   | Conclusion .....                             | 100 |
| 4.2.2   | Recommendation .....                         | 101 |
| 5       | Appendices .....                             | 115 |

## List of Figures

|  |    |
|--|----|
| <b>Figure 1- 1-</b> Drug release profile of conventional dosing versus controlled release .....  | 2  |
| <b>Figure 1- 2-</b> Drug transport mechanisms and barriers in ocular delivery .....  | 4  |
| <b>Figure 1- 3-</b> Structure of the eye .....   | 4  |
| <b>Figure 1- 4-</b> Structure of the tear film .....   | 5  |
| <b>Figure 1- 5-</b> Schematic of mucin structure and its mucoadhesive moieties .....   | 11 |
| <br>   |    |
| <b>Figure 2- 1-</b> <sup>1</sup> H NMR spectrum of hyperbranched POEGMA-co-AA synthesized with EGDMA as the cross-linker and DDT as the chain transfer agent .....   | 40 |
| <b>Figure 2- 2-</b> Polymer structure resulting from preparing hyperbranched polymers with varying DDT (chain transfer agent) and EGDMA (cross-linker) concentrations .....  | 41 |
| <b>Figure 2- 3-</b> Effect of EGDMA (cross-linker) mole percentage on hyperbranched polymer M <sub>w</sub> .....   | 43 |
| <b>Figure 2- 4-</b> Effect of increasing the EGDMA (cross-linker) concentration on hyperbranched polymer polydispersity at two different DDT (chain transfer agent) concentrations .....   | 44 |
| <b>Figure 2- 5-</b> Molar mass distribution curves of hyperbranched polymers (from GPC refractive index detection) for polymers prepared with different concentrations of EGDMA and a) 1.23 mole % of DDT and b) 1.45 mole % of DDT .....  | 45 |
| <b>Figure 2- 6-</b> (a) Visual appearance and (b) UV/vis transmittance value at 500 nm wavelength for a 15wt% solution of hyperbranched polymer with 1.45 mol % DDT and 6.2 mol % EGDMA .....  | 48 |
| <b>Figure 2- 7-</b> Hydrodynamic diameter of hyperbranched polymers prepared with varying EGDMA (cross-linker) contents at fixed DDT (chain transfer agent) concentrations before and after sample filtration .....  | 49 |
| <b>Figure 2- 8-</b> Viscosity versus shear rate as a function of increase in EGDMA content for hyperbranched polymers prepared with a) 1.23 mole % DDT and b) 1.45 mole % DDT .....  | 51 |
| <b>Figure 2- 9-</b> Rheological comparison of hyperbranched polymers prepared with the highest EGDMA content and 1.45 mole% and 1.23 mole% DDT (from Figure 2-5) with the hyperbranched polymer prepared with the highest EGDMA and DDT contents resulting in a soluble hyperbranched polymer (EGDMA 10.4%-DDT 3.7%); Inset: polymer composition map showing location of the three polymers considered in the sample space ..... | 53 |

|   |    |
|---|----|
| <b>Figure 2- 10-</b> Viscosity versus shear rate for hyperbranched polymer 20 (6.45 mole% EGDMA,1.45 mole% DDT) as a function of polymer concentration .....  | 55 |
| <b>Figure 2- 11-</b> Rheology of hyperbranched polymer (10.4 mole% EGDMA, 3.7 mole% DDT) mixed with (a) PVP (b) linear hydrophobically grafted poly(N-vinylpyrrolidone) linear polymers (55 kDa molecular weight, 1.7 mol % C <sub>x</sub> hydrophobes) mixed with CD-grafted hyperbranched polymer .....   | 56 |
| <b>Figure 2- 12-</b> Rheology of CD-grafted hyperbranched polymer (10.4 mole% EGDMA, 3.7 mole% DDT): (a) comparison of viscosity profile of hyperbranched polymer before and after CD grafting; (b) rheology of mixtures of linear hydrophobically grafted poly(N-vinylpyrrolidone) linear polymers (55 kDa molecular weight, 1.7 mol % C <sub>x</sub> hydrophobes) mixed with CD-grafted hyperbranched polymer ..... | 58 |
| <br>  |    |
| <b>Figure 3- 1-</b> Degree of ionization for C12-P(VP(75)-VA)-66kDa and the corresponding PBA grafted polymer C12-P(VP(75)-PBA (4))-66kDa.....  | 79 |
| <b>Figure 3- 2-</b> Transmittance of polymers at as a function of wavelength (15 wt % solutions) .....  | 81 |
| <b>Figure 3- 3-</b> Percent cell viability of HCEC cells exposed to polymers grafted with hydrophobic groups of different chain lengths, PBA content and molecular weight .....   | 84 |
| <b>Figure 3- 4-</b> Viscosity versus shear rate of C <sub>12</sub> -P (VP-VA)-60kDa before and after PBA conjugation .....  | 85 |
| <b>Figure 3- 5-</b> Viscosity versus shear rate of dual C <sub>x</sub> -PBA grafted P(VP(91)-PBA)-60kDa polymer functionalized with different hydrophobe chain lengths .....  | 85 |
| <b>Figure 3- 6-</b> Viscosity versus shear rate of dual C <sub>x</sub> -PBA grafted C12-P(VP-PBA) polymers with different molecular weights.....  | 86 |
| <b>Figure 3- 7-</b> Viscosity versus shear rate of dual C <sub>x</sub> -PBA grafted C <sub>12</sub> -P (VP-PBA) polymers with different PBA contents.....   | 87 |
| <b>Figure 3- 8-</b> Examples of dynamic oscillation responses of dual C <sub>x</sub> -PBA grafted polymers for a) a polymer with low PBA content (C <sub>12</sub> -P(VP(90)-PBA(4))-178kDa) and b) a polymer with high PBA content (C <sub>12</sub> -P(VP(78)-PBA(19))-66kDa) and c) a polymer before PBA conjugation (C <sub>12</sub> -P(VP(75)-VA)-66kDa) .....   | 90 |
| <b>Figure 3- 9 -</b> tan δ versus frequency profile for high-PBA content C <sub>12</sub> -P(VP(78)-PBA(19))-66kDa) dual C <sub>x</sub> -PBA grafted polymer (30 wt%) in the absence and presence of mucin (4 wt%) .....   | 91 |

**Figure 3- 10** - Representative example of a) excess storage modulus and (b) relative synergism parameter or  $C_{12}$  - P(VP(78)-PBA(18.8))-66kDa measured as a function of frequency for dual  $C_x$ -PBA grafted polymers .....92

**Figure 3- 11** - Rheological synergism of polymer-mucin interactions: (a) excess modulus ( $\Delta G'$ , blue series, or  $\Delta G''$ , red series); (b) relative synergism parameter ( $\Delta G'/G'$ , blue series, or  $\Delta G''/G''$ , red series) .....94

## List of Tables:

|   |    |
|---|----|
| <b>Table 2- 1</b> -UV/vis transmittance value at 500 nm wavelength for 15wt% solution of hyperbranched polymer with varying percentages of DDT and EGDMA before and after filtration. Measured wt% of mass loss due to filtration (via gravimetry) are also included for reference.....             | 48 |
| <b>Table 3- 1</b> -Recipes and molecular weights of poly(vinyl pyrrolidone-co-vinyl formamide) (P(VP-co-VF)) graft platform polymers and mole percentage of monomer residues bearing a primary amine group in P(VP-co-VA) copolymers based on <sup>1</sup> H NMR and conductometric titration ..... | 76 |
| <b>Table 3- 2</b> -Degree of alkylation and the resulting mole% of total monomer residues functionalized with hydrophobic grafts in P(VP-co-VA)-C <sub>x</sub> polymers as measured by titration.....   | 77 |
| <b>Table 3- 3</b> -Degree of amine substitution (i.e. percentage of amine groups in the original P(VP-co-VA) polymer grafted with PBA) and the resulting PBA content (mole% of total monomer units) of graft copolymer .....  | 80 |
| <b>Table 3- 4</b> -Percent transmittance of dual C <sub>x</sub> -PBA grafted polymers at 600 nm (15 wt% solutions) .....  | 82 |
| <b>Table 3- 5</b> -Refractive index of 15 wt% solutions (in water) of dual C <sub>x</sub> -PBA grafted P(VP-VA) polymers .....  | 83 |

# 1 -Literature review

## 1.1 Drug delivery

The effectiveness of a drug depends on both its concentration at the site of action and its ability to carry out its intended physiological action. In most applications of drug delivery systems, a local increase in concentration of the drug immediately following administration is followed by a rapid decrease in its concentration in a short period of time until the next dosage occurs [1] (Figure 1-1). Therefore in order for the drug to be effective, it is essential to keep its concentration in the therapeutic window for as long as possible; lower concentrations are ineffective while higher concentrations can lead to drug toxicity.

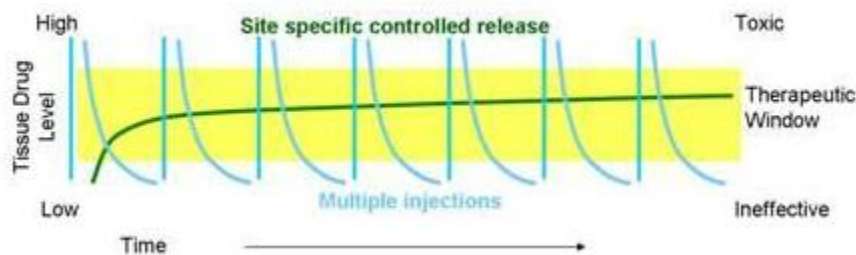


**Figure 1- 1-**Drug release profile of conventional dosing versus controlled release [2]

Advances in synthetic chemistry have led to the development of drug delivery systems with increased efficacy. In particular, polymer-based drug delivery systems can carry the drug to site of action and protect it from interacting with small molecules and/or macromolecules such as proteins that may change the pharmacokinetics or activity of the drug. A critical consideration for these materials is how they can be removed from the body after use; typically, the materials have to be either biodegradable so they are cleared from the body through metabolism or be excreted directly through kidneys.

## 1.2 Barriers to ocular drug delivery

The drug bioavailability is low at the intraocular tissues due to the eye's intricate protective mechanisms. Therefore, it is essential to understand the structure of the eye in order to understand the barriers of ocular drug delivery.

### 1.2.1 Eye structure and anatomy

In order to improve the drug delivery to a specific target site, it is critical to understand the barriers and limitations for the biopharmaceutical vehicles to access that site. The human eye has been called the most complex organ in the body. The eye is a slightly asymmetrical globe, about one inch in diameter. Its structure can be divided into two sections: the anterior segment which occupies one-third of the eye and the posterior segment which takes up the rest of the structure. The anterior segment includes the cornea, conjunctiva, aqueous humor, iris, and the ciliary bodies while the sclera, choroid, retinal pigment epithelium, neural retina, optic nerve and vitreous humor comprise the posterior segment. Both of these segments can be affected by various vision diseases. Anterior segment diseases include glaucoma, allergic conjunctivitis, anterior uveitis and cataract, while the most prevalent diseases affecting the posterior segment are age-related macular degeneration (AMD) and diabetic retinopathy.

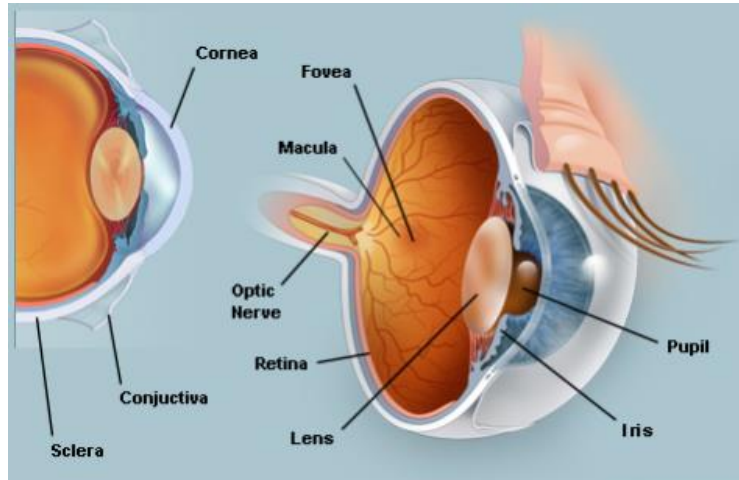


Figure 1- 2-Structure of the eye [3]

The anatomical structure of the eye provides numerous barriers which will result in reduction of bioavailability of the drug in both the anterior and posterior segments. Figure 1- 3 shows the drug movement and barrier/clearance in the case of ocular drug delivery with the key barriers described in more detail in the subsequent sections.

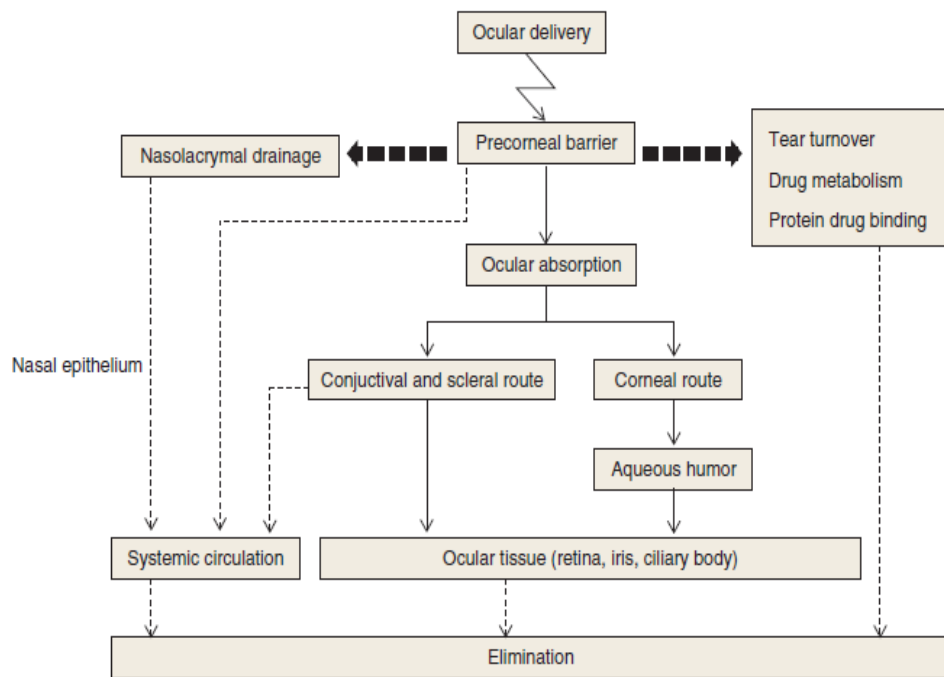
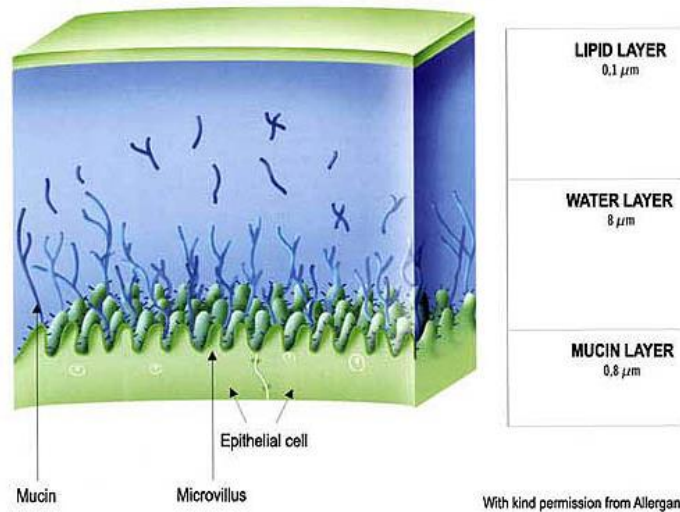


Figure 1- 3-Drug transport mechanisms and barriers in ocular delivery [4]

### 1.2.2 Tear film

While the tear film plays an important role in functionality of eye, it acts as a barrier for the bioavailability of biopharmaceutical formulations. Figure 1- 4 shows the structure of the tear film.



**Figure 1- 4**-Structure of the tear film

The main role of tear film is to protect the eye from harmful foreign substances by trapping or washing them through blinking. In addition, it provides smooth refractive surface, lubricates the conjunctival surfaces and carries the nutrients for cornea. The human tear film is made of three layers. The outermost layer is the lipid layer, produced by the meibomian glands. The lipid layer is 0.1 μm thick [5] and controls the evaporation rate in order to maintain the tear osmolarity even at low tear flow. The middle layer is the aqueous layer, which has a total volume of  $7 \pm 2 \mu\text{L}$  [6] with the thickness of 7-10 μm [5] and relatively fast turn-overs, as an average of 1.2 μL/min with a range of 0.5-2.2 μL/min of tears are secreted by the lachrymal glands [6]. Its main function is maintaining the hydration of the epithelium layer of cornea. The aqueous layer also contains a significant concentration of mucin which contributes to the reduction of tear drainage by increasing the viscosity. The innermost layer is the mucus layer, which is ~0.2-1 μm thick [5]

and comprised of glycoprotein chains which are bound to each other through the disulfide bonds; coupled with the chain flexibility, these bonds form a loose gel like network through non-covalent interactions like hydrogen bonding. Mucin is highly anionic at eye pH (7.0-7.4) since it has sialic acid in its structure [7]. Mucin covers the corneal and conjunctival epithelial cells which are highly hydrophobic due to their high concentration of lipoproteins and produce a hydrophilic extracellular matrix through the differentiation of glycosylated glycocalix. The mucous layer associates with the epithelium layer through this glycocalix. The mucin layer is viscous and highly hydrated and plays a crucial role in physiological functionality of the eye including the wetting of the corneal surface and lubrication against the eyelid movement.

Collectively, these three layers of the tear form a significant mucoaqueous barrier that continuously removes the particles and foreign substances at the anterior surface of the eye. Protein and mucin in the tear film can bind to drugs and reduce the effective drug concentration in contact with cornea. The high buffer capacity of the eye (facilitated by weak organic acids and carbonic acids) can control the extent of ionization of the drug and consequently its bioavailability. The high tear turnover rate (restoration time of 2-3 min [8] ) shortens the residence time of drug and reduces the penetration time of drug through the ocular tissues. In addition, given that the tear film has a natural volume on the order of 7-10  $\mu\text{L}$  and most eye drops dispensed have a volume of 20-50  $\mu\text{L}$ , drug administration via eyedrops results in rapid drainage of the formulation through the nasolacrimal duct, reflex blinking, overflow of fluid onto the face and eventually dilution of the formulation within the first minutes of application.

### 1.2.3 Cornea

The cornea is composed of an epithelial cell layer, Bowman's layer, stroma, Descemet's membrane and an endothelial cell layer. The corneal epithelium (the innermost layer) in

particular has a significant defense mechanism against drug permeation. The epithelium consists of 5-6 layers of cells that are packed closely together. The tight junctions between the cells results in the low permeation of biopharmaceutical between or through the epithelium cells [9]. The stromal layer is comprised mainly of collagen fibers and is highly aqueous and hydrated, a potential barrier for biopharmaceutical penetration depending on the lipophilicity of the drug. The innermost layer, the endothelium, consists of just a single cell layer and is considered a weak barrier, as it is 200 times more permeable than the epithelium [10].

#### 1.2.4 Conjunctival and sclera

The conjunctiva and sclera are considered as alternative routes for ophthalmic drug delivery for biopharmaceuticals that are poorly absorbed across the cornea. However, they too have their own limitations and restrictions. The conjunctiva is a mucus tissue and a thin transparent membrane which lines the inner surface of the eye lids and is reflected on the globe. The conjunctiva functions as a lubricatant and protects the eye by producing mucin and antimicrobial peptides. Molecules up to 20,000 kDa are able to permeate the conjunctival tissue while the permeation limit for corneal tissue is 5000 kDa [11]. However, the conjunctiva is commonly considered as a non-productive way of drug delivery since it is highly vascularized, such that drug penetrating the conjunctiva reaches blood circulation instead of significantly enhancing the intraocular drug level. The sclera, whose main role is to maintain the shape of the eye, is made of extracellular collagenous fibrils and glycoproteins. The permeability of this layer is less than conjunctiva but more than cornea [9] with hydrophilic substances in particular more permeable through this layer. Molecular radius and geometry as well as the charge can significantly influence the permeation of drug molecule through this layer since glycoproteins have typically a

large negative charge; as such, they can trap positively charged and/or larger drugs, making the sclera more permeable to small and anionic molecules [5].

### 1.3 Ocular drug delivery systems

The anatomical and physiological characteristics of the eye make it uniquely challenging in the context of drug delivery. Several drug delivery systems have been investigated over years for ocular drug delivery, including polymeric solutions, ointments and inserts.

#### 1.3.1 Inserts

Ocular inserts are erodible and non-erodible polymer rods and that are implanted in the eye and will either gradually dissolve in the tear film to release drug or serve as matrices retarding the diffusion of drug into the eye. Inserts can take many forms, including contact lenses, tablets placed in the conjunctival cul-de-sac, collagen shields, punctal plugs, and scleral plugs. Incorporation of drugs and lubricants into the matrix of these inserts results in a controlled release, in some cases over months [12]. However, they have low patient compliance due to difficulties in the application as well as interference with vision; in addition, they are often uncomfortable since they may increase the friction associated with blinking and thus induce corneal inflammation [13]. Release is also dependent on natural tear production, which restricts their use across all ocular diseases. Thus the use of inserts as the drug delivery vehicles is limited according to their relatively high cost and low patient compliance.

#### 1.3.2 Ointments

Ointments are another class of carrier systems for ophthalmic drug delivery and typically consist of petrolatum or mineral oil incorporated with pharmaceutically active substances or wetting agents. These formulations are able to increase the viscosity of the tear film and subsequently

enhance the bioavailability of a drug by limiting the rapid drainage of the drug from the eye. However, they cause a sticky sensation and blurred vision [14], again leading to typically low patient compliance in practical use.

### 1.3.3 Eyedrops

Eyedrops are the most frequently used formulation for ocular drug delivery due to their patient compliance and ease of application. The disadvantage of eye drops is their low bioavailability (BA, typically 1-10 %). This poor BA is contributed to precorneal loss factors such as solution drainage, lachrymation, tear evaporation and tear turnover in addition to the low permeability of the corneal epithelial membrane which hinders the drug delivery to anterior and posterior of the eye.

## 1.4 Eyedrop delivery improvement strategies

### 1.4.1 Viscosity and permeation enhancers

The low BA of the drug requires frequent instillation of the eyedrop in order to maintain a therapeutic level of drug in the tear film as well as the ultimate site of action, resulting in a large amount of drug administered which may result in both local and systematic side effects [15], [16]. Numerous strategies have been employed to increase the retention time of the drug. Consideration of factors such as the breakup time of tear film and mucin layer as well as the dispersion forces and interfacial tension are all essential in designing a topical formulation. From a kinetics perspective, the higher the viscosity of the tear film, the slower the release and the higher the drug bioavailability; however, solutions with high viscosities can be uncomfortable for patients during blinking and cause blurring by creating a thick, uneven pre-corneal film which can be uncomfortable. One approach to improving the comfort of such materials is to mimic the highly non-Newtonian viscosity behaviour of the natural tear. The mucin component

of the tear film is highly non-Newtonian in that its viscosity depends strongly on the shear rate; as such, the shear force applied during blinking reduces the viscosity of tear to promote patient comfort [17]. Natural tears have a viscosity of only  $2.8 \pm 0.2$  cps at a shear rate of less than  $4 \text{ s}^{-1}$  [18]; however, the eye can comfortably tolerate solutions with viscosities up to 15 cps as measured under the extremely high shear rates (between  $1000\text{-}30000\text{s}^{-1}$ ) induced by blinking [19]. The shear rate during blinking is estimated to be around  $20,000\text{s}^{-1}$  and the relative velocity of the lid and globe during blinking is  $\sim 15\text{-}25 \text{ cm/s}$  [20]. Thus, non-Newtonian solutions show significantly less resistance to blinking and show greater acceptance compared with viscous Newtonian formulations. To increase the contact time of drug and enhance its bioavailability, highly non-Newtonian, medium-to-high molecular weight polymers such as hydroxyl ethyl cellulose [21] and sodium carboxymethyl cellulose [22] have been widely used. Permeation enhancers like benzalkonium chloride [23], [24] can also be added to the formulations to improve corneal uptake; however, while such permeation enhancers can increase the bioavailability of the drug, they have also shown a toxicological complications in some studies due to their role in disrupting cellular tight junctions that serve as barriers to drug as well as other small molecule transport [25].

#### 1.4.2 Mucoadhesion

In a drug delivery context, bioadhesion is the adherence of a drug carrier system to a distinct biological location. In the case of ophthalmic drug delivery, the two logical targets for bioadhesion in terms of enhancing drug bioavailability are the epithelial tissue or the mucous coating covering that tissue (the latter of which is referred to as mucoadhesion) [26].

### 1.4.2.1 Structure and function of mucosal membranes

Mucosal membranes line the wall of body cavities such as the gastrointestinal, respiratory, and reproductive tracts, the nostrils, the mouth, and the eye that are in direct contact with the surrounding environment. Biological mucus can be divided into two types: membrane-based or soluble [27]. Membrane-based mucous forms a gel layer, is highly hydrated, and is highly viscoelastic, while soluble (secreted) mucins serve to enhance the local viscosity of the fluid in which they are found. Secreted mucins are high molecular weight glycoproteins with a molecular weight in the range of 0.5-40 MDa [27]. This high molecular weight structure can be divided into 500 kDa subunits that are linked together through cysteine-cysteine disulfide linkages [28]. The subunits are made of protein backbone which comprises 12-17% of the mucin and has large fractions of serine, threonine and proline amino acids [27]. The protein base is grafted with oligosaccharide chains made of N-acetylgalactosamine, N-acetylglucosamine, galactose, fucose and N-acetylneuramic acid (sialic acid) [27].

Figure 1-5 shows the structure of the mucin.

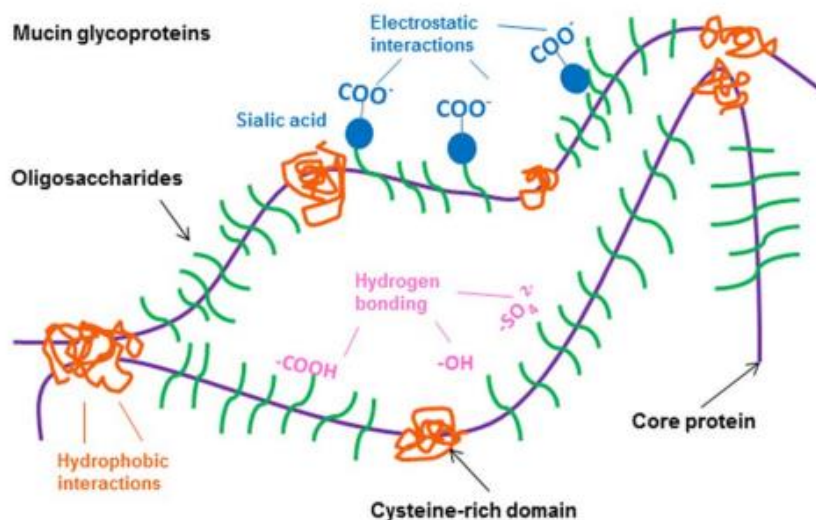


**Figure 1- 5-**Schematic of mucin structure and its mucoadhesive moieties [29]

Corneal and conjunctival epithelial cells secrete mucin to provide a gelatinous lubrication layer to facilitate the spread of the tear film over the hydrophobic epithelial cells [30]. The secreted mucins as well as some of the membrane bound mucin are able to diffuse into the aqueous layer by the turbulence created during blinking. The mucus gel is a semi-permeable system which permeates water, nutrients and small molecules while stays impermeable to bacteria and other notorious microorganisms thus it can also inhibit diffusion of many drugs [21].

The carboxylic group of the sialic acid residues give a negative charge to most of mucins. These acid groups are completely ionized in the physiological conditions since sialic acid has a  $pK_a$  of 2.6 [27]. Mucin is able to show different physiochemical behavior depending on the local pH; for example, it becomes a soft gel at the acidic pH of the stomach while it is a viscoelastic solution at neutral pH values. The pH of the mucus layer itself varies in different parts of the body [31], with the lungs and nasal cavity mucus slightly acidic with pH of 5.5- 6.5 [31], ocular mucus slightly basic with a pH of  $\sim 7.8$  [31], mouth mucus approximately neutral with a pH of 6.2 - 7.4 [31], and the gastric mucus ranging from highly acidic at the lumen (1.0-2.0) to  $\sim 7$  at the epithelial surface [31]. Toxic and irritating substances can irritate mucin secretion which results in thickening of the mucus layer, while gastric mucus characteristics also vary depending on food consumption. The lifetime of mucus is generally short, although its clearance time is different in different parts of the body [31]. As a result, in all these systems, the mucus gel is a dynamic system, with both stimuli from the environment and new mucus being produced constantly by the goblet cells dynamically changing the nature of the mucosal layer.

### 1.4.2.2 Factors affecting mucoadhesion

There are many factors that can enhance the mucoadhesion of a drug delivery system to the tear film. These factors are related to the composition, structure and physiochemical properties of different layers of the tear film [32]. A drug delivery system can interact with different layers of tear film through electronic effects, physical adsorption, wetting, diffusional interpenetration, or covalent bonding. Consideration of aspects such as contact time, the flexibility of the polymer chains, and capacity for polymer interdiffusion are essential. In addition, the formulation of the delivery system can also influence mucoadhesion; for example, the ionic strength of the drug delivery system can influence mucoadhesion through hydrogen bonding, electrostatics or hydrophobic interactions as the degree of ionization of the functional groups can influence the shielding of the functional groups and the repulsion and expansion of the mucus network. In general, the following polymer properties are manipulated to tune mucoadhesion responses.

#### 1.4.2.2.1 Molecular weight

Generally a minimum limit of molecular weight is needed for mucoadhesion to be successful, with the threshold values varying for different polymers. An enhancement in mucoadhesion is typically gained by increasing the molecular weight, an effect attributable to the improved interpenetration and chain entanglements achievable with high molecular weight polymers. As an example, 20 kDa polyethylene glycol (PEG) is slightly adhesive while 200 kDa PEG shows improved bioadhesion and 400 kDa PEG shows extremely improved bioadhesion properties [32], [33]. The trend seen for linear polymers might not be the same for non-linear (branched, comb, etc.) polymers. For example, dextran with a molecular weight of 19500 kDa shows the same adhesion as PEG with a molecular weight of 200 kDa as a result of helical conformation and

spatial formation of dextran that can screen the bioadhesive functional groups of dextran from efficient interactions [32], [33].

#### **1.4.2.2.2 Polymer concentration**

The concentration of the mucoadhesive polymer also plays a role in mucoadhesion. In systems with a concentration higher than an optimum level, the mucoadhesion decreases; this trend is attributed to the compaction of polymer chains in more concentrated solutions that drives a change in conformation from the extended conformation to coiled molecules less prone to interpenetrating into the mucosal gel [33], [34].

#### **1.4.2.2.3 Flexibility of the polymer chains**

Polymer chain mobility typically enhances the degree of mucoadhesion. The chains should be able to move freely and interpenetrate into the mucosal gel to form the entanglement. If the polymers become crosslinked, their movement and mobility decreases; therefore, the interpenetration and length of polymer chain that can diffuse into the mucus layer decreases and subsequently the mucoadhesion decreases [35].

#### **1.4.2.2.4 Swelling**

An optimum level of hydration is needed during the process of mucoadhesion [33]. The magnitude of swelling observed depends on the chemistry of the mucoadhesive system, its concentration, and the ionic strength of the medium. Polymer hydration results in the relaxation of stretched, entangled or twisted macromolecules, exposing the adhesive functional groups and enabling stronger mucoadhesive interactions [36], [37]. Furthermore, chain interdiffusion is favoured by polymer–water interactions dominating the corresponding polymer–polymer

interactions [36]. Exceeding an optimum level of water can, however, reduce the mucoadhesion (sometimes even to the point of resulting in nearly zero adhesive bond) [33].

#### 1.4.2.2.5 pH of the polymer–substrate interface

If the mucoadhesive interaction occurs through hydrogen bonding of the carboxyl groups, pH changes the degree of interaction. At lower pH values, proton donating carboxyl groups promote higher hydrogen bonding compare to ionized carboxyl groups at high pHs. On the other hand, at high pH values, the carboxyl groups are ionized, inducing expansion of the polymer coil that promotes polymer chain mobility, interdiffusion, and physical entanglement. Thus, while mucoadhesion typically occurs across all pH values, the relative contributions of hydrogen bonding and physical entanglements to the adhesive bond strength depends on the  $pK_a$  value of the functional group [32], [38]. For example, Park and Robinson showed that the mucoadhesion of polycarbophil decreases as the pH increases given that the hydrogen bonding contributions to mucoadhesion are stronger than those of interpenetration in this polymer system [37].

#### 1.4.2.2.6 Initial contact time

The degree of swelling and penetration of the mucoadhesive carrier system in mucus is determined by the initial contact time. Increasing the initial contact time promotes the interaction to facilitate enhanced mucoadhesion [39].

#### 1.4.2.2.7 Mucin turnover

The mucin turnover time is rapid enough to be considered in the concept of mucoadhesion as a means for drug clearance, as it results in detachment of mucoadhesive carrier system from the surface [40]. Consequently, the carrier does not have the contact time needed for the mucoadhesive interaction to take place, even though it can result in high strength interaction. The

mucoadhesive polymer can itself change the turnover time of mucin by acting as an effective cross-linker for the native mucosal gel. While the exact turnover time of mucin remains somewhat unclear (and may vary between patients), it is estimated to be ~15-20 hours [41], significantly slower than the tear turnover. On this basis, mucoadhesion can be considered as an efficient method to increase the bioavailability of ocular formulations, although the duration of this benefit is limited to timescales on the order of days as opposed to weeks or months.

### 1.4.2.3 Mucoadhesive polymers

The first report of a mucoadhesive polymer formulation goes back to 1947 in a study done by Scrivener and Schantz, in which tragacanth gum was mixed with dental adhesive for penicillin application to the oral mucosa [27]. Typically, mucoadhesive polymers have high molecular weights, making natural polymers (which have natively high molecular weights) often the polymers of choice for such applications, with polysaccharides attracting particular interest.

Natural polymers that can form in situ gels when they are used as ophthalmic carriers have attracted particular interest as mucoadhesive polymers in eyedrop formulations. Xanthan gum, a polysaccharide made of glucose, mannose and glucuronic acid with high molecular weight, and carrageenan, a sulfated polysaccharide, are both examples of non-cellulosic mucilages that form gels upon their application and crosslinking with native lysozyme in the tear film to form a shear-thinning gel with a long residence time in the ocular surface [42], [43]. Crosslinking can also take place between alginate, an anionic polysaccharide, and calcium ions natively found in the tear film [44]. The drawback of these natural polymer gelation approaches is their dependence on native tear composition that can vary in different patients.

Alternately, highly swollen carbohydrates that can effectively build viscosity can enhance residence time and thus improve mucoadhesion. Hyaluronic acid (HA) is naturally found in the

vitreous humor and is a natural, non-irritating polysaccharide that shows pseudoplastic properties in that it is a viscous liquid at low frequency and behaves as an elastic 'shock absorber' at high frequency. Many studies have used HA polymers for ophthalmic applications due to its pseudoplastic properties as well as mucoadhesive properties, primarily due to its structural homology with native mucin [10], [45]–[47]. HA has shear thinning properties in addition to having a high-water binding capacity as well as being a viscous mucoadhesive polymer with low ocular irritancy [45]. Anionic cellulosic derivative like sodium carboxy methylcellulose (CMC) can enhance mucoadhesion by similar mechanisms. In an study done by Kyyronen et al [48], the bioadhesion of timolol was improved three to nine times when the formulation was made in the presence of sodium CMC.

Alternately, charge can be used to drive mucoadhesive interactions. For example, chitosan (produced by deacetylation of chitin in alkaline environment) is widely used in ophthalmic formulations. The mechanism of mucoadhesion for this cationic polymer is through the attraction between opposite charges of the cationic polymer with the negative charges of sialic acid groups in mucin structure [49], [50]. Genta et al. showed that acyclovir-loaded chitosan microspheres are able to promote the prolonged release of drug and enhance its bioavailability [51].

Natural polymers are not structurally homogeneous, which means the degree of functional groups substitution in cellulosic and molecular weight can vary within batches as well as batch-to-batch. Therefore synthetic polymers have attracted interest as substitutes to mimic the functionality of natural polymers while exerting improved control over polymer structure at lower cost.

Analogous to the success of HA and CMC in mucoadhesive applications, polyanionic synthetic polymers such as poly(acrylic acid) (crosslinked and non-crosslinked) show greatly enhanced mucoadhesion and shear thinning properties; for example, the viscosity of a 0.1 wt% solution of linear PAA with a molecular weight of 1-2 million decreases from 40-70 cps at  $1 \text{ s}^{-1}$  shear to 2-10 cps at  $1000 \text{ s}^{-1}$  shear [19]. Both linear polymers (Carbomer) and gels lightly crosslinked using polyalkenyl ethers (Carbopol) or divinyl glycol (Polycarbophils) [45], [52] exhibit enhanced mucoadhesion, with improved drug penetration in the eye also demonstrated with these materials [53]. The disadvantage of these polymers is that they have high viscosities (1000cps at  $1 \text{ s}^{-1}$  shear), causing patient discomfort and blurring shortly after its application [54]. Neutral but highly flexible polymers have also been used, taking advantage of the improved mucosal interpenetration achievable with such polymers. In particular, grafting poly(ethylene glycol) (PEG) or its higher molecular weight analog polyethylene oxide (PEO) can increase the mucoadhesivity of the polymers due to the high mobility of these grafts (facilitating physical entanglements with the native mucus) as well as the capacity of the ether linkage in PEO to form hydrogen bonds with mucin. Different mucoadhesive approaches may also be combined together; for example, PAA grafting to Pluronic (PEO-poly(propylene oxide)-PEO) polymer, which undergoes a phase change from liquid to semisolid at ocular temperature, increases drug delivery to the eye and results in retention of the drug at the mucosal surface [41].

#### 1.4.2.4 Boronic acid copolymers as a mucoadhesive polymer

While electrostatics is the most common method used in mucoadhesion, its use is limited due to charge screening by counterions in the tear fluid. Therefore, a novel class of mucoadhesive polymers have been developed in which labile covalent bond formation between boronate residues on polymers and protic groups on mucins can enhance mucoadhesion [27], [55], [56]. In

particular, phenylboronic acids (PBA) and derivatives are able to adhere to the *cis*-diol residues of sialic acid, the terminal groups in a nine-carbon backbone of the glycan structure dominant in mucins. Boronic acid-mediated mucoadhesion has attracted significant interest since the intermolecular interaction results in the formation of a pair of covalent bonds [57], [58]. The boronate containing polymers are mucoadhesive at alkaline pH of 8-9 and physiological ionic strength, with the maximum level of mucoadhesion achieved when PBA is in its ionized form (tetrahedral compare to the neutral trigonal form). Ivanov et al. showed that the porcine stomach mucin is able to form insoluble complexes with a copolymer of N-acryloyl-m-aminophenylboronic acid and N,N-dimethyl-acrylamide at pH 9 [59]. However, since PBA has a  $pK_a$  of 9 (significantly higher than physiological pH), PBA-mediated mucoadhesion is relatively ineffective at physiological pH, given that a relatively low fraction of PBA groups are ionized in this case. The presence of an amine linkage near the PBA functional group can reduce its  $pK_a$  to pH of 7.4 and subsequently enhance the covalent complex formation [60]–[63], thought to be associated with the lone pair on the amine nitrogen coordinating with the trigonal boronate groups to create a tetrahedral geometry ideal for *cis*-diol interactions. Fluorination of the benzene ring can also lower the  $pK_a$  due to electronic induction effects.

### 1.4.3 Hyperbranched polymers

Given that the shape of a macromolecule is a determining factor in its properties, there has been a growing interest in synthesizing polymers with different structural architectures, sizes and functionalities. In practice, most polymers now used in industry are linear or cross linked networks, but progress in synthetic chemistry has led to the discovery of new nanostructures of polymeric materials. One of these classes of materials is dendritic polymers, symmetrically branched polymers with a well-defined molecular mass. Dendrimers are made from a central

core based on three different types of repeat units which are defined as terminal (repeat units bonded to one other monomer), linear (a repeat unit bonded to two other monomers) and dendritic (a repeat unit bonded to three or more other monomers). Such materials offer versatile structural platforms for drug delivery and gene delivery applications due to their high functionality, high solubility, and small (10-30 nm) molecular sizes. However, their extreme symmetrical structure and step-by-step synthesis makes their synthesis time consuming and thus expensive.

As an alternative, hyperbranched polymers (HBPs) have been introduced. Unlike dendrimers, HBPs have random distributions of linear, terminal and dendritic units in their backbone, making them highly irregular in both size and internal structure compared to their monodispersed dendritic analogous. However, also unlike dendrimers, they can typically be synthesized in a single synthetic step and show similar characteristics to dendrimers such as having a large population of surface functional groups, lower solution or melt viscosities, and higher solubilities relative to linear polymers with similar molecular weights [64]. Given their synthetic ease and desirable properties, hyperbranched polymers have attracted interest in industrial applications such as additives for coatings and resin formulations [65] and molecular templates for the growth of inorganic molecules to produce nanomaterials [66]. They have also shown potential to be used in biomedical applications such as drug and gene delivery [67].

The first hyperbranched molecule was discovered by Berzelius in 19<sup>th</sup> century when he was reacting a  $A_2B_2$  monomer (tartaric acid) with a  $B_3$  monomer (glycerol) [68]. In 1901, Watson Smith reacted a  $A_2$  type monomer (phthalic anhydride or phthalic acid) with a  $B_3$  monomer (glycerol)[68]. However, in all these reactions based on polycondensation of bifunctional and trifunctional monomers, gelation can happen at higher degree of polymerization. In 1952 Flory

developed the idea of synthesizing hyperbranched polymers using  $AB_n$  ( $n \geq 2$ ) monomer in which the monomer has one A functional group and two or more B functional groups, creating a highly branched polymer with a mixture of dendritic (fully reacted B) and terminal (no reacted B function) units with one focal unit (A function). This reaction is a typical step growth reaction of multifunctional monomers that avoids (or at least minimizes) the risk of gelation and crosslinking. The  $AB_2$  monomer is the most common monomer used in these reactions but  $AB_3$ [69],  $AB_4$  and  $AB_6$  [70] have also been used for preparing branched polymers with different patterns. In 1995, Fréchet et al. introduced the concept of self-condensing vinyl polymerization. SCVP is based on an inimer, a vinyl functional group that carries an initiator group [71], [72]. The propagation in these monomers occurs through the double bond (chain growth) and the condensation of the initiating site (step growth). Fréchet et al. also reported on using living cationic, group transfer, and living free radical processes in self-condensing living polymerization for the production of hyperbranched polymers [71]. The disadvantage of this method is that special monomers are required to allow the self-condensing to begin. This will limit the use of SCVP in polymerizations such as reversible addition fragmentation termination polymerization (RAFT), nitroxide mediated polymerization (NMP) or atom transfer radical polymerization (ATRP) [72].

A simpler and more generic route to synthesizing hyperbranched polymers is the free radical copolymerization of a vinyl monomer and divinyl monomer with inclusion of a chain transfer agent which can inhibit the gelation. This method is called the “Strathclyde methodology” and was introduced by Sherrington and co-workers [73]. This method relies on the fact that free radical polymerizations containing a bifunctional monomer can undergo macrogelation if the system is too concentrated or microgelation if the system is diluted and

these branched polymers are considered as the precursors for network systems [74]. This methodology is a solution to scaling up and synthesizing large quantities of branched polymers without manipulation the conditions of polymerization and/or diluting the system to high levels.

#### 1.4.3.1 Nanoparticles as ocular delivery systems

Nanoparticles such as nanomicelles, nanospheres, nanocapsules, liposomes, nanogels, and dendrimers have been widely investigated as promising drug delivery systems for the eye [75]–[77]. Their small size (~10-100 nm) enables them to diffuse across the tight junctions in the corneal membrane and enhances the corneal permeability of drugs [75], [77]. In addition, their high surface area to volume ratio increases their retention time by increasing their interaction with mucus membrane of the corneal surface [75], [78]. An effective nanocarrier should be able to enhance drug permeation while controlling the release mechanisms of the drug. In addition, specific targeting is possible using these nanoparticles through surface modification with ligands targeting particular cell surface receptors. Using nanoparticles for drug delivery reduces the variation in drug concentration and therefore the risk of toxic effects caused by having excess amount of drug in a specific location; in addition, their small size does not introduce any disruption in the aqueous layer and thus frictional contributions to blinking. For example, Zimmer and Kreuter showed that ophthalmic formulations with the size of higher than 10  $\mu\text{m}$  can cause sensation once they are applied on the ocular surface [79].

Nanospheres (in which drug is dispersed throughout the solid polymer particle) and nanocapsules (in which drug is entrapped in solution inside the nanoparticle) can be made with different release properties depending on the preparation method. The simplest method is to emulsify a water insoluble polymer into an aqueous suspension and then evaporate the polymer

solvent to form a solid polymeric nanoparticle. The most common chemistry used for this purpose is polylactide (PLA) or poly(lactide-co-glycolic acid) (PLGA), which can release drugs both via simple diffusion as well as degradation of the nanoparticles (via hydrolytic degradation of the ester backbone) over timescales of several days to several months [80]. Block copolymers combining PLA/PLGA with poly (ethylene glycol) (PEG) or poly (ethylene oxide) (PEO) can significantly enhance the residence time of such particles by blocking non-specific protein adsorption and promoting chain interpenetration into native mucus. Chitosan-coated poly( $\epsilon$ -caprolactone) (PCL) nanocapsules and PCL-PEG block copolymers have also been reported to enhance the drug permeation through the corneal epithelium while still preserving the capacity for degradation via ester backbone hydrolysis [81]. PECL nanocapsules have also been extensively investigated for ophthalmic drug delivery since they can permeate through the corneal epithelium without damaging the membrane to increase drug bioavailability [82], [83]. Non-degradable particles have also been reported, although are less common and unlikely to find real applications in the clinic. One potentially interesting system though involves cellulose acetate phthalate nanoparticles that can *in situ* gel in contact with the lacrimal fluid at pH of 7.2-7.4 [84]. Although such nanoparticles significantly improve the bioadhesivity of the drug, they have the disadvantage of causing vision blurring. Polyacryl-cyanoacrylate (PACA) nanoparticles and nanocapsules have also been investigated for enhancing the bioavailability and permeability of hydrophobic and hydrophilic drugs on the cornea [85], although corneal epithelium cell membrane disruption has been reported using such nanoparticles [86].

Self-assembly of amphiphilic polymers to result in core/shell nanoparticle structures has been extensively explored in the field of drug delivery. If micelles are formed, the hydrophobic

drug is trapped in the core of micelle to enhance the half-life of the drug in the vascular circulation. In contrast, if liposomes or polymersomes are instead assembled, the hydrophilic drug partitions inside the nanoparticle while hydrophobic drug can be carried in the bilayer structure. To date, the most popular approach is to form micelles of Pluronic F127, a triblock copolymer of poly(ethylene oxide)-block-poly(propyleneoxide)-block-poly(ethylene oxide) (PEO-PPO-PEO), that has been used by several scientists to encapsulate drugs for eye drops formulations [87], [88]. Pluronic F127 has also been used in fabricating bulk hydrogel network systems. Since it is temperature sensitive and has a sol-gel temperature below the physiological temperature of 37-38 °C, it has been widely used in enhancement of bioavailability of drugs in ophthalmic applications [5]. Liquid Pluronic F127 (at room temperature) is mixed with the drug of interest and then gelled upon contact with the eye to trap the drug and control its release from the polymer matrix [89].

Natural amphiphiles (lipids) have also been widely used for ophthalmic drug delivery, with commercial formulations including Visudyne® (QLT Ophthalmics, Inc., Menlo Park, CA, United States) for the delivery of the photosensitizer verteporfin [90] and Tears Again® (Optima Pharmaceutical GmbH, Germany) for the treatment of dry eye [91]. Surface modification to enhance mucoadhesion has also been attempted in a couple of studies, using chitosan as the mucoadhesive agent. Diebold et al. showed that the corneal and conjunctiva uptake of drug (FITC-conjugated BSA) using liposome/chitosan nanoparticles (LCS/NP) is increased without inducing significant *in vitro* toxicity [92]. In another study, liposomes were coated with low molecular weight chitosan to use its positive charge to improve the interaction with the mucus membrane which subsequently results in higher bioavailability of the drug [93]. The

disadvantage of liposomes as a drug carriers is the challenges of maintaining their structural stability.

Nanogels are comprised of water-soluble polymers crosslinking into a nanoparticulate form via physical, ionic or covalent interactions. Nanogels have the ability to maintain their structure while absorbing water hundreds or thousands-fold higher than their dry weight. Nanogels are useful for delivering hydrophilic drugs since the drug can be trapped in the pores of matrix and be released either by simple diffusion or by using external stimuli like pH and temperature.

Dendrimers are highly branched, symmetric macromolecules with tree-shape structure arranged around their core. Given that the branches can be easily functionalized, hydrophilic or hydrophobic drugs can be transported in their internal cavities depending on the properties of the functional groups. Alternately, drugs can be facilely conjugated (typically via covalent bond formation) to the dendrimer surface [94]. Surface modified poly(amidoamine) (PAMAM) dendrimers have been investigated particularly widely. In one study Vandamme and Brobeck showed that surface modified PAMAM (with an  $-NH_2$  surface, a  $-COOH$  surface, and an  $-OH$  surface) is able to increase the residence time of tropicamide (pyridinylmethylbenzeneacetamide) and pilocarpine nitrate (parasympathomimetic alkaloid) to the eye [95]. Shaunak et al. showed that conjugating glucosamine-6-sulfate (DGS) to a G3.5- $CO_2H$  PAMAM glucosamine dendrimers introduces well-defined immuno-modulatory and antiangiogenic characteristics that can be used synergistically to prevent scar tissue formation [96]. Dendrimer-fluocinolone acetonide-G4-OH PAMAM showed a sustained release of drug over 90 days [97]. Majoral showed that carteolol (an ocular anti-hypertensive drug for glaucoma) conjugated in a soluble G1-2- $CO_2H$  phosphorus-containing dendrimer is able to penetrate more in the aqueous

humor of the eye compare to carteolol alone [98]. DPTs (dendrimeric polyguanidilyated translocators) have been investigated by Durairaj et al for delivery of gatifloxacin across the biological barriers, with the dendrimers able to permeate into corneal epithelial cells in 5 minutes and facilitate increased transportation of GFX across the sclera-choroid-retinal pigment epithelium barrier (40 % increase over 6 hours) [99]. Ease of functionalization and encapsulation of hydrophilic and hydrophobic drugs in these nano-sized drug vesicles has made dendrimers an attractive ophthalmic drug delivery system. Since hyperbranched polymers have similar properties to dendrimers in the context of drug delivery but are less dependent on the multi-step synthetic procedures required for dendrimers, they also offer significant potential interest in this context.

#### 1.4.4 Hydrophobic modified water soluble polymers

Hydrophobically associative polymers (HAPs) are a class of water soluble polymers with a hydrophilic backbone with hydrophobic grafts. These polymers can be synthesized through two different methodologies. The first method is to copolymerize the hydrophobic monomer with the principal hydrophilic monomer [100]; the second strategy is to chemically graft the hydrophobic group to the polymer backbone following the synthesis [101]. The advantage of the latter is the capacity to use commercially available polymers; however the grafting yield is lower compare to monomer incorporation (provided a common solvent can be found to effective perform a solution polymerization with both monomers). Alternately, micellar polymerizations in which a surfactant such as sodium dodecyl sulfate (SDS) is used to solubilize the hydrophobic monomer can be used [102]. Microemulsion polymerization can also be used to synthesize associative polymers, but this method has been largely supplanted by the micellization technique. In addition

surfomers, are monomers that are also surfactants, can also be used for making associative polymers [100].

Given that self-associations can occur between different polymer chains via the side-chain hydrophobes, the rheological properties of such materials have attracted particular interest. Associative polymers have high viscosities at low shear rate due to 3D network formation facilitated by the hydrophobic segments of these polymers; however, these interactions can be broken at higher shear to exhibit strong shear thinning characteristics. Entropy is the driving force for chain entanglement of hydrophobically modified polymers to reduce their exposure to the solvent; however, if too many hydrophobes are added, the polymer solubility decreases to the point that intrachain interactions begin to dominate and the solution viscosity decreases (and/or the polymer becomes insoluble) [101].

One of the advantages of making associative polymers is that effectively high viscosities can be achieved without increasing the molecular weight too much. The properties of these solutions are controlled via the degree of substitution and the nature and functionality of hydrophobic substitutes. In addition the temperature, molecular weight of polymer backbone, the ionic strength of the solution, and the polymer concentration all affect the properties of the associative polymer. In particular, there is a critical polymer concentration for intermolecular hydrophobic association to take place [103]. The overlap concentration ( $C^*$ ) is the concentration above which polymer chains are on average close enough together that intermolecular hydrophobic interactions occur and an enhancement is seen in viscosity [103], [104]. The study of associative polymer solution is usually done at concentrations both below and above this critical concentration. Below the critical concentration, there is a competition between the intermolecular and intramolecular interaction such that the viscosity can either decrease or

increase relative to the non-hydrophobically modified polymer depending on the competition between these interactions. Intramolecular associations results in the contraction of the polymer chains and a subsequent decrease in the intrinsic viscosity; however, above the critical aggregation concentration, the inter-chain crosslinking is more dominant which results in an increase in the viscosity [103], [105].

Another factor affecting the viscosity of these solutions is the length and degree of substitution of the hydrophobic groups. Longer polymer chains and higher degrees of substitution are more effective in increasing the viscosity [106]. For example, Desbrieres et al. showed that a minimum length of six carbons is needed in order to see an enhancement in viscosity of the [106]. Lower hydrophobic content is needed for polymers made with higher molecular weight backbones and longer alkyl chains to preserve overall polymer solubility. In addition, incorporating ionic functional groups in the base polymer can increase the solubility of associating polymers in water to facilitate increased hydrophobic functionalization.

In addition to their interesting rheological properties in the context of lubricating the blinking response, amphiphilic polymers are able to dissolve hydrophobic chemicals through their hydrophobic domains [107]. This approach is one of the few available that facilitates the delivery of a hydrophobic drug target using a water-soluble polymer precursor, offering advantages in terms of formulation as well as patient compliance.

## 1.5 Objectives

The main objective of this research is to develop synthetic polymers with improved shear-thinning properties and mucoadhesion by controlling the morphology and composition of those polymers in order for more effective use in ophthalmic formulations. First, to investigate the effect of polymer morphology on shear-thinning behaviour, poly(oligoethylene glycol

methacrylate)-based hyperbranched polymers were prepared using ethylene glycol dimethacrylate as the cross-linker and dodecanethiol as the chain transfer agent. These hyperbranched polymer building blocks provide a dense, nanoscale structure (similar to a dendrimer) for potential drug release while still maintaining solution transparency due to their small size. In addition, the branched structure of these polymers provides unique flow properties which we hypothesize may enhance the speed of network recovery following shearing, critical for ophthalmic applications due to the speed and frequency of blinking. Finally, the use of dodecanethiol as the chain transfer agent imparts shear thinning properties with high viscosities at low shear rates and low viscosities at high shear rates, providing ease of administration and comfort during blinking.

Second, to evaluate the role of mucoadhesion (or, more broadly, polymer-mucous interactions), dual-grafted poly(vinyl pyrrolidone-co-vinyl formamide) (P(VP-co-VF)) copolymers were prepared. The hydrolysis of vinylformamide groups gives reactive amine groups for further grafting of alkyl groups ( $C_{12}$  and  $C_{18}$  chain lengths, for shear thinning properties) and phenylboronic acid groups (for mucoadhesion). The high hygroscopicity of PVP facilitates the grafting longer hydrophobes while maintaining a soluble, hydrated polymer. Interactions between mucin on the mucin layer as well as in the aqueous, coupled with interactions between the polymers themselves, is expected to lead to improved properties for dry eye therapies.

## **2 -Manipulating Shear Thinning Properties of Ophthalmic Polymer Solutions as a Function of Polymer Morphology and Functionalization**

## 2.1 Introduction

The unique anatomy and physiology of the eye pose significant challenges with ocular drug delivery. Topical administration in the form of eye drops (typically used for anterior segment diseases) is limited by precorneal and anatomical barriers that can change the bioavailability of the drug upon administration. Less than 5% of the applied dose typically reaches the intraocular tissues, given that most drugs are washed away by blinking or lachrymal drainage within 15-30s after application; furthermore, the tear restoration time is only 2-3 minutes, providing minimal contact time for the drug to reach the intraocular tissues even if it is not quickly washed away. Therefore, frequent drug instillation is needed in order to maintain a therapeutic drug level in the tear film, potentially causing toxic side effects and cellular damage at the ocular surface [108].

The retention of an eyedrop in the eye is influenced by viscosity, hydrogen ion concentration, the osmolality, and the instilled volume. To improve the drug contact time, different additives such as viscosity modifiers and permeation enhancers can be added. Increasing the viscosity is particularly of interest in the context of artificial tears; however, while enhanced viscosities can improve the residence time on the ocular surface, they also decrease the lubricity between the eye lid and the ocular surface by increasing the friction coefficient [14]. As such, a balance must be struck in terms of optimizing the viscosity as a function of shear rate for the design of effective artificial tear formulations.

Current eyedrop formulations employ polymeric materials such as cellulose derivatives, poly (vinyl alcohol) (PVA), carbomer (a lightly cross-linked poly(acrylic acid)), poly (vinyl pyrrolidone), polyethylene glycol, and dextran are used to lubricate and increase the bioavailability of drug formulations [36], [44]. However, additives at the relatively low molecular weights used in current artificial tear formulations behave as Newtonian fluids in that they do not

shear thin upon blinking, either demanding the use of lower concentrations (and thus facilitating lower retention times and thus efficacy) or resulting in high friction between the ocular surface and eyelid (resulting in patient discomfort).

To overcome this issue, growing interest has been directed toward shear-associative polymers [19]. Such polymers are able to increase the viscosity of the formulation at rest by forming physical intermolecular interactions between the polymer chains, facilitate disruption of these interactions when the shear is applied during blinking (providing the required lubrication), and re-form the interactions once the shear is removed. As such, shear-associative polymers can express high viscosities even at relatively low molecular weights, often desirable for *in vivo* applications in the context of clearance as well as avoiding potential mechanical degradation of the higher molecular weight polymers at the high deformation rates induced upon blinking. The most common method to induce such shear-responsive behavior is to graft hydrophobic side-chains to water-soluble polymers that can form a physical network via hydrophobic interactions [109], although other physical interactions such as charge, inclusion complexes [110], or hydrogen bonding are used as well [111].

We have recently reported the use of hydrophobically-grafted poly(vinyl pyrrolidone-co-vinyl formamide) (PVP-co-VF) polymers as shear-thinning ophthalmic materials [112]. PVP is a highly hygroscopic polymer, such that its solubility and gel-forming potential can be maintained even after hydrophobic modification. Grafting of  $C_8 - C_{18}$  hydrophobes to hydrolyzed vinylformamide residues produces shear-associative polymers with over four decades of shear thinning from zero shear to infinite shear, while at the same time being well-tolerated *in vivo*. However, the potential use of these materials as anterior segment drug delivery vehicles is limited by two factors: (1) the viscous recovery of the network following shearing is

slower than ideal for the case of blinking, where recovery must be extremely fast (within a second or two) to prevent significant lachrymal drainage and (2) drug delivery from such networks is extremely fast, particularly for small hydrophilic drugs.

Hyperbranched polymers offer a potential solution to this problem. Hyperbranched polymers are highly branched polymers analogous to structurally imperfect dendrimers; however, unlike dendrimers, they can be produced in a single synthetic step using the Strathclyde methodology by balancing the quantities of added cross-linker and chain transfer agent in a free radical polymerization process [72], [73], [113]–[116]. Relative to linear polymers, hyperbranched polymers are significantly denser (assisting with drug delivery) and stiffer (keeping the orientation of hydrophobes more stationary during the shear process), both potentially favorable properties in the context of artificial tear solutions.

In this work, we prepare hyperbranched polymers based on poly (oligoethylene glycol methacrylate) (POEGMA) using the Strathclyde methodology and use them as additives to PVP-co-VF-based ophthalmic solutions. POEGMA has been demonstrated to be non-immunogenic and non-cytotoxic, making it of interest for drug delivery applications [117]. Using 1-dodecanethiol as the chain transfer agent will introduce  $C_{12}$  hydrophobes at the branch chain ends of the hyperbranched polymer that are capable of forming association between each other (and between hydrophobically-modified linear polymers) that can be disrupted under shear. We anticipate that hyperbranched POEGMA with DDT in its structure will have utility in the context of ocular drug delivery since (1) its nano-size structure can introduce denser drug delivery domains into the solution without inducing significant light scattering and (2) either the residual double bonds (from single-reacted cross-linker) as well as acrylic acid functional groups

copolymerized into the network can be used to cross-link hyperbranched polymers together, graft drugs/drug binding domains to the network, or graft affinity groups to the matrix.

In addition, we exploited these functional groups to graft cyclodextrins (CDs) to these hyperbranched polymers. CDs, while water soluble, have a 1-2 nm hydrophobic pockets which are able to interact with hydrophobic entities due to the orientation of carbons and ethereal oxygens of constituents' glucose residues. CDs are frequently used in drug delivery applications to increase the bioavailability of hydrophobic drugs by solubilizing and stabilizing the drug inside a water-soluble matrix [118]. CDs are also widely reported to form inclusion complexes with hydrophobic graft copolymers to act as a gelation aid via host-guest interactions [119]–[121]. As such, incorporating CDs in the hydrophobically-modified hyperbranched polymer building blocks offers the potential for host-guest interactions to support the network formation via simple hydrophobic graft self-assembly, providing an additional shear-dependent network forming unit of potential interest for ophthalmic formulations. We hypothesize that improved shear responses can be achieved by combining different building blocks with different morphologies and functionalization (i.e. CD grafts) relative to any single component alone.

## 2.2 Experimental

### 2.2.1 Materials

Oligo(ethylene glycol) monomethyl ether methacrylate (OEGMA300,  $M_n = 300$  g/mol, Sigma Aldrich, 98%), was passed over a column of basic aluminum oxide (Aldrich, type CG-20) to remove the inhibitor and stored at 5 °C prior to polymerization. Ethylene glycol dimethacrylate (EGDMA, Sigma Aldrich, 98%), acrylic acid (AA, Sigma Aldrich, 99%), 1-dodecanethiol (DDT, Sigma Aldrich,  $\geq 98\%$ ),  $\beta$ -cyclodextrin ( $\beta$ -CD, Sigma Aldrich,  $\geq 97\%$ ), chloroacetic acid

(Sigma Aldrich,  $\geq 99.0\%$  purity), adipic acid dihydrazide (ADH, Alfa Aesar, 98%), sodium hydroxide pellets (EMD Chemicals, Mississauga, Ontario), glacial acetic acid (Caledon Laboratory Chemicals, Georgetown, Ontario), N'-ethyl-N-(3-dimethylaminopropyl)-carbodiimide (EDC, Carbosynth, Compton CA, commercial grade), and dimethyl-2,2'-azobis(2-methylpropionate) (AIBME, Wako Chemicals, 98.5%) were used as received. All HCl and NaOH solutions used for titration were prepared from Acculute standards. All water used was of Milli-Q grade (resistivity 18 M $\Omega$ -cm).

## 2.2.2 Synthesis

### 2.2.2.1 Hyperbranched POEGMA-co-AA

Hyperbranched polymers were prepared by free radical polymerization method in dioxane, where OEGMA and AA were comonomers, EGDMA was the cross-linker, and DDT was the chain transfer agent. The polymerizations were conducted in a 250mL three-necked flask with a condenser under magnetic stirring (200 RPM) under a N<sub>2</sub> purge at 70°C. The reactants in the flask were purged with N<sub>2</sub> for 30 minutes prior to the injection of the initiator solution. The reaction was carried out for 4 hours, after which the polymers were purified by evaporating the dioxane solvent and precipitating the polymer in ethyl ether. The precipitates were left in a desiccator connected to a vacuum pump overnight for evaporation of residual ethyl ether.

### 2.2.2.2 Preparation of $\beta$ CD hyperbranched polymer derivatives

#### 2.2.2.2.1 Synthesis of carboxymethyl cyclodextrin (CM-CD)

$\beta$ CD was dissolved in a 3 M solution of NaOH. Chloroacetic acid was added to the solution, and the mixture was then stirred at room temperature until all components were dissolved. The flask was submerged in a water bath with the temperature of 60°C, and the reaction was allowed to

proceed for 15 min. Following, the solution was cooled to room temperature and glacial acetic acid was used to neutralize the solution to pH 7.0. Methanol was used to precipitate the product and collect it through vacuum filtration. The product was stirred in acetone overnight to reduce its syrupy consistency followed by collection through vacuum filtration. The product was left in an oven at 60 °C until it is dry [122].

#### 2.2.2.2.2 Synthesis of hydrazide-functionalized cyclodextrin (Hdz-CD)

In the subsequent reaction, hydrazide is grafted onto cyclodextrin by carbodiimide chemistry. 5 g of carboxymethylated  $\beta$ CD was mixed with ADH (5 molar excess relative to carboxymethyl groups) in 120 mL of deionized water. The pH of the solution was adjusted to 4.75 with 1 M HCl, and the reaction was started with the addition of EDC (5 molar excess of carboxymethyl groups). The reaction was conducted for 4 hours, over which time a pH 4.75 was maintained via the addition of 1 M HCl. The solution was cooled to room temperature and 1 M NaOH was used to neutralize the solution to pH 7.0. Rotatory evaporation was then used to remove water, after which the product was precipitated using a large excess of acetone. The product was stirred in acetone overnight to reduce its syrupy consistency followed by its collection through vacuum filtration [122].

#### 2.2.2.2.3 POEGMA-co-AA-g-cyclodextrin hyperbranched polymers

In the subsequent reaction, Hdz-CD was grafted to POEGMA-co-AA hyperbranched polymer using carbodiimide chemistry. In a typical experiment, 2 g of POEGMA-co-AA was mixed with Hdz-CD (2 molar excess of acrylic acid groups in the hyperbranched polymer) in 100 mL of water. The reaction was then initiated via the addition of EDC (2 molar excess of acrylic acid groups in the hyperbranched polymer) at a constant pH of 4.75. The resulting product was

purified by dialyzing against Milli-Q water (MWCO 3500) followed by lyophilization and storage of the polymer at room temperature in sealed containers.

#### 2.2.2.2.4 Hydrophobic grafted Poly (N-Vinylpyrrolidone) linear polymers

Free radical polymerization of N-vinylpyrrolidone and N-vinyl formamide was performed using isopropanol as both the solvent and the chain transfer agent and dimethyl-2,2'-azobis(2-methylpropionate) (AIBME) as the free radical initiator. This step was followed by basic hydrolysis of the N-vinylformamide monomer residues to N-vinylamine residues to provide the necessary platform for grafting alkyl groups. The third step is the condensation reaction of alkyl halide (1-chlorododecane – C<sub>12</sub>) and amine groups of the graft platform [112].

### 2.2.3 Characterization

#### 2.2.3.1 Nuclear magnetic resonance

Hyperbranched polymer composition was analyzed by <sup>1</sup>H-NMR (Bruker 600 MHz spectrometer) in deuterated dimethylsulfoxide.

#### 2.2.3.2 Potentiometric-conductometric titrations

Potentiometric-conductometric titration of the polymers was used to evaluate the acrylic acid content of the hyperbranched polymers. The polymers were dissolved in water at a concentration of 1 mg/mL, and (KCl) salt was added to reach an initial conductivity of 5 mS/m. 1 M HCl was added drop-wise to set the solution initial pH~2.5. Samples were then titrated using NaOH (0.1M), recording pH and conductivity as a function of the base volume added (Mandel PC Titrator). The data was analyzed using the derivative of the pH-versus-volume curve to identify the inflection point onset-offset corresponding to the acrylic acid titrated.

### 2.2.3.3 Gel permeation chromatography

Gel permeation chromatography was performed using a Waters 2996 photodiode array detector, Waters 2414 refractive index detector, Waters 2475 multi- $\lambda$  fluorescence detector, and four Polymer Labs PLgel individual pore size columns maintained at 40 °C with a 5 $\mu$ m bead size and pore sizes of 100, 500, 103 and 105 Å. THF was used as the eluent at a flow rate of 1.0 mL min<sup>-1</sup>, and polystyrene standards were used to calibrate the instrument. All polymers were dissolved in THF at a concentration 10 mg/mL followed by filtering the solution through a 0.2  $\mu$ m PTFE membrane.

### 2.2.3.4 Transmittance by UV-vis spectroscopy

The transparency of the hyperbranched polymer solutions was measured using a Variant Cary Bio 100 UV-vis spectrometer. Polymers were dissolved in PBS (pH 7.4) at a concentration of 1 mg mL<sup>-1</sup>. The absorbance of the solution was recorded at a wavelength of 500 nm at 0.5°C intervals over a temperature range of 10°C to 80°C, with the temperature ramped at a rate of 1°C min<sup>-1</sup>.

### 2.2.3.5 Particle size measurements by dynamic light scattering

Particle size measurements were conducted using dynamic light scattering with a 632.8nm light source. Detection was conducted using a 90° angle and photomultiplier tube detector (Brookhaven Instruments Corporation). All polymers were dissolved in 1 mM KCl, with pH adjusted if necessary using 1 M HCl. The concentrations were varied for different polymers to achieve a count rate that facilitates sufficient signal:noise while avoiding multiple scattering (100-250 counts per second). The effective diameter was reported as the average of five repeat measurements, with the error bars representing the standard deviation of those measurements.

### 2.2.3.6 Rheological measurements

A cone/plate rheometer (ATS, Rheologica Instrument, USA) was used to measure the shear thinning potential of hyperbranched polymer solutions. A cone of diameter of 4 cm and cone angle of 20° was used. Polymer solutions at a concentration of 20 wt% were prepared in Milli Q water and left in the vials for 48 hours and at room temperature to reach a level of equilibrium self-association prior to testing. After the sample was loaded on the plate, a wait time of 5 minutes was used to dissipate any residual stress. Shear dependent viscosity was measured by applying stresses from 0.01 to 100 Pa and measuring the resulting strain. The range of the stress was divided over 35 intervals, and an integration time of 60 seconds was used per sample.

## 2.3 Results and discussion

### 2.3.1 Characterization

#### 2.3.1.1 POEGMA-co-AA characterization

The one-pot Strathclyde methodology was used to prepare hyperbranched polymers via facile free radical polymerization of OEGMA and AA with varying amounts of EGDMA as the cross-linker and 1-dodecanethiol (DDT) as the chain transfer agent. DDT was used as the chain transfer agent since it was reported to be an efficient transfer agent in methacrylate polymerizations, has a low volatility, and provides hydrophobic groups on the branch ends that are relevant for self-associative hydrogel formation [114]. The  $^1\text{H}$  NMR spectra (Figure 2- 1) confirm the incorporation of all these units into the final hyperbranched polymer, showing peaks for the COOH group (from acrylic acid, ~12.24 ppm), O-CH<sub>3</sub> (from OEGMA, 3.35-3.45 ppm), O-CH<sub>2</sub>-CH<sub>2</sub>-O (from OEGMA, 3.5-3.58 ppm), O=C-CH<sub>2</sub> (from OEGMA and EGDMA, 4-4.4 ppm), S-CH<sub>2</sub>-CH<sub>2</sub> (from DDT, 0.5-1 ppm), and S-CH<sub>2</sub> (from DDT, 1-1.5 ppm).

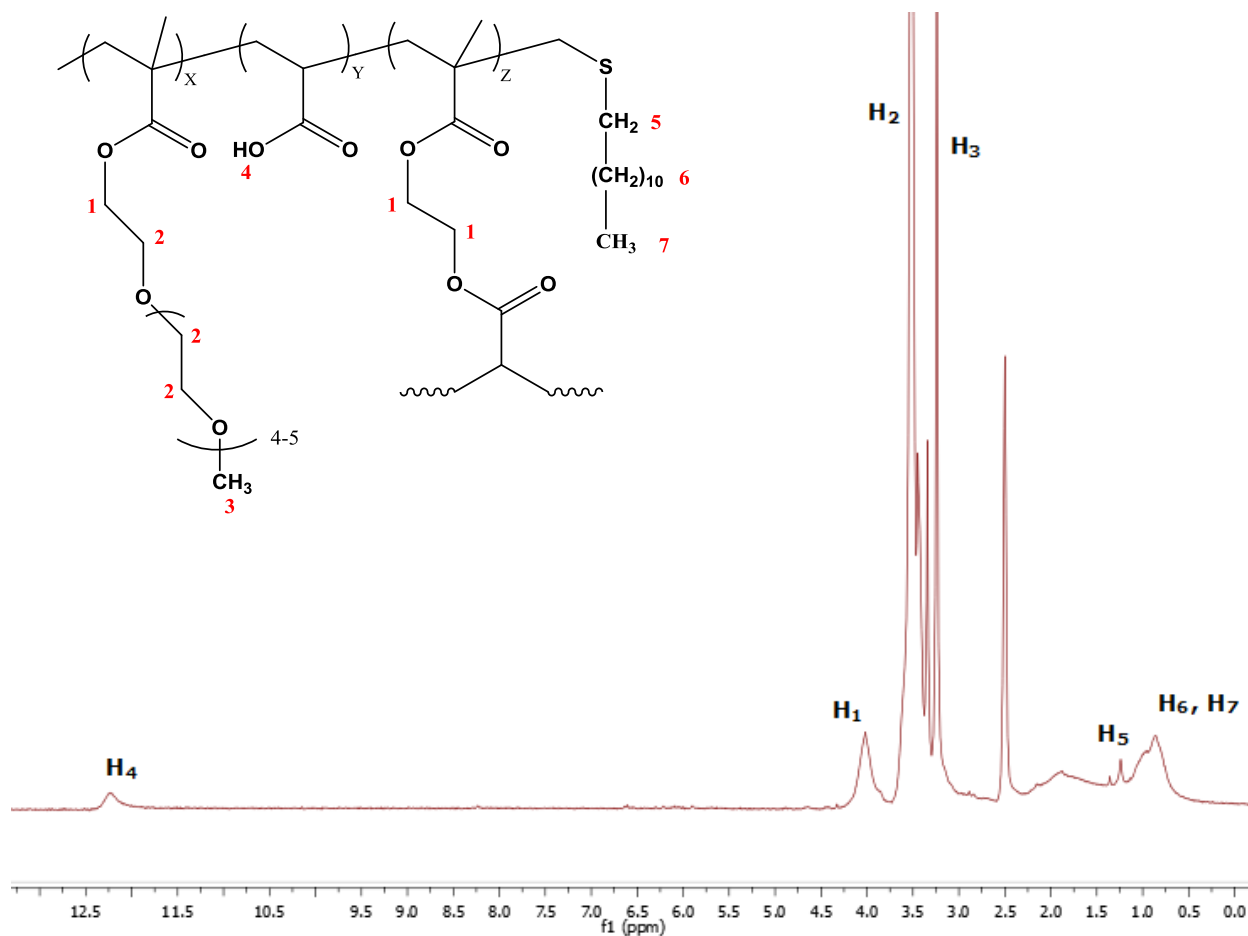


**Figure 2-**  $^1\text{H}$  NMR spectrum of hyperbranched POEGMA-co-AA synthesized with EGDMA as the cross-linker and DDT as the chain transfer agent

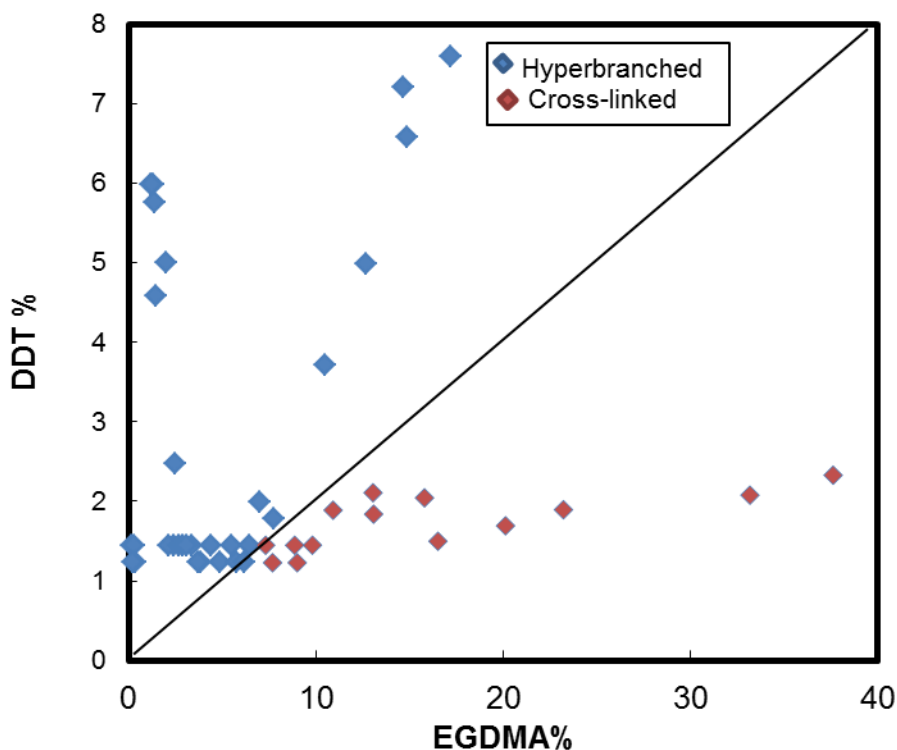
The NMR can be used for calculating the degree of branching by calculating the mole fraction of EGDMA incorporated in these polymers using the methodology reported by the Wang group [123]. Unfortunately, in this case, the mol% of EGDMA is very low compared to OEGMA and the DDT  $(\text{CH}_2)_9$  signal overlaps with the other  $-\text{CH}_2$  signals from the polymer backbone, making NMR of limited quantitative utility for this purpose.

The degree of incorporation of acrylic acid in the hyperbranched polymers was quantitatively measured by potentiometric-conductometric titration to be 15- 17 wt % AA, which on a monomer-only basis (assuming the amount of OEGMA incorporated in the copolymer is much greater than the amounts of EGDMA and DDT) results in a copolymer composition of

approximately 60 mole% OEGMA and 40 mole% AA. This acrylic acid fraction can further be used for conjugation other chemicals on the polymer backbone and/or as an affinity group for cationic drugs.

### 2.3.1.2 Optimization

The hyperbranched polymer recipe was optimized in order to achieve the maximum levels of both EGDMA and DDT without having an insoluble network. Figure 2- 2 summarizes the results, with recipes yielding hyperbranched polymers denoted in blue and recipes yielding bulk gel formation denoted in red. The detailed recipes used for each of the data points are given in Appendix A Table A 1.



Initially, two distinct groups of hyperbranched polymers were prepared to explore the reaction space. In the first set, all hyperbranched polymer were made using 1.23 mole% DDT and varying the mole% of EGDMA from 0.19 to 9 mole%, effectively reducing the DDT/EGDMA ratio from 6.36 to 0.13. The polymerization proceeds homogeneously without any gelation for polymers with EGDMA mole% of 0.19-6.88, with gelation observed at higher EGDMA concentrations. In the second set, the DDT mole% was increased to 1.45 mole% and was kept constant while the EGDMA content was varied in the range of 0.15 to 9.8 mole %, covering DDT/EGDMA ratios from 9.66 to 0.15. In both sets macrogelation occurs when the ratio of chain transfer to cross-linker falls below 0.2.

Based on the results of these initial two libraries, additional polymers were prepared using different ratios of DDT to EGDMA to obtain polymers with highest ratios of DDT and EGDMA while still lying in the hyperbranched region of the graph. As the level of cross-linker in the feed increases, more chain transfer is needed to avoid gelation. In addition, if the DDT and cross-linker content is too high, while macrogelation is avoided, the polymers become insoluble in water; for example, polymers 31-34 prepared with > 5 mole% DDT and >12 mole% EGDMA were not water soluble. This result can be attributable to an increase in polymer molecular weight (due to more EGDMA being used) coupled with an increase in the hydrophobicity of that polymer (due to the enhanced incorporation of DDT). These insoluble polymers were not used for further experiments.

### 2.3.1.3 Molecular weight optimization

Gel permeation chromatography was conducted on the hyperbranched polymers to obtain their molecular weights and polydispersities, with the results of both series of polymers generated shown in Figure 2- 3.

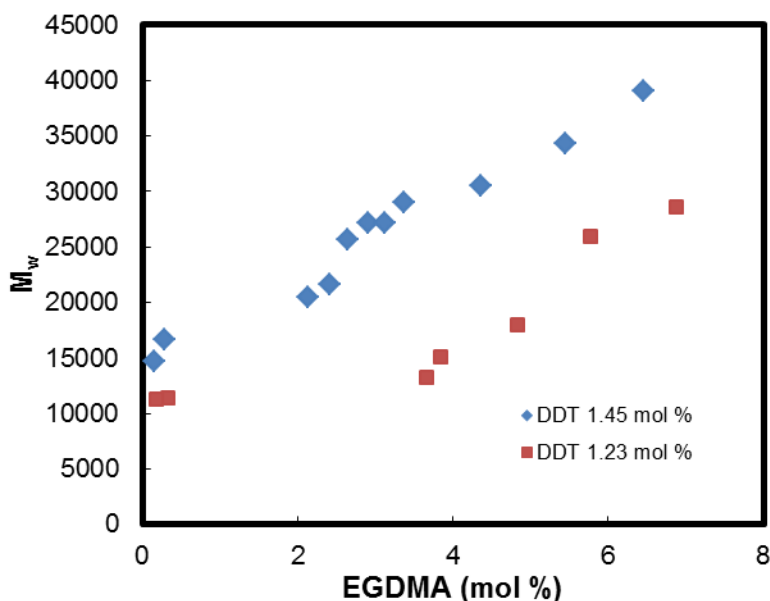


**Figure 2- 3**-Effect of EGDMA (cross-linker) mole percentage on hyperbranched polymer  $M_w$

By comparing polymers prepared using the same amount of chain transfer and different amounts of cross-linker, it can be concluded that higher cross-linker fractions result in hyperbranched polymers with higher molecular weights and broader molecular weight distributions (independent of what fixed amount of DDT is used to prepare the polymers). This result is consistent with the general free radical mechanism by which these polymers are made. At lower cross-link levels, the number of pendant methacrylate groups is small (for a given amount of initiator) and decreases to low levels as the reaction proceeds to high conversions. However, as the dimethacrylate monomer content increases in the feed, more pendant double bonds are incorporated into the polymer structure and thus a larger number of reactive groups for

propagation become accessible, resulting in higher molecular weight polymers. The molecular weight can be controlled by tuning the ratio of branching agent and chain transfer agent. For example, polymer 35, which was prepared using the highest amount of EGDMA (10.5 mole%) and DDT (3.7 mole %) that still produces a branched and water-soluble polymer, has a molecular weight of 55 kDa, significantly higher than polymers produced using lower cross-linker and/or chain transfer agent concentrations. Figure 2- 4 shows the polydispersity value and Figure 2-5 shows the full molecular weight distributions associated with the various hyperbranched polymers produced.

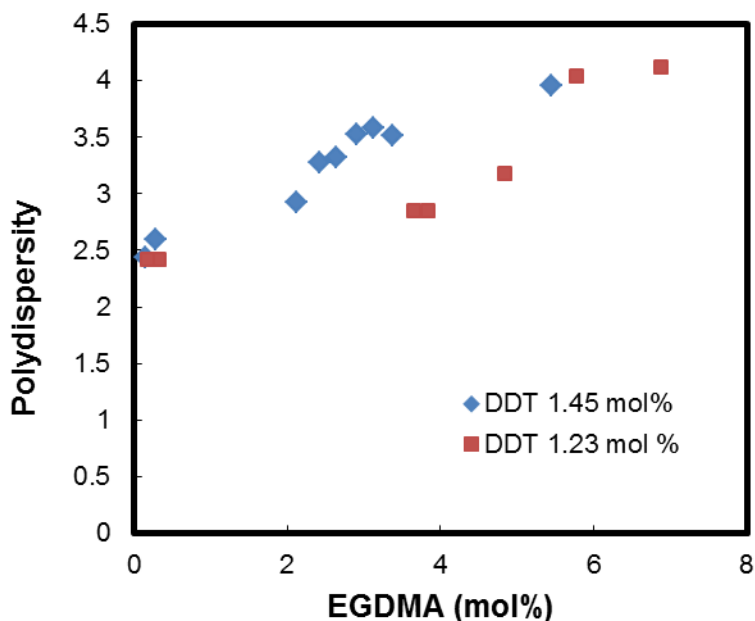


**Figure 2- 4**-Effect of increasing the EGDMA (cross-linker) concentration on hyperbranched polymer polydispersity at two different DDT (chain transfer agent) concentrations

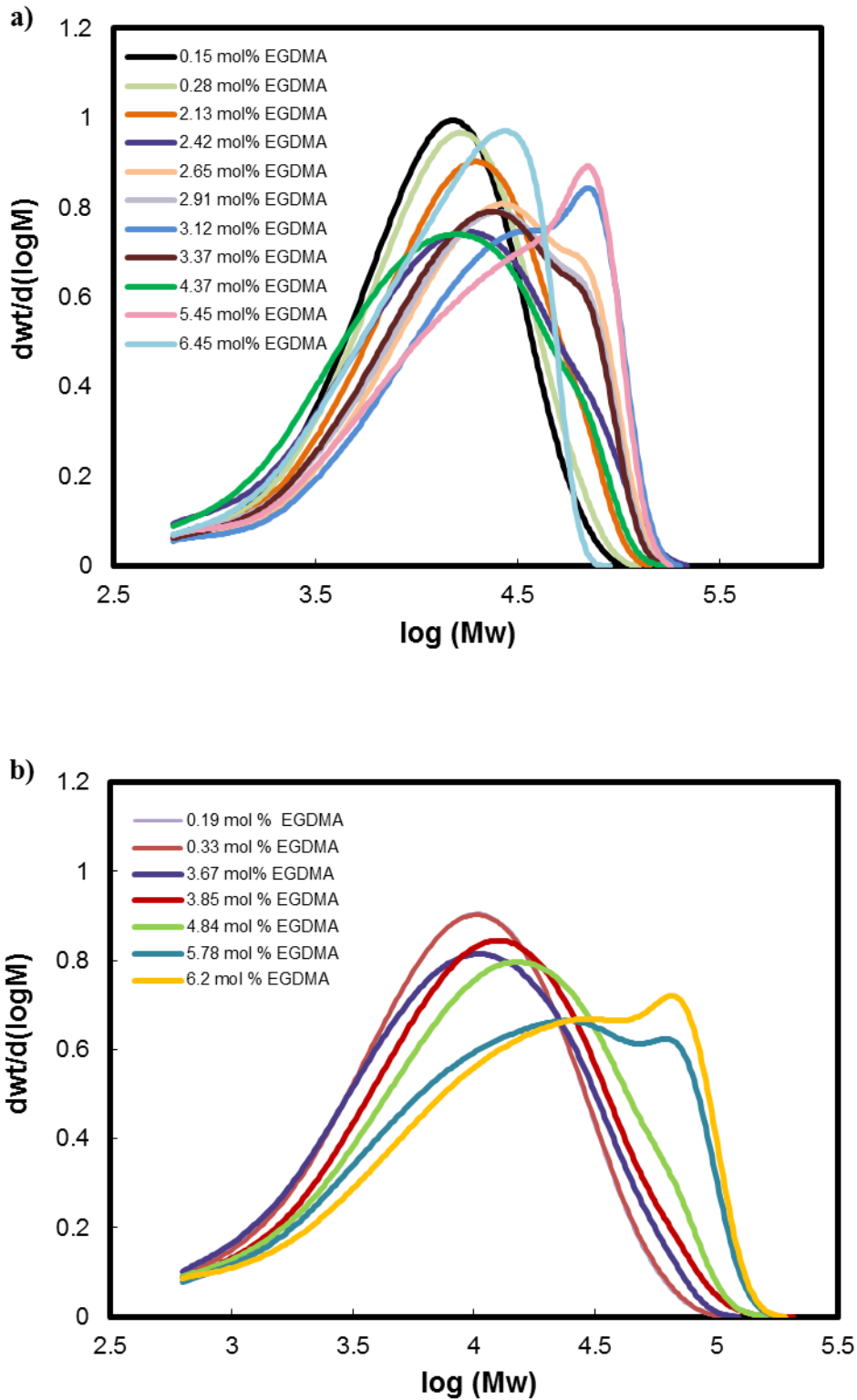


**Figure 2- 5-**Molar mass distribution curves of hyperbranched polymers (from GPC refractive index detection) for polymers prepared with different concentrations of EGDMA and a)1.23 mole % of DDT and b)1.45 mole % of DDT

In discussing these results, we should first note that each datum point at a specific elution volume represents polymer chains with complex and different structures (i.e. different degrees of branching, densities, cross-linking, etc.) that coincidentally have the same hydrodynamic volume. Therefore, on this basis, the high polydispersities and broad molar mass distribution curves observed are expected and indeed characteristic of hyperbranched polymer systems in which chain transfer and the chain branching are happening at the same time as the propagations steps in the polymerization [113], [114]. For polymers prepared with constant DDT concentrations, the polymers become significantly more polydisperse (with wider molecular weight distributions) as the level of EGDMA was increased. This result is again related back to the fundamental mechanism of the free radical copolymerization used to prepare these materials, since the number of primary chains is controlled by the chain transfer agent while the level of branching is controlled by the level of fully reacted brancher (cross-linker) incorporated. As a result, for a relatively fixed number of primary chains (constant DDT content in each series), more cross-linker results in higher molar mass and, due to the increased uncertainty related the length of each branch formed as more branching occurs at the same level of chain transfer agent, a more multimodal distribution. In addition, the polydispersity increase is higher at a lower EGDMA concentration for hyperbranched polymers prepared with higher DDT concentrations (Fig. 2-3). We anticipate this result is a function of increased chain transfer agent again increasing the degree of polydispersity within the different branches, as the values of chain transfer agent used here are not so high that propagation would be significantly limited for the vast majority of the branches formed.

#### 2.3.1.4 Transparency

Any ophthalmic application of these polymers requires them to be highly transparent. However, the % transmittance of 15 wt% (in water) solutions of purified hyperbranched polymers prepared with different EGDMA contents and measured at 500 nm with a 1 cm path length is consistently <30% (Figure 2- 6). We hypothesize that this poor transmittance result is a consequence of a few, larger polymers (more akin to microgels) being formed during the Strathclyde methodology synthetic process, which is a relatively uncontrolled process that may result in the formation of a microgel fraction that would have a disproportionate impact on solution transparency according to Mie scattering theory [124]. To test this hypothesis, samples were filtered through a 0.45 $\mu$ m filter and re-tested for transparency, with the weight percent of polymer lost due to filtering also measured by lyophilizing the filtrate and measuring the residual mass relative to the initial filtered mass. Results for an example 1.45 mol % DDT and 4.65 mol % EGDMA hyperbranched polymer indicate that while only <10 wt% of the initial polymer mass is lost through filtration, the transparency of the resulting solution increases to >90% ( Figure 2- 6). This result supports our hypothesis of a (small) microgel fraction that can be eliminated via filtration disproportionately influencing the light scattering of the solution. This result is echoed across a broad spectrum of hyperbranched polymers with different cross-link densities tested, with mass losses of <10% resulting in transparencies increasing from 20-30% to >90% (Table 2- 1). We should also note that these results are collected using a 1 cm path length cell while the tear film has a thickness of only ~10  $\mu$ m, making this result of high significance for an artificial tear formulation.

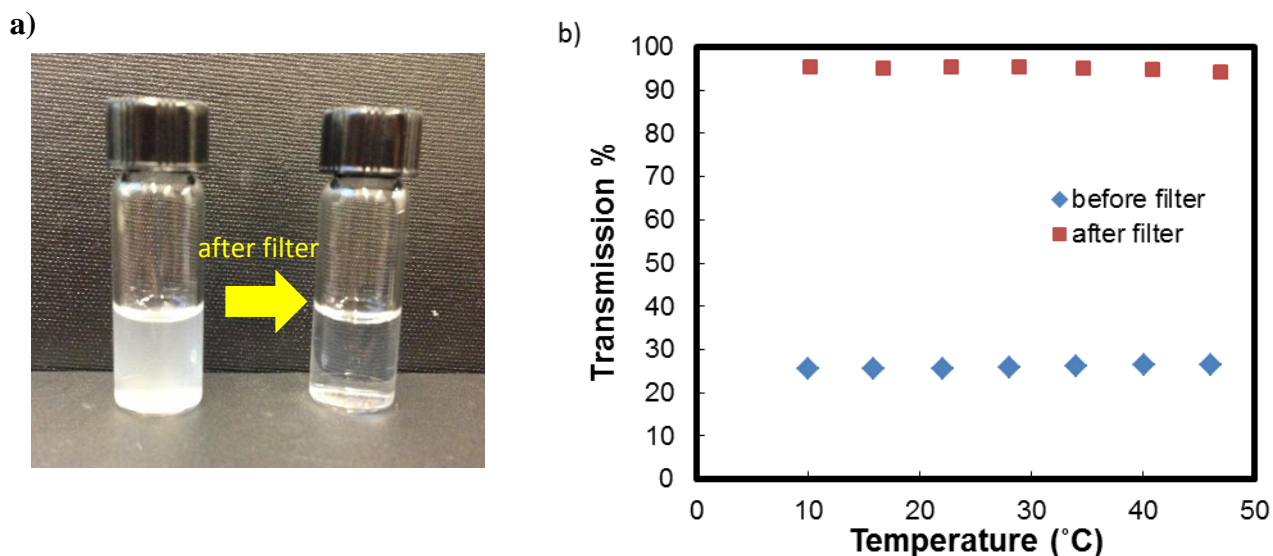


**Figure 2- 6-**(a) Visual appearance and (b) UV/vis transmittance value at 500 nm wavelength for a 15wt% solution of hyperbranched polymer with 1.45 mol % DDT and 6.2 mol % EGDMA

**Table 2- 1-**UV/vis transmittance value at 500 nm wavelength for 15wt% solution of hyperbranched polymer with varying percentages of DDT and EGDMA before and after filtration. Measured wt% of mass loss due to filtration (via gravimetry) are also included for reference.

| Polymer | EGDMA<br>(mol %) | DDT<br>(mol %) | Mass loss<br>(wt%) | %Transmission<br>before filter | %Transmission<br>after filter |
|---------|------------------|----------------|--------------------|--------------------------------|-------------------------------|
| 1       | 0.19             | 1.23           | 9                  | 25                             | 93                            |
| 7       | 6.2              | 1.23           | 10                 | 23                             | 94                            |
| 10      | 0.15             | 1.45           | 10                 | 25                             | 92                            |
| 20      | 6.45             | 1.45           | 12                 | 26                             | 94                            |
| 35      | 10.47            | 3.72           | 8                  | 21                             | 89                            |

### 2.3.1.5 Size

The hyperbranched polymer building block represents a dense, nanoscale structure (akin to a dendrimer, only one that can be made in a single synthetic step and with much less expensive

precursors) with a defined size that may be tuned according to the target application. In this application, given that transparency was the principal goal, smaller sizes are preferred; however, in the context of drug delivery, larger sizes (or at least a fraction of larger sized hyperbranched units) may be desirable to prolong release kinetics. Dynamic light scattering measurements of hyperbranched polymers of particular interest in this work are shown in Figure 2- 7.

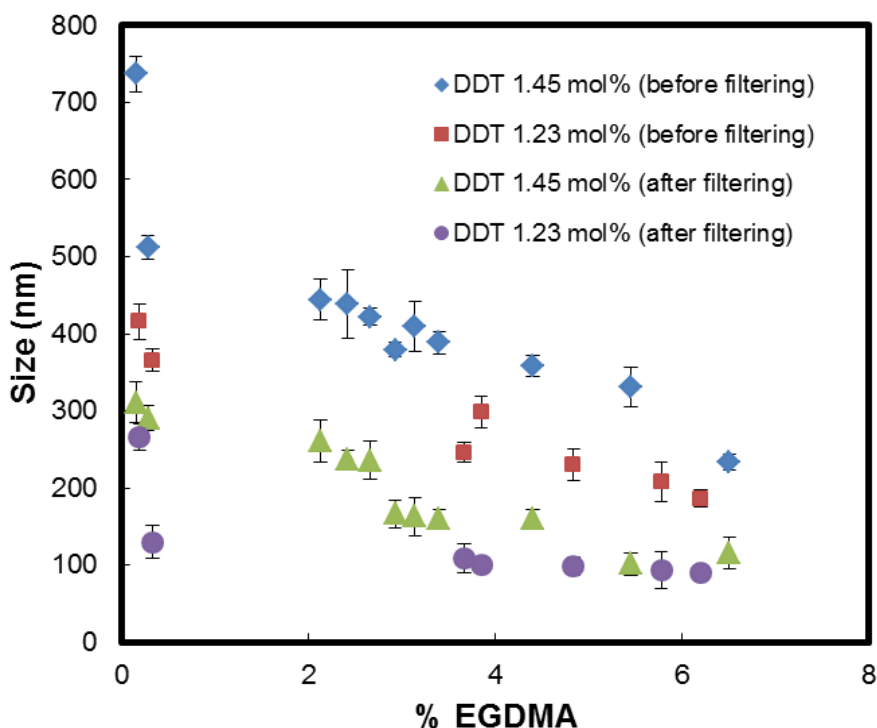


**Figure 2- 7**-Hydrodynamic diameter of hyperbranched polymers prepared with varying EGDMA (cross-linker) contents at fixed DDT (chain transfer agent) concentrations before and after sample filtration

First, filtration clearly decreases the average particle size measured independent of the DDT or EGDMA concentration used. This result again suggests that the small (<10 wt%) of mass eliminated via filtration was disproportionately larger than the majority of the hyperbranched polymers produced. The broad polydispersity of the hyperbranched polymers produced is also further demonstrated by comparing the light scattering results with the GPC results. GPC gives a

number-weighted result while light scattering is an intensity-weighted result, which (according to Mie scattering theory [124]) will significantly more highly weight the larger particles in the mixture (particularly when the primary particle population is as small as GPC suggests). In addition, the effective diameter of the polymers decreases as the mole% of cross-linker used to prepare the polymer increases. This is consistent with the expected result of higher cross-link densities resulting in more compact and branched polymer structures that are less able to swell in water. Thus, increased cross-linker content both increases the refractive index gradient of the hyperbranched polymers with water (leading to increased scattering) and reduces the size of the particles (leading to reduced scattering according to Mie theory), accounting for the roughly equivalent transmittances observed as a function of EGDMA content in the previous section. In this context, using more EGDMA can be dually effective by both increasing the molecular weight (increasing the viscosity) and decreasing the size of these nanoparticles (lower light scattering).

#### 2.3.1.6 Viscosity optimization

Rheological experiments confirm that the use of DDT as the chain transfer agent imparts shear thinning properties to the hyperbranched polymers. Figure 2-8 shows that increasing the EGDMA content in hyperbranched polymers prepared using a fixed 1.4 mole% DDT has a significant impact on the infinite shear (blinking) viscosity of the hyperbranched polymers but minimal to no influence on the zero shear (at rest) viscosities of the polymers.

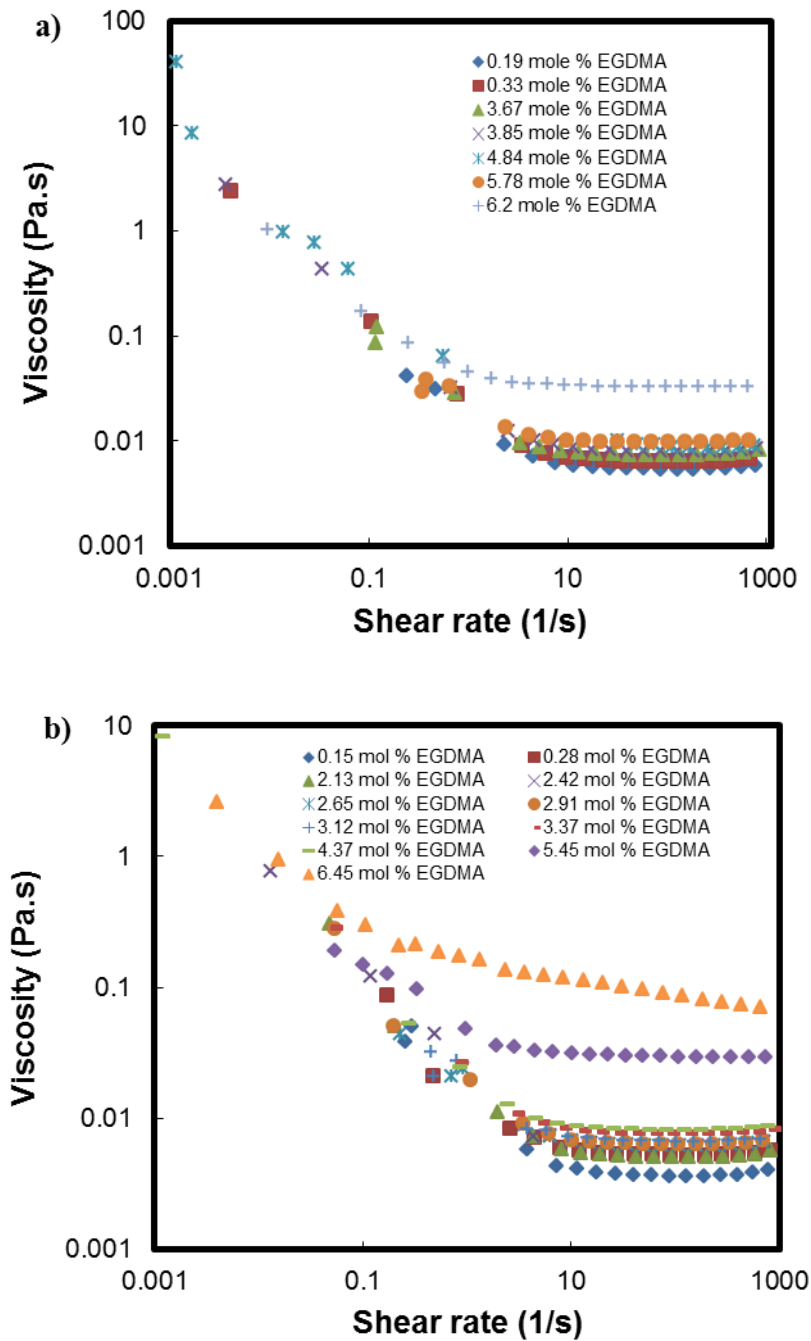


**Figure 2- 8-**Viscosity versus shear rate as a function of increase in EGDMA content for hyperbranched polymers prepared with a) 1.2 mole % DDT and b) 1.4 mole % DDT

All DDT-containing hyperbranched polymers exhibit 3-4 magnitude higher viscosities at low shear compared to higher shear rate viscosities. This is desirable in ophthalmic formulations

given that the enhanced low shear viscosity enhances the retention time of drug or any other substances trapped in the branch structures. Increasing the cross-link density has two competing effects on viscosity: (1) the hyperbranched polymer becomes denser and thus more compact, decreasing the hydrodynamic radius of the polymer at a fixed molecular weight and thus acting to reduce the viscosity and (2) the hyperbranched polymer molecular weight increases, resulting in the need for fewer distinct polymer chains to self-associate in order to create a network structure but also increasing the probability of intramolecular versus intermolecular interactions. The net result of these competing factors is a slight increase in infinite shear viscosity (and concurrent reduction in shear thinning potential) for the highest molecular weight (i.e. highest EGDMA content) hyperbranched polymers. This general trend was observed independent of the DDT content of the hyperbranched polymer studied (Figure 2-8 (a) and (b)).

Comparing the viscosity of the two hyperbranched polymers prepared with the highest amount of EGDMA in each set (Figure 2-8 (a) and (b)) with the hyperbranched polymer made with the highest amount of DDT and EGDMA possible while still producing a soluble polymer (polymer 35, Figure 2-9) shows that there is a limit to the degree of viscosity increase observed at higher shear rates.

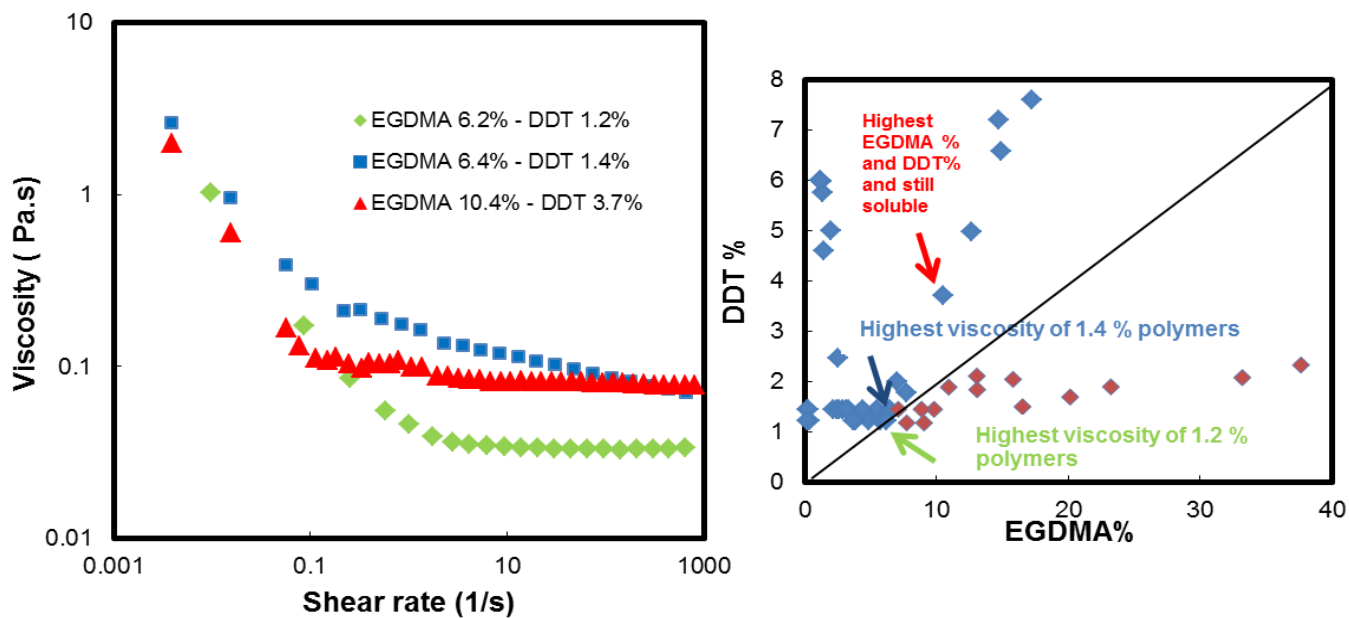


**Figure 2- 9**-Rheological comparison of hyperbranched polymers prepared with the highest EGDMA content and 1.45 mole% and 1.23 mole% DDT (from Figure 2-5) with the hyperbranched polymer prepared with the highest EGDMA and DDT contents resulting in a soluble hyperbranched polymer (EGDMA 10.4%-DDT 3.7%); Inset: polymer composition map showing location of the three polymers considered in the sample space

Polymer 35, even though has the highest molecular weight as well as incorporating the highest amount of DDT and EGDMA, shows essentially the same viscosity profile as the hyperbranched polymer prepared with significantly lower amounts of EGDMA and DDT. Again, this result can be attributed to the competing factors regulating the viscosity of hyperbranched polymers. Here, where both the DDT and the EGDMA content are varied, the viscosity of the hyperbranched polymer solution is correlated with both the molecular weight (EGDMA content) and the DDT content (degree of branching and hydrophobicity) according to the Mark-Houwink-Sakurada equation  $[\eta]=KM_v^\alpha$  in which  $M_v$  is the molar mass of the polymer and  $k$  and  $\alpha$  are constants determined by the specific solvent-polymer combination at a certain temperature. For a random coil in a theta solvent, the  $\alpha$  value is  $\sim 0.5$ ; in the same solvent,  $\alpha$  for hard sphere is zero whereas for semicoils and rigid rods it is  $\sim 1$  and  $\sim 2$  respectively. Hyperbranched polymers, due to their

internally cross-linked and highly branched internal structures, behave more like a sphere such that  $\alpha \rightarrow 0$ ; in addition, as the content of DDT increases, the polymers also become more hydrophobic, resulting in chain deswelling according to the reduced polymer-solvent interactions (and concurrent effect on the Flory  $\chi$  parameter). Thus, the more branched structure coupled with the reduced polymer-solvent affinity counteract the increased molecular weight of polymer 35 in terms of determining its infinite shear viscosity. This result demonstrates clearly that changing the composition of the hyperbranched polymer has a relatively limited effect on its viscosity profile. While this result is not ideal in the context of manipulating the shear thinning properties of an artificial tear formulation, this property is highly desirable from a formulation perspective in that the viscosity of the artificial tear solution can be kept largely constant irrespective of the composition of hyperbranched polymer used, allowing for facile switching between denser, higher affinity and less dense, lower affinity hyperbranched units to (for example) change the drug delivery kinetics within the formulation.

The shear thinning potential of hyperbranched polymers can be tuned, however, by changing the concentration of the polymer, as demonstrated in Figure 2- 10. Reducing the polymer concentration significantly decreases the infinite shear viscosity while it has little to no effect on the lower shear viscosity values. This result is consistent against multiple hyperbranched polymers tested. Note that, consistent with the similar low-shear viscosity profiles measured, the macroscopic appearance of the material remains as a gel or a viscous solution even upon dilution from 60 wt% to 20 wt%; this result is in contrast to previous observations with linear hydrophobically-modified polymers, in which higher concentrations led to significantly higher zero shear viscosities as well as infinite shear viscosities (at least over the concentration range explored here for the hyperbranched polymers). Since the polymer

concentration is diluted within the tear film immediately after administration and further diluted over time due to tear turn-over, maintaining the capacity for gel/viscous solution formation and shear thinning over such a broad concentration range represents a significant advantage of these hyperbranched polymers in terms of potential ophthalmic applications.

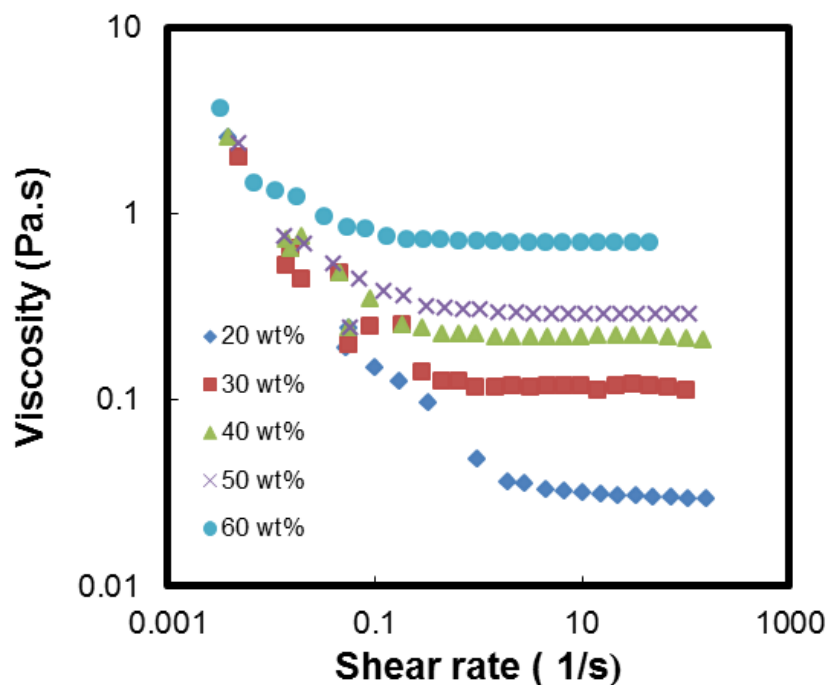


**Figure 2- 10-**Viscosity versus shear rate for hyperbranched polymer 20 (6.45 mole% EGDMA,1.45 mole% DDT) as a function of polymer concentration

Combining linear, hydrophobically-modified polymers with  $C_{12}$ -terminated hyperbranched polymers results in a significantly higher viscosity at higher shear rates but minimal changes in the viscosities observed at lower shear rates, as shown in Figure 2- 11.

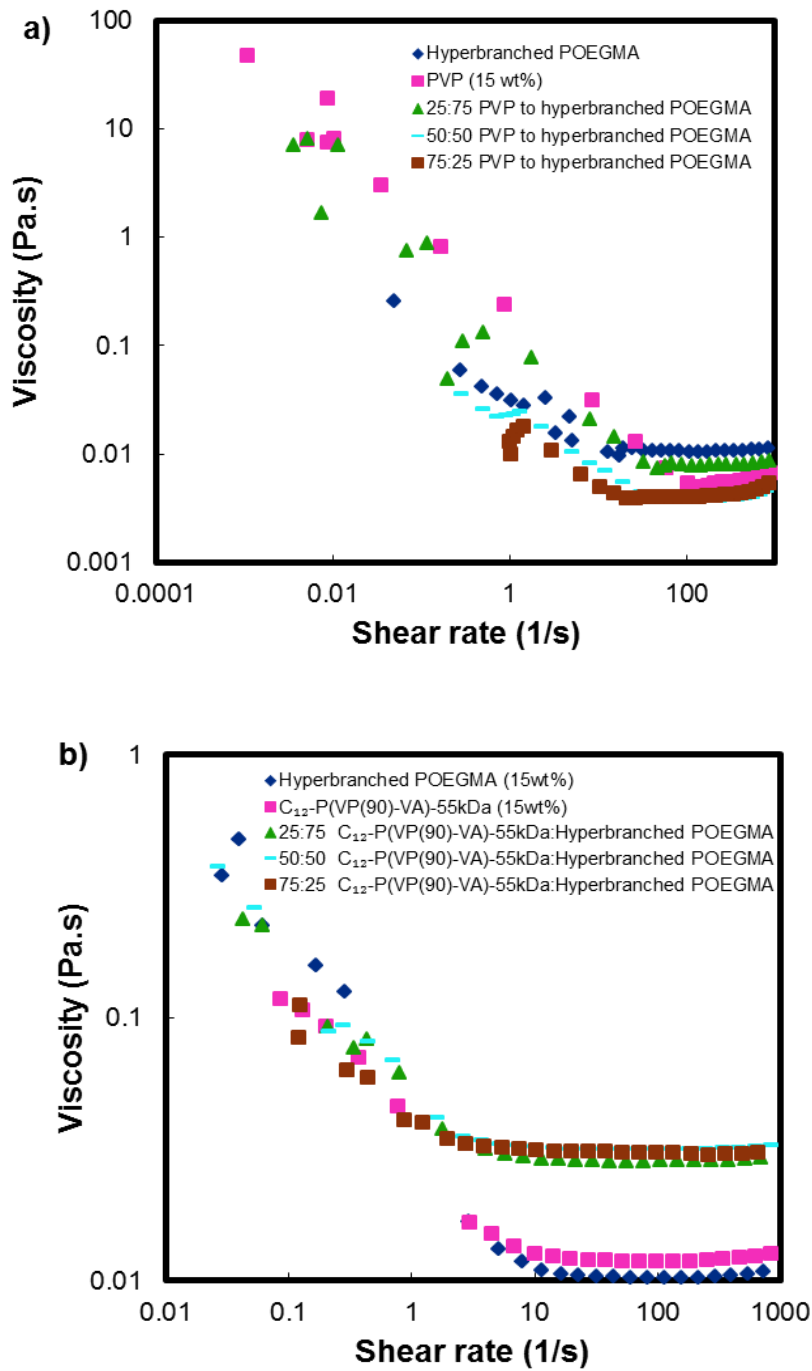


**Figure 2- 11-** Rheology of hyperbranched polymer (10.4 mole% EGDMA, 3.7 mole% DDT) mixed with (a) PVP (b) linear hydrophobically grafted PVP linear polymers (55 kDa molecular weight, 1.7 mol % C<sub>12</sub> hydrophobes) mixed with CD-grafted hyperbranched polymer

In the absence of hydrophobic grafts on the PVP component, no significant change in viscosity is observed upon mixing linear PVP and hyperbranched hydrophobically-modified polymers at different ratios (Fig. 2-11(a)). This result indicates the lack of latent interactions between the pyrrolidone groups in PVP and the ether groups on the POEGMA side-chain. However, when the PVP polymer is hydrophobically grafted, a significant enhancement in infinite-shear viscosity is observed together with minimal changes in zero-shear viscosity. This result suggests that the hydrophobic networks formed by mixing hydrophobically-modified linear and hyperbranched polymers together are stiffer than those formed with either component alone. We hypothesize this result is related to the rigidity and high multivalency of the hydrophobic-grafted POEGMA hyperbranched polymers being combined with the flexibility and bridging capacity of the hydrophobic-grafted linear PVP polymers, combining the advantages of both individual components while mitigating their weaknesses in terms of promoting the formation of stronger, more shear-stable networks. This result, however, would only be relevant to eye drop formulations if the zero shear viscosity needed to be enhanced to minimize tear drainage during blinking in the context of avoiding higher molecular weight polymers that are more challenging to biologically clear (provided the resulting, higher viscosity during the blink did not induce patient discomfort).

## 2.3.2 Cyclodextrin complex inclusion

### 2.3.2.1 POEGMA-co-AA-g-CD characterization

<sup>1</sup> H NMR of hyperbranched POEGMA-co-AA grafted with cyclodextrin confirms the incorporation of Hdz/ $\beta$ -CD in the final hyperbranched polymer, showing peaks for the NH-C=O hydrogen of Hdz/ $\beta$ -CD ~ 9 ppm (Appendix B Figure B 1). The degree of incorporation of

Hdz/ $\beta$ -CD in the hyperbranched polymers was quantitatively measured by potentiometric-conductometric titration, tracking the consumption of  $-\text{COOH}$  groups following CD grafting. From this result, the degree of substitution of CD on the available AA monomer residues is  $\sim 41\%$ , resulting in 8 mole % of the total monomer residues containing CD in these samples.

#### 2.3.2.2 Rheology of POEGMA-co-AA-g-CD

The incorporation of cyclodextrin in the hyperbranched polymers significantly modifies the rheological properties of the material over the full range of shear rates studied, as shown in Figure 2-12.

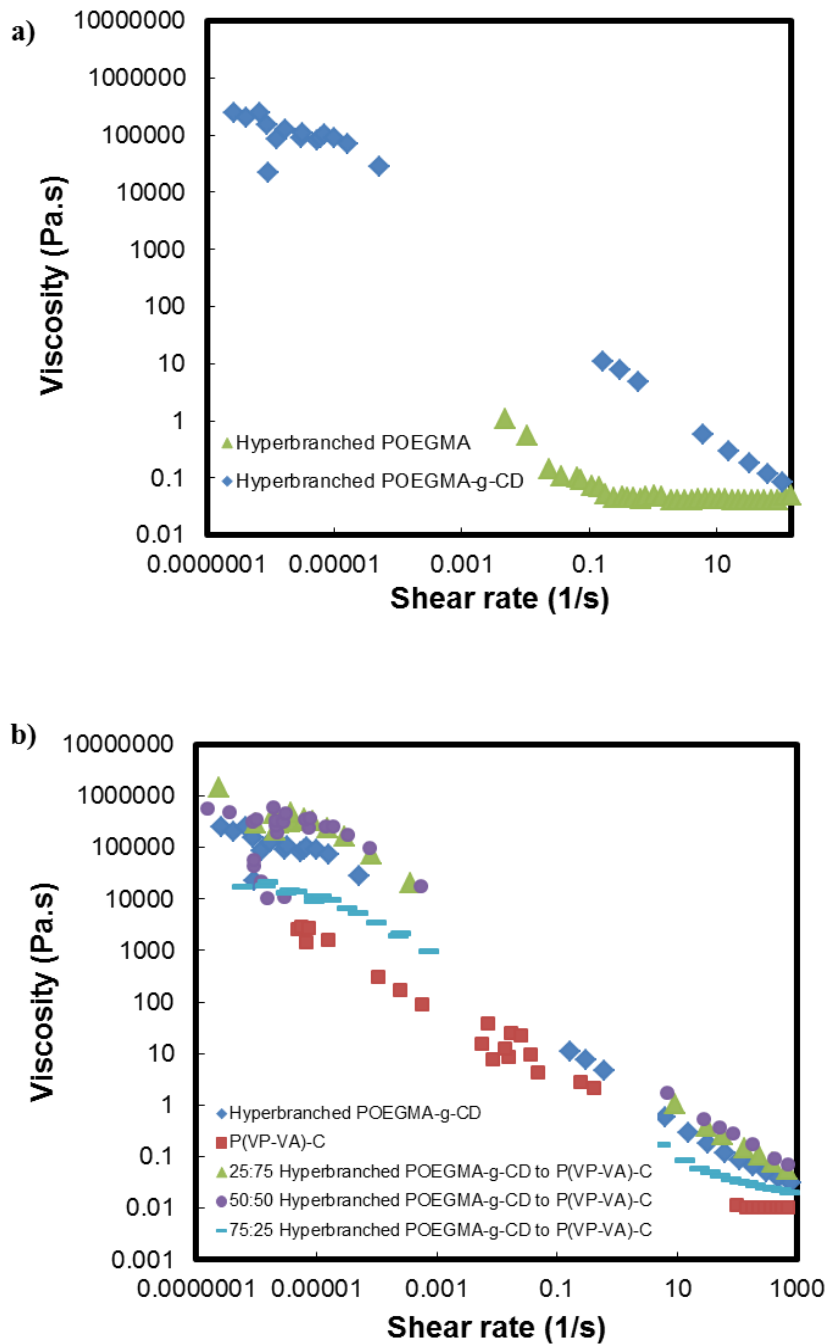


**Figure 2- 12-**Rheology of CD-grafted hyperbranched polymer (10.4 mole% EGDMA, 3.7 mole% DDT): (a) comparison of viscosity profile of hyperbranched polymer before and after CD grafting; (b) rheology of mixtures of linear hydrophobically grafted poly(N-vinylpyrrolidone) linear polymers (55 kDa molecular weight, 1.7 mol % C<sub>x</sub> hydrophobes) mixed with CD-grafted hyperbranched polymer

Rheological experiments suggest that hydrophobic dodecanethiol chains are able to form inclusion complexes with the hydrophobic cavity of cyclodextrin, with a 10 wt % solution of CD-functionalized hyperbranched polymer exhibiting significantly higher viscosities at all shear rates tested relative to the same polymer before CD grafting (Figure 2-12 (a)). In addition, when CD-functionalized hyperbranched polymers were mixed with hydrophobic grafted poly(N-vinylpyrrolidone) linear polymers, significantly higher zero-shear viscosities and lower-shear increases in viscosity as a function of shear rate (both attributable to stronger interpolymer interactions) are achieved with only a slight enhancement of the viscosity at higher shear rates relative to using either of the two components alone. We attribute this result to the formation of an inclusion complex between hydrophobes grafted to the PVP-based polymers with the CDs on the hyperbranched polymers. Combining the advantages of the increased flexibility of the linear polymer component (acting as more effective bridges between CD-functionalized hyperbranched units) with the relative structure and rigidity of the hyperbranched polymer component is hypothesized to lead to the significantly enhanced increase in viscosity as the shear rate is reduced as well as the significantly higher zero-shear viscosity achieved. As a result, the 50:50 mixture of the two polymers leads to the lowest-shear thickening response and the highest zero-shear viscosity, as the favorable properties of both building blocks are most effectively leveraged (and the negative properties of both building blocks on viscosity are effectively minimized). Both these properties (gelation at higher shear and stiffer gel formation at zero shear) are highly desirable in the context of ophthalmic formulations, as the gel-like properties of the polymer solution can be recovered faster following shearing and the gel formed is effectively stronger, minimizing clearance without significantly sacrificing lubricity at higher shear rates.

## 2.4 Conclusions

Hyperbranched polymers offer potential utility in the context of functional shear-thinning materials. Hyperbranched polymers can be prepared with a broad range of cross-linker contents (related directly to molecular weight) and branching densities (related to cross-linker and chain transfer agent content). Functionalization of the polymers with  $C_{12}$  groups by using dodecanethiol as the chain transfer agent results in shear thinning materials that can shear thin over up to 4 orders of magnitude and whose shear thinning potential is surprisingly independent of the cross-linker and chain transfer agent concentrations used in the polymer recipe, with reduced shear thinning only observed at extremely high (>6 mole%) cross-linker contents. This independence offers potential to tune the properties of the hyperbranched additive (for tuning drug delivery kinetics, for example) without significantly changing the rheological properties relevant to their use. Filtering to remove the small (<10 wt%) fraction of larger, microgel-like particles results in solutions that are functionally transparent even at high concentrations (15-20 wt%), and dilution of the solutions does not significantly affect the low shear viscosity of the solution over a broad concentration range (15-60 wt%), both ideal properties for use in the highly diluting environment of the eye. Finally, by combining linear, hydrophobically-modified polymers with  $C_{12}$ -terminated hyperbranched polymers, the infinite shear viscosity of the mixture solution significantly increases, potentially useful for enhancing the retention time of an artificial tear formulation made from these polymers without requiring the use of very high molecular weight polymers that may be challenging to biologically clear. Mixing linear, hydrophobically-modified polymers with cyclodextrin-functionalized hydrophobic hyperbranched polymer introduces additional benefits in terms of generating extremely stiff gels at zero shear (due to the combination of hydrophobic interactions and inclusion complex

formation in these systems) and lower-shear viscosity build-up, with potential benefits in terms of more rapidly reforming a gel-like structure following blinking to minimize drainage between blinks without compromising lubricity. We anticipate these materials have significant potential both for the treatment of dry eye (i.e. hydration can be maintained with fewer eyedrop administrations) as well as drug delivery to the front of the eye (i.e. enhanced residence time of the drug on the corneal surface).

### **3 -Mucoadhesive, Shear-Associative Polymers based on Dual Hydrophobe-Phenylboronic Acid Grafted Poly(vinyl pyrrolidone)**

### 3.1 Introduction

Eye drops are the primary method of delivering therapeutic agents to the anterior segment of the eye [125]. Due to several effective defence mechanisms at the front of the eye, the bioavailability of drugs using an eye drop is low, and most of the administered drug is eliminated from the ocular surface after a couple of blinks [108], [126]. Other methods of delivery such as implants [127], viscous solutions [21], ointments [12], and contact lenses [128] have been used as alternatives to eye drops. Implants can increase the bioavailability of the drug but they have issues with poor patient compliance or patient discomfort. Ointments can provide a sustained contact with the eye, but at the same time they typically result in blurred vision and irritation, leading to characteristically low patient compliance [14]. The use of highly concentrated, viscous polymer solutions has been demonstrated to increase the bioavailability of the drugs by reducing the tear turn-over time but can also increase the local and systematic toxicity as a consequence of that drug therapy [108]. Contact lenses have low patient compliance and difficulties associated with administration, especially for elderly people who are typically more at risk for developing the type of ophthalmic diseases the drug is intended to treat (e.g. dry eye, glaucoma, etc.). As such, a significant need exists to develop novel, patient-friendly, and effective approaches to address the challenge of low drug bioavailability associated with eye drops.

Formulations using mucoadhesive polymers as drug carriers have been proposed to overcome the limitations associated with topical administration methods. Mucoadhesive polymers are able to interact with mucin through a combination of electrostatic interactions, hydrophobic interactions, hydrogen bonding, covalent bond formation, and/or interdiffusion of the polymer chains into the mucin network (resulting in mechanical interlocking). Natural polymers such as chitosan [49], [50], cellulosic derivatives like sodium carboxymethylcellulose

(CMC)[48], and natural polysaccharides like hyaluronic acid [129], [130] and alginate [130] have all been used as mucoadhesive polymers to increase the residence time of the drug at the ocular surface. Synthetic polymers, which offer the advantage of improved compositional homogeneity batch-to-batch, have also been investigated as mucoadhesives, with poly(acrylic acid) and its lightly cross-linked derivatives (trade names Carbopol and Carbomer) in particular showing a high degree of mucoadhesion due to its anionic nature [41], [52], [131]. Carbopol has been used to increase the concentration of drug in the corneal and aqueous humor [132].

Alternately, functional groups that can bind to mucin may be grafted to or copolymerized with synthetic polymers to promote mucoadhesive bond formation. In particular, phenylboronic acid (PBA)-functionalized polymers have been widely investigated due to their ability to attach to mucin through covalent bonding of PBA in its charged form and *cis*-diols of mucin [56]. Using covalent binding can strengthen the mucoadhesion observed, and the interaction is not influenced by counterions in the tear fluid like other mucoadhesives.

Recently, we have reported on shear-associative polymers based on poly(vinyl pyrrolidone-co-vinyl formamide) (P(VP-co-VF)) grafted with  $C_8 - C_{18}$  hydrophobes [112]. Shear-associative polymers such as these are able to form physical intermolecular interactions between their hydrophobic grafts which can subsequently be disrupted by applying shear and reformed once the shear is removed, facilitating enhanced residence times at the ocular surface (via viscous solution/gel formation at low shear) while also promoting lubrication during blinking. These P(VP-co-VF) hydrophobically grafted polymers exhibited significant shear thinning (~4 orders of magnitude between zero shear and infinite shear), remained transparent up to extremely high concentrations (~30 wt%), and were well-tolerated both *in vitro* by corneal and retinal epithelial cells as well as *in vivo* following both anterior and posterior administration.

However, to effectively use these materials for longer-term anterior segment drug delivery or longer-term dry eye relief, the retention time of the polymer needs to be enhanced; an enhancement we anticipate may be achieved by making this polymer mucoadhesive.

In this study, we investigated the conjugation of PBA groups to these hydrophobically-modified P(VP-co-VF) backbones to enhance the mucoadhesion of the polymer. Sequential grafting of two different grafts (hydrophobes and PBA) is uniquely facilitated by this initial copolymer design, as the hygroscopicity of the PVP backbone maintains a highly hydrated system, the random copolymerization kinetics facilitates effective spacing of the grafts along the polymer backbone, and the capacity to hydrolyze the VF residues (exposing reactive amine groups) to different degrees as a function of hydrolysis time can facilitate sequential grafting of alkyl halides (as shear associative groups) and PBA (as mucoadhesive groups). In addition, by grafting the PBA functional groups to the exposed amine groups via reductive amination (producing a secondary amine bond that serves as an electron donor to the aromatic group in PBA), the  $pK_a$  of PBA groups is effectively lowered from  $\sim 8.8$  (in the free state) to  $\sim 7.4$  (in the grafted state), significantly enhancing the percentage of PBA groups in the charged, trigonal state that can strongly bind to *cis*-diol groups in mucin. Such a design is thus anticipated to have significant advantages in terms of both shear thinning and mucoadhesion, promoting enhanced retention times of polymer on the ocular surface while still lubricating blinking.

## 3.2 Experimental

### 3.2.1 Materials

N-vinylpyrrolidone (NVP, >99%, Sigma Aldrich) and N-vinyl formamide (NVF, 98%, Sigma Aldrich) were purified prior to use by mixing the monomers with Dowex 50W X8 (hydrogen

form, Sigma-Aldrich) for 24 hours followed by passing them through an alumina basic column for inhibitor removal. Dimethyl-2,2'-azobis(2-methylpropionate) (AIBME, Wako Chemicals, 98.5%), sodium hydroxide (EMD Chemicals, Mississauga ON), alkyl halides 1-chlorododecane ( $\geq 99.5\%$ , Sigma-Aldrich), and 1-chlorooctadecane (96%, Sigma-Aldrich), 4-formyl phenylboronic acid ( $\geq 95.0\%$ , Sigma-Aldrich), triethylamine ( $\geq 99\%$ , Sigma-Aldrich), and sodium cyanoborohydride (95%, Sigma-Aldrich) were all used as received. HCl and NaOH solutions used for titration were Acculute standards. All water used was of Milli-Q grade (resistivity 18 M $\Omega$ -cm).

### 3.2.2 Synthesis

#### 3.2.2.1 P (VP-co-VF)

Free radical polymerization of N-vinylpyrrolidone and N-vinyl formamide was performed using isopropanol as both the solvent and the chain transfer agent and dimethyl-2,2'-azobis(2-methylpropionate) (AIBME) as the free radical initiator. Molecular weights of the copolymers can be changed by using different amounts of solvent and initiator, while the maximum amine content of the copolymer can be changed by changing the VP:VF monomer ratio ( Table 3- 1). The reactants and initiator were mixed in a 3-neck glass round bottom flask with a condenser attached under 200 rpm magnetic stirring and a nitrogen purge. The reaction was carried out at 75°C for 24 hours, followed by evaporation of isopropanol using a rotatory evaporator to isolate the crude polymer product. The polymer was then dissolved in water, dialyzed using cellulose membranes (MWCO 3.5 kDa, minimum 6 cycles), and lyophilized for storage.

#### 3.2.2.2 P (VP-co-VA)

Basic hydrolysis was performed to convert the N-vinylformamide monomer residues of P(VP-co-VF) to N-vinylamine residues. 500 mg of P(VP-VF) was dissolved in 1N NaOH (0.2 wt%

polymer) in a three-necked round bottom flask under 200 rpm magnetic stirring, heated to 75°C, and left to react for 24 hours. Upon cooling, the reaction is stopped by neutralization of the solution with 1M HCl followed by dialysis against MilliQ water for 6 cycles using a cellulose membrane (MWCO 3.5 kDa) and lyophilisation for storage at room temperature.

### 3.2.2.3 P (VP-co-VA)- C<sub>x</sub>

Alkylated P(VP-VA) was prepared via a condensation reaction of alkyl halides (1-chlorododecane – C<sub>12</sub>, or 1-chlorooctadecane – C<sub>18</sub>) and amine groups of the graft platform. 0.1 wt% P(VP-VA) was first dissolved in a 1:10 water:methanol mixture containing 0.02wt% sodium hydroxide, after which the alkyl halide was gradually added. The flask was submerged in an oil bath (65°C), and the reaction was carried out for 48 hours. At completion, the methanol solvent is evaporated using a rotatory evaporator and the solution was mixed with hexanes for 4 hours to separate the unreacted alkyl halides into the organic phase. A separatory funnel was then used to separate the aqueous phase (containing the grafted polymer and water) from the organic phase (containing the unreacted alkyl halide), with three sequential extractions performed to the point that the lower aqueous phase in the funnel is clear (i.e. no emulsified component). The solution was then dialyzed against Milli-Q water for 6 cycles using a cellulose membrane (MWCO 3.5 kDa) and was lyophilized to dryness for storage at room temperature.

### 3.2.2.4 P(VP-co-VA)-C<sub>x</sub>-PBA

Phenylboronic acid functional groups were grafted to the residual free amine groups left unreacted in the alkylation reaction using a reductive amination procedure. A 10 mg/mL solution of P(VP-VA)-C<sub>x</sub> is dissolved in methanol followed by addition of 2 equivalents of sodium cyanoborohydride as the reducing agent, a 2-fold excess of 4-formylphenylboronic acid relative

to the available amine groups for grafting, and 2 equivalents of triethylamine to convert amine salts to free amine groups to facilitate reductive amination. The solution was purged with nitrogen and stirred at room temperature for 24 hours to complete the reaction. The resulting polymer was dialyzed against Milli-Q water (6 cycles, MWCO 3500) followed by lyophilization for storage at room temperature.

### 3.2.3 Characterization

#### 3.2.3.1 Nuclear magnetic resonance

The degrees of grafting of  $C_x$  groups and PBA groups to the P(VP-co-VF) polymer backbone were assessed using  $^1H$ -NMR on a Bruker AVANCE 600 MHz spectrometer using deuterated water as the solvent.

#### 3.2.3.2 Potentiometric-conductometric titration

Potentiometric-conductometric titration of the polymers was used to evaluate the amine content on the P(VP-VA) polymer backbone (to assess the degree of hydrolysis) as well as the amine content after alkyl grafting (to assess the mole% alkyl grafting achieved). Polymers were dissolved in water at a concentration of 1 mg/mL, after which KCl salt was added to reach an initial conductivity of 5 mS/m. 1 M HCl was added drop-wise to adjust the initial pH of the solution to  $\sim 2.5$ , after which samples were titrated using NaOH (0.1M). pH and conductivity were measured as a function of the base volume added (Mandel PC Titrator). The titration endpoints were analyzed using the derivative of the pH-versus-volume curve to identify the inflection point onset-offset corresponding to the quantity of amine titrated.

#### 3.2.3.3 Gel permeation chromatography

Polymer molecular weights are determined by gel permeation chromatography (GPC) using a Waters 590 HPLC pump, three Waters Ultrastaygel Linear columns (30 cm  $\times$  7.8 mm (i.d.);  $< 10$

$\mu\text{m}$  particles) operating at  $40^\circ\text{C}$ , and a Waters 410 refractive index detector operating at  $35^\circ\text{C}$ . The eluent used was 50 mM LiBr in N,N-dimethylformamide (DMF), and the system was calibrated with narrow molecular weight PEG standards (Waters).

#### 3.2.3.4 Transmittance by UV/visible spectroscopy

The % transmittance of the samples (representing the transparency with respect to optical clarity) were measured over the full UV and visible spectrum (300 - 700 nm) using a DU 800 UV/vis spectrophotometer (Beckman Coulter). The transmittances of the samples were recorded using a 15 wt% solution (in phosphate buffered saline) of each P(VP-VA)-C<sub>x</sub>-PBA polymer tested and a 1mm path length quartz cuvette.

#### 3.2.3.5 Refractive index

The refractive indices of P(VP-VA)-C<sub>x</sub>-PBA polymers (dissolved at x wt% in phosphate buffered saline) were measured at  $25^\circ\text{C}$  using a digital PAL-RI hand-held pocket refractometer (ATAGO).

#### 3.2.3.6 Rheology

A cone/plate rheometer (ATS, Rheologica Instrument, USA) using a cone with a 4 cm diameter and  $20^\circ$  cone angle was used to measure the dynamic viscosity of P(VP-co-VA)-C<sub>x</sub>-PBA polymer solutions. Polymer solutions were prepared at a concentration of 15 wt% in Milli Q water and equilibrated for 48 hours at room temperature prior to testing. Stresses from 0.01 to 100 Pa were then applied and the resulting strain was measured to assess the viscosity as a function of shear rate. The stress range is divided into 35 intervals, with an integration time of 60 seconds applied at each shear stress point.

### 3.2.3.7 Mucoadhesion via Rheological Synergism

Oscillatory rheology measurements were performed to assess the magnitude of mucoadhesive bond formation between different P (VP-co-VA)-C<sub>x</sub>-PBA polymer solutions and mucin (in this case from porcine stomach typeII). Measurements were performed on 30 wt% solutions of polymers (dissolved in phosphate buffered saline), 4 wt% mucin (also dissolved in phosphate buffered saline) and the combination of 30 wt% polymer and 4 wt% mucin (in phosphate buffered saline). Solutions were stored at 4°C for 48 hours prior their use to ensure they are completely hydrated and any mucoadhesive equilibrium was reached. An oscillation stress sweep was first performed to find the linear viscoelastic region; following, an intermediate stress within this linear regime was selected and held constant as the oscillation frequency was varied from 0.01 to 100 Hz (30 intervals). The magnitude of mucoadhesion observed was quantified based on the theory of rheological synergism, referring to the excess property measured within a mixture of mucus gel and the test material compared to the arithmetic sum of that same property measured for the two components individually [133]. Both G' (storage modulus, elastic component) and G'' (loss modulus, viscous component) may be considered in terms of this concept of an excess property, with G' of particular interest in the context of gel formation. The excess modulus representing the rheological synergism can be calculated using Equations 3-1 (elastic modulus) or 3.2 (loss modulus):

$$\Delta G' = G'_{mix} - (G'_{polymer} + G'_{mucin}) \quad \text{Equation 3- 1}$$

$$\Delta G'' = G''_{mix} - (G''_{polymer} + G''_{mucin}) \quad \text{Equation 3- 2}$$

The higher the G'(mix) value (the measured modulus value of the combination of the polymer and mucin) relative to the geometric sum of the two individual component G' values, the higher

the excess modulus property and thus the stronger the mucoadhesion between mucin and the polymer. Alternately, this synergism can be expressed in terms of the relative synergism (i.e. the relative increment in viscoelasticity with regard to the polymer and mucin solutions alone) based on Equations 3-3 and 3-4.

$$\Delta G' / G' \quad G' = G' \text{ polymer} + G' \text{ mucin} \quad \text{Equation 3-3}$$

$$\Delta G'' / G'' \quad G'' = G'' \text{ polymer} + G'' \text{ mucin} \quad \text{Equation 3-4}$$

### 3.2.3.8 In vitro cytotoxicity assay

The cytotoxicity of the dual grafted polymers was assessed using an MTT assay against human corneal epithelial cells (HCECs, anterior segment). Thiazolyl blue tetrazolium bromide (MTT) assay is a metabolic process in which the concentration of the purple metabolite of the MTT dye can be related to the level of cell metabolism and thus the total number of viable cells in the presence of various concentrations of the tested polymers reported relative to the cell viability in a non-treated control well. Cell viability was calculated based on the following equation:

$$\text{Cell Viability (\%)} = \frac{\text{Absorbance}_{\text{polymer solution}}}{\text{Absorbance}_{\text{Blank}}} \quad \text{Equation 3-5}$$

HCECs were cultured in complete KSFM media (Gibco), including the provided bovine pituitary extract and EGF supplement, and 1% penicillin/streptomycin. Cells were plated in a 24-well polystyrene multiwell plate at a density of 100,000 cells per well, with a total volume of 1 mL of the appropriate media added to each well. Cells were allowed to adhere for 24 hours, after which 2 mg/ml polymer solutions prepared in PBS (sterilized via filtration through a 0.2 mm syringe filter and a 3 hr exposure to UV) with concentrations ranging from 100 to 1000 µg/ml were

transferred into wells with cultured cells and incubated for 24 h. The MTT assay test was done by exposing the cells to 150  $\mu\text{L}$  of a 40 mg/mL MTT reagent solution for four hours, lysing the cells with 250  $\mu\text{L}$  DMSO, and reading the resulting absorbance at 570 nm using a multiwell plate reader. Percentages of cell viability were calculated in reference to a positive control of cells grown under the same conditions but not exposed to any polymers, with the absorbance of the media itself measured as a negative control and subtracted from the measured MTT signal. A total of four replicates was performed for each polymer and each plate was scanned 3 times, with the reported error bars representing the standard deviation of the replicates.

### 3.3 Results and discussion

#### 3.3.1 Characterization

##### 3.3.1.1 P (VP-VF)

The chemical composition of the P (VP-co-VF) polymer backbone was quantitatively verified by  $^1\text{H}$  NMR by comparing the peak area of  $\text{CH}_2$  groups in pyrrolidone ring ( $\sim 2.8\text{-}3.9$  ppm) with the CH peak from the formamide group ( $\sim 7.7\text{-}8.4$  ppm). The reactivity ratio of the two monomers is  $\sim 1$  [134], resulting in functional monomers being incorporated randomly and nearly quantitatively in the polymers (Table 3-1). Polymers intended to have 10 mole% NVF incorporation yielded 8.8-9.4 mole% NVF in the synthesized samples, while 17 mol% and 28 mol% NVF was incorporated for the intended 20 mole% and 30 mole% NVF polymers respectively.

Molecular weights of these graft platform polymers were determined using a DMF GPC, first calibrated with narrow molecular weight PEG standards. However, commercial (albeit

broader polydispersity) polyvinylpyrrolidone samples with known  $M_w$  values (10 kDa, 40 kDa, and 50 kDa, Sigma Aldrich) show significantly lower molecular weights compared to what is anticipated when the PEG standards are used, with the calculated molecular weights roughly 2-fold lower than the provided  $M_w$  values of the commercial PVP samples. Therefore, to achieve more accurate measurements of molecular weight, all  $M_w$  values obtained from the GPC were calibrated against the PVP samples instead of the PEG standards. The resulting  $M_n$ ,  $M_w$ , and PDI values for the polymers produced are shown in Table 3- 1, with graft platform molecular weights ranging between ~60-180 kDa achieved by varying the solvent:monomer ratio in the polymerization. Note that overall, two sets of graft platform polymers are produced: (1) same molecular weight (~60-66 kDa) but different mole percentages of functional monomer (~9-25 mole% of amine-bearing monomer) and (2) same mole percentage of functional monomer (~8-9 mole% of amine-bearing monomer) but different molecular weights (~60-180 kDa). This data set allows for independent assessment of the effects of graft platform molecular weight and functionalization on the ultimate polymer properties.

### 3.3.1.2 P (VP-VA)

VF can undergo both basic and acidic hydrolysis. Acidic conditions result in lower conversions due to cationic nature of amine groups at lower pHs which results in repulsion with  $H^+$  ions [135]; in contrast, basic hydrolysis can result in quantitative hydrolysis of the amide groups [136]. Following base hydrolysis on our graft platform P(VP-co-VF) polymers,  $^1H$  NMR indicates the complete disappearance of the formamide amide group at 7.7-8.4 ppm, suggesting quantitative hydrolysis in these polymers. However, potentiometric/conductometric titration analysis of the polymer-bound amine groups suggests that the amine % calculated from the titration is consistently lower than the quantitative conversion suggested by NMR (Table 3- 1).

We anticipate this difference is a result of a side-reaction that can convert formamide residues into OH groups, resulting in a copolymer consisting of vinylamine with a negligible amount of vinyl alcohol. Thus, synthesizing these samples slight excess of VF is required to produce stoichiometric equivalents of reactive amine groups available for grafting following hydrolysis.

**Table 3- 1-**Recipes and molecular weights of poly(vinyl pyrrolidone-co-vinyl formamide) (P(VP-co-VF)) graft platform polymers and mole percentage of monomer residues bearing a primary amine group in P(VP-co-VA) copolymers based on <sup>1</sup>H NMR and conductometric titration

| Sample code               | Monomer Vol% | Initiator wt% | Solvent/chain transfer | Initiator | M <sub>n</sub> (Da) | M <sub>w</sub> (Da) | PDI  | Corrected M <sub>w</sub> (Da) | Targeted amine mole % (theoretical) | Amine mole % based on NMR | Amine mole% based on titration |
|---------------------------|--------------|---------------|------------------------|-----------|---------------------|---------------------|------|-------------------------------|-------------------------------------|---------------------------|--------------------------------|
| <b>P(VP(91)-VF)60kDa</b>  | 15           | 0.015         | Isopropanol            | AIBMe     | 10100               | 25500               | 2.5  | 60000                         | 10                                  | 9.4                       | 8.8                            |
| <b>P(VP(84)-VF)65kDa</b>  | 15           | 0.015         | Isopropanol            | AIBMe     | 11800               | 27600               | 2.37 | 65000                         | 20                                  | 17.7                      | 15.8                           |
| <b>P(VP(75)-VF)65kDa</b>  | 15           | 0.015         | Isopropanol            | AIBMe     | 11900               | 27900               | 2.4  | 65700                         | 30                                  | 28                        | 25                             |
| <b>P(VP(91)-VF)83kDa</b>  | 20           | 0.03          | Isopropanol            | AIBMe     | 11600               | 35300               | 3.05 | 83000                         | 10                                  | 9.9                       | 8.9                            |
| <b>P(VP(92)-VF)178kDa</b> | 30           | 0.1           | Isopropanol            | AIBMe     | 23500               | 75800               | 3.22 | 178200                        | 10                                  | 8.8                       | 8.2                            |

### 3.3.1.3 P(VP-VA)-C<sub>x</sub>

Hydrophobically-modified polymers were prepared with different backbone molecular weights, different hydrophobic graft lengths, and different degrees of functionalization (based on different amine mole fractions in the P(VP-co-VA) graft platform) to create a shear-thinning polymer material. While both <sup>1</sup>H NMR and titration can theoretically be used for determination of degree of alkylation, calculation of the degree of alkylation with NMR is challenging due to low degree of alkylation targeted in these materials and the overlap of the signal from the hydrophobe CH<sub>2</sub> groups and the CH<sub>2</sub> groups in the polymer backbone; instead, titration was used for this purpose.

Table 3- 2 shows the degree of alkylation (i.e. the percentage of amine residues grafted) and mole% of alkyl chains in polymer (i.e. the total mole percentage of all monomers in the graft platform functionalized with alkyl grafts) for the hydrophobically-modified polymers produced.

**Table 3- 2-** Degree of alkylation and the resulting mole% of total monomer residues functionalized with hydrophobic grafts in P(VP-co-VA)-C<sub>x</sub> polymers as measured by titration

| Sample code                           | Degree of alkylation | Mole % of monomer units with alkyl chains |
|---------------------------------------|----------------------|---|
| C <sub>12</sub> -P(VP(91)-VA)-60kDa   | 20%                  | 1.8                                       |
| C <sub>18</sub> -P(VP(91)- VA)-60kDa  | 20%                  | 1.8                                       |
| C <sub>12</sub> -P(VP(84)- VA)-65kDa  | 7.9%                 | 1.2                                       |
| C <sub>12</sub> -P(VP(75)- VA)-66kDa  | 6.25%                | 1.6                                       |
| C <sub>12</sub> -P(VP(91)- VA)-83KDa  | 25%                  | 2.25                                      |
| C <sub>12</sub> -P(VP(92)- VA)-178KDa | 13.5%                | 1.1                                       |

The degree of alkylation is relatively low for all polymers tested, presumably due to steric inhibition associated with long hydrophobes (both in terms of blocking additional grafting to

adjacent reactive functional groups and, as the grafting reaction proceeds, self-associating to further reduce the accessibility of the reactive functional groups). This hypothesis is supported by the particularly low graft yield achieved with the highest molecular weight polymer (C<sub>12</sub>-P(VP(90)-VF)178kDa), which could be interpreted as a direct result of the higher affinity for these polymers to self-associate and increase the steric hindrance. Interestingly, the ultimate graft density on a per monomer unit basis is similar regardless of the number of free amines present in the graft platform polymer, further confirming the impact of steric hindrance on this reaction but also facilitating an opportunity to compare the properties of polymers with different residual reactive group contents but similar graft densities.

#### 3.3.1.4 P(VP-VA)-C-PBA

Given the relatively low graft yields of hydrophobes, a relatively large fraction of the amine groups on the original graft platform polymer are still available for conjugation with PBA via reductive amination with 4-formylphenylboronic acid. The choice of the reducing agent is essential in this reaction given that it must selectively reduce imines (or iminium ions) without affecting aldehydes and ketones. Cyanoborohydride (NaBH<sub>3</sub>CN) is used as the reducing agent given its solubility in the methanol (used as the solvent for this step) and its reported pH-sensitive selectivity [137], with aldehydes and ketones reduced at pH 3-4 but iminium moieties selectively reduced at pH of 6-7 in the absence of significant aldehyde or ketone reactivity; pH 6 was subsequently chosen to perform the reductive amination step. The secondary amine linkage produced effectively reduces the pK<sub>a</sub> of PBA (Figure 3- 1) such that it is significantly more ionized at tear pH, increasing the strength and frequency of bond formation with the sialic acid residues in mucin.

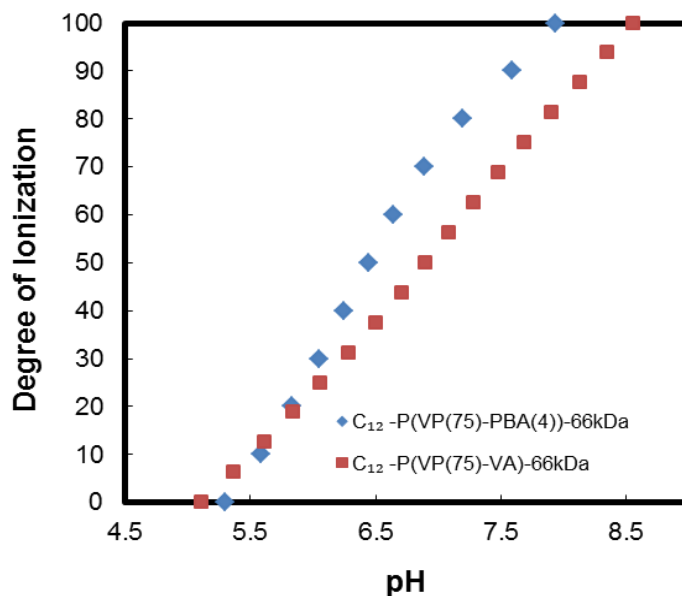


**Figure 3- 1**-Degree of ionization for C<sub>12</sub>-P(VP(75)-VA)-66kDa and the corresponding PBA grafted polymer C<sub>12</sub>-P(VP(75)-PBA (4))-66kDa

<sup>1</sup>H NMR was used for determination of PBA content conjugated in these polymers by comparing the integration of the phenyl ring protons from phenylboronic acid (7.5-8.5 ppm) with all the other protons of polymer backbone (1.5-4.5 ppm). Table 3- 3 shows the degree of substitution of amine groups (normalized to the total number of amines present in the original graft platform P(VP-co-VA) polymer by PBA groups and the resulting PBA mole% (expressed as the percentage of total monomer units functionalized with a boronic acid graft) in the polymer backbone.

**Table 3- 3-**Degree of amine substitution (i.e. percentage of amine groups in the original P(VP-co-VA) polymer grafted with PBA) and the resulting PBA content (mole% of total monomer units) of graft copolymer

| Sample Code                           | Degree of substitution | mole% of PBA<br>(based on total<br>monomer residues) |
|---------------------------------------|------------------------|--|
| P(VP(91)-PBA)-60kDa                   | 58%                    | 5.2  |
| C <sub>12</sub> -P(VP(91)-PBA)-60kDa  | 63%                    | 5.3  |
| C <sub>18</sub> -P(VP(91)-PBA)-60kDa  | 60%                    | 5.1  |
| C <sub>12</sub> -P(VP(84)-PBA)-65kDa  | 84%                    | 12.8   |
| C <sub>12</sub> -P(VP(75)-PBA)-66kDa  | 87%                    | 18.8   |
| C <sub>12</sub> -P(VP(91)-PBA)-83kDa  | 51%                    | 4.3  |
| C <sub>12</sub> -P(VP(92)-PBA)-178kDa | 46%                    | 4.0  |

The graft yield in the reductive amination is significantly higher compared to the alkylation step, likely attributable to the smaller size of 4-formylphenylboronic acid graft relative to the hydrophobic grafts. However, it should be noted that we intentionally kept PBA contents at relatively low values in these copolymers for two reasons: (1) PBA grafting increases the hydrophobicity of the polymer and thus can sacrifice the favorable humectancy associated with the PVP backbone at higher degrees of incorporation and (2) extremely high amounts of PBA might increase the residence time of the artificial tear on the ocular surface too significantly and result in corneal epithelium inflammation.

### 3.3.2 Transmittance

One of the requirements for the use of these materials for ophthalmic application is that they are transparent at high concentrations. Table 3- 4 shows the percent transmittance at 600 nm of 15

wt% solutions of PBA/C<sub>x</sub> dual-grafted polymers prepared using different hydrophobe chain lengths, different molecular weight graft platforms, and different PBA contents, while Figure 3-2 shows the percent transmittance of these polymers over the full visible wavelength scan. The higher PBA content polymers exhibit lower transmissions at all wavelengths than polymers prepared with lower PBA contents. However, transmittance values of >80% over the visible light range (~400-700 nm) are consistently observed for these materials; given that these measurements are performed using a 1 mm path length cuvette, such transmittance values are likely acceptable in the tear film (thickness ~10 μm) in a practical application.

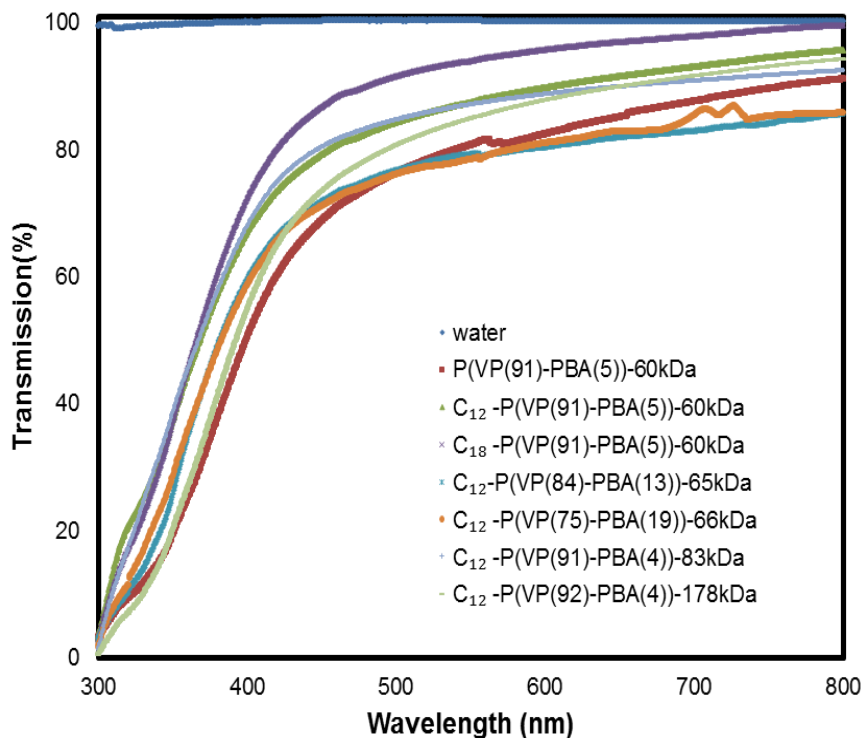


Figure 3- 2-Transmittance of polymers as a function of wavelength (15 wt % solutions)

**Table 3- 4-**Percent transmittance of dual C<sub>x</sub>-PBA grafted polymers at 600 nm (15 wt% solutions)

| Sample Code                              | Transmission % |
|--|----------------|
| P(VP(91)-PBA(5))-60kDa                   | 82.41          |
| C <sub>12</sub> -P(VP(91)-PBA(5))-60kDa  | 89.68          |
| C <sub>18</sub> -P(VP(91)-PBA(5))-60kDa  | 95.63          |
| C <sub>12</sub> -P(VP(84)-PBA(13))-65kDa | 80.29          |
| C <sub>12</sub> -P(VP(75)-PBA(19))-66kDa | 80.98          |
| C <sub>12</sub> -P(VP(91)-PBA(4))-83kDa  | 88.69          |
| C <sub>12</sub> -P(VP(92)-PBA(4))-178kDa | 87.80          |

### 3.3.3 Refractive index

The refractive index of dual C<sub>x</sub>-PBA grafted P(VP-VA) polymer solutions (at 15 wt%) with different molecular weights and PBA contents was measured to assess the suitability of concentrated solutions of this polymer in the context of potential ophthalmic use (Table 3- 5). Given the similarity in the measured refractive index values to water (1.33) and the natural cornea and lachrymal fluid values of 1.34-1.36 [138], the results shown in Table 3- 5 indicate that this polymer solution should not pose any problems with refraction and thus vision impairment even at high concentration in ophthalmic applications.

**Table 3- 5-**Refractive index of 15 wt% solutions (in water) of dual C<sub>x</sub>-PBA grafted P(VP-VA) polymers

| Sample Code                              | Refractive index |
|--|------------------|
| Water                                    | 1.3328           |
| P(VP(91)-PBA(5))-60kDa                   | 1.3478           |
| C <sub>12</sub> -P(VP(91)-PBA(5))-60kDa  | 1.3500           |
| C <sub>18</sub> -P(VP(91)-PBA(5))-60kDa  | 1.3479           |
| C <sub>12</sub> -P(VP(84)-PBA(13))-65kDa | 1.3465           |
| C <sub>12</sub> -P(VP(75)-PBA(19))-66kDa | 1.3482           |
| C <sub>12</sub> -P(VP(91)-PBA(4))-83kDa  | 1.3479           |
| C <sub>12</sub> -P(VP(92)-PBA(4))-178kDa | 1.3477           |

### 3.3.4 In vitro cytotoxicity assay

MTT assay results indicate no significant cell toxicity of dual C<sub>x</sub>-PBA grafted polymers with different molecular weights and PBA contents over a wide concentration range (Figure 3- 3). Although the concentrations tested in this *in vitro* assay are significantly lower than those envisioned for use in eyedrop formulations, cytocompatibility to this degree using a closed, *in vitro* system such as that used is typically predictive of the material being well-tolerated even at much higher concentrations in the context of *in vivo* applications.

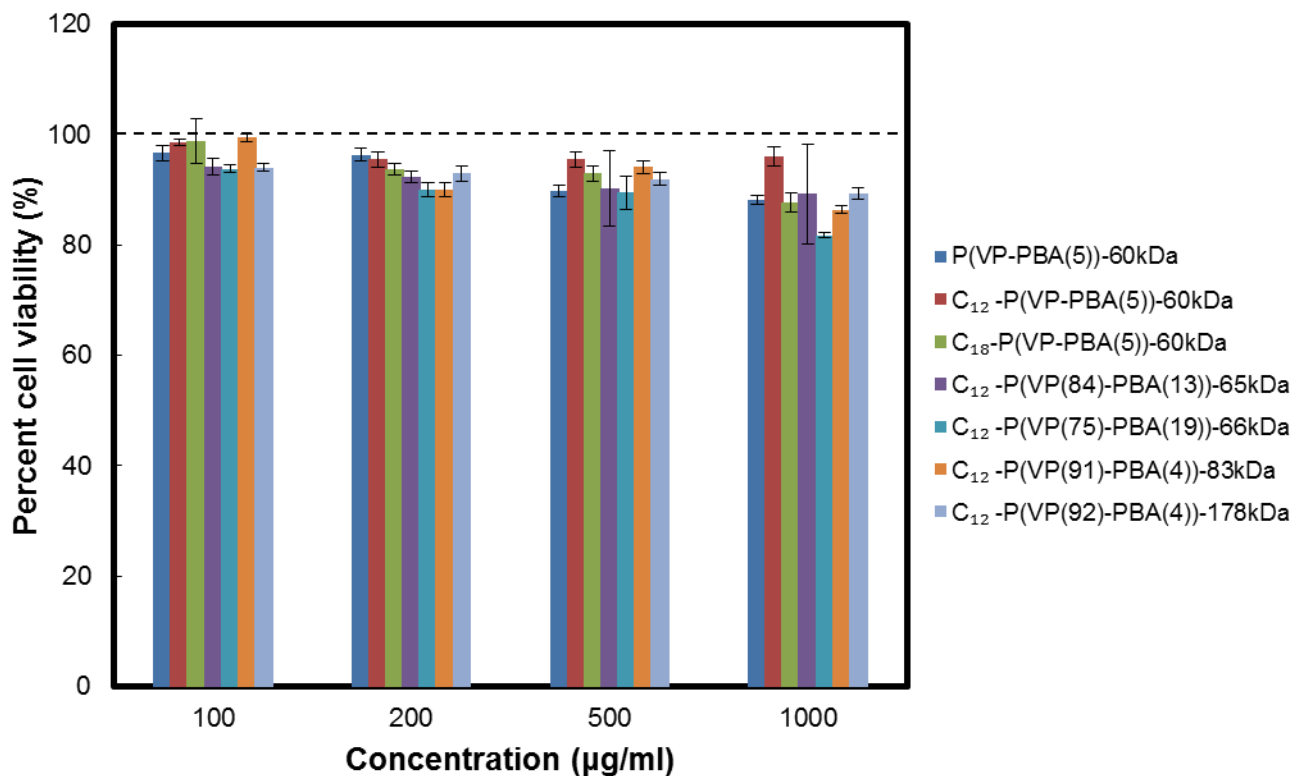


**Figure 3- 3-** Percent cell viability of HCEC cells exposed to polymers grafted with hydrophobic groups of different chain lengths, PBA content and molecular weight relative to cell-only (i.e. no polymer) controls

### 3.3.5 Rheology

Relative to the C<sub>x</sub>-only polymers (previously reported to exhibit shear thinning over at least 4 orders of magnitude of viscosity between zero and infinite shear [112]), dual grafted C<sub>x</sub>-PBA polymers exhibit similar rheological behavior.

Figure 3- 4 compares the shear-dependent viscosity of a representative C<sub>12</sub>- P(VP-VA)-60kDa polymer before and after PBA conjugation.

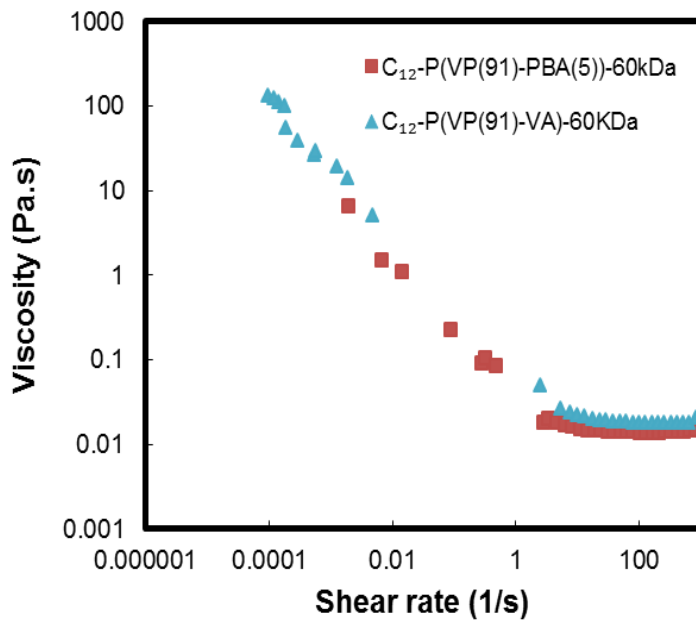


Figure 3- 4-Viscosity versus shear rate of C<sub>12</sub>-P (VP-VA)-60kDa before and after PBA conjugation

Figure 3- 5 compares the effect of hydrophobe chain length on the viscosity of polymers.

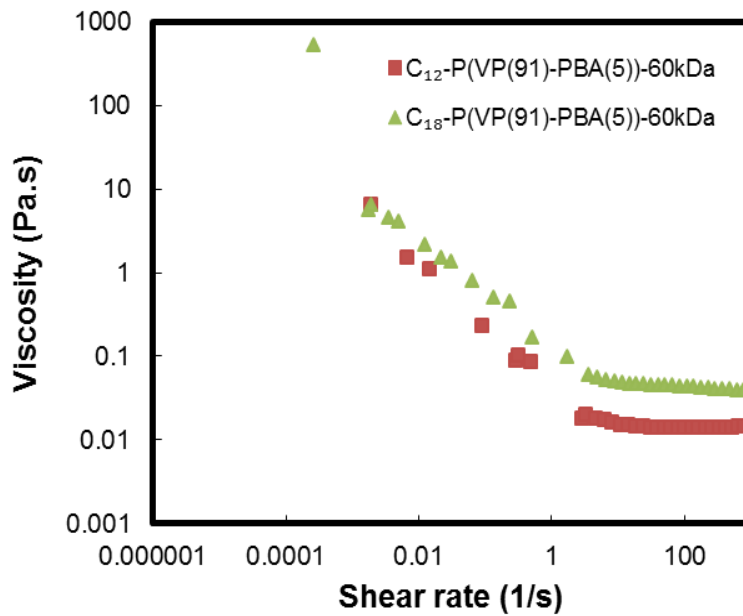
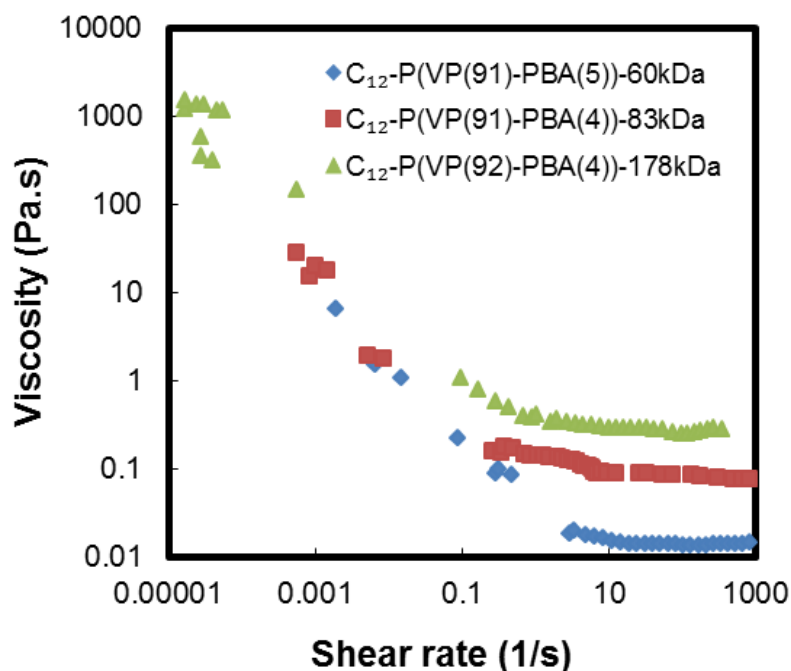


Figure 3- 5-Viscosity versus shear rate of dual C<sub>x</sub>-PBA grafted P(VP(91)-PBA)-60kDa polymer functionalized with different hydrophobe chain lengths

Again consistent with observations with polymers grafted with only  $C_x$  grafts, the incorporation of longer hydrophobes facilitates stronger interpolymer interactions and thus higher viscosities at all shear rates tested.

The rheological properties can be further tuned by changing the molecular weight of graft platform. Figure 3- 6 shows viscosity versus shear rate data for  $C_{12}$ -P(VP-PBA) polymers prepared using different molecular weight graft platforms.



**Figure 3- 6-**Viscosity versus shear rate of dual  $C_x$ -PBA grafted  $C_{12}$ -P(VP-PBA) polymers with different molecular weights

Again consistent with the  $C_x$ -only grafted materials, the lower molecular weight polymers are significantly more shear thinning, with only slightly lower zero shear viscosities but significantly (nearly 2 orders of magnitude) lower infinite shear viscosities. Thus lower molecular weights

are thus more preferred to be used in ophthalmic applications, both in the context of promoting clearance as well as facile injectability and effective lubricity during blinking.

Interestingly, based on the results in Figure 3-4 in particular, the rheology of the polymer is observed to be relatively constant as a function of the absence or presence of PBA groups. This observation is further investigated in Figure 3-7, in which the PBA content of the polymer is systematically increased by using polymers of the same molecular weights (and similar hydrophobe graft densities, Table 3-3) but different PBA contents.

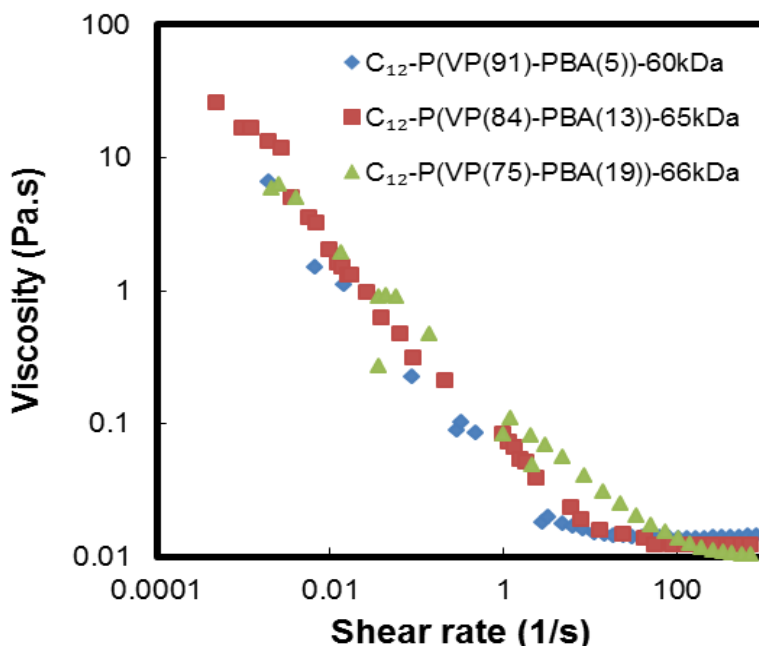


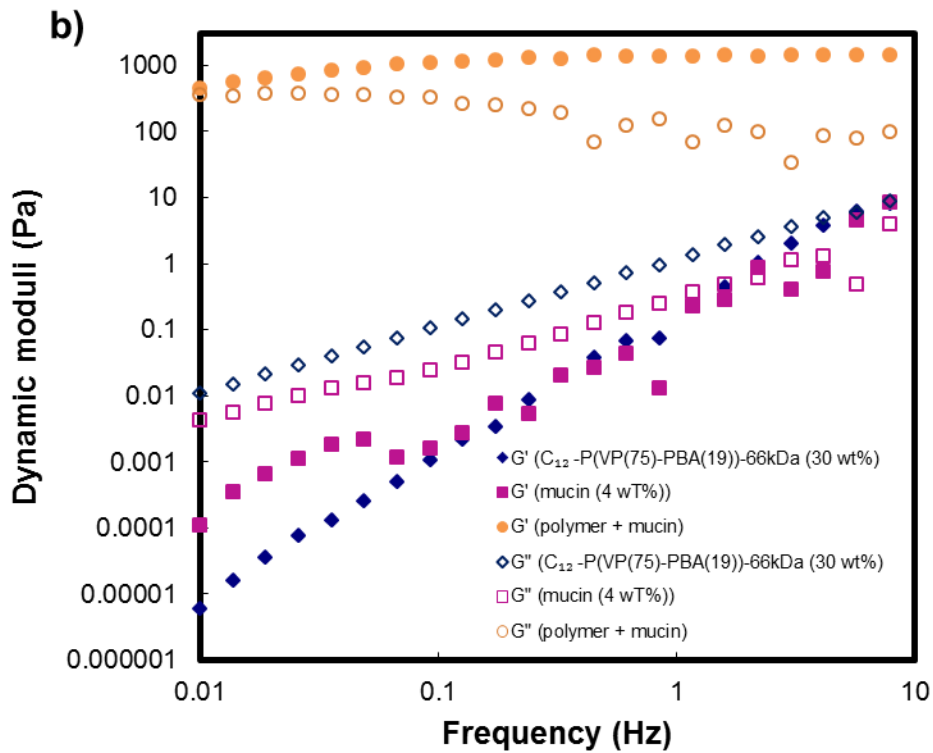
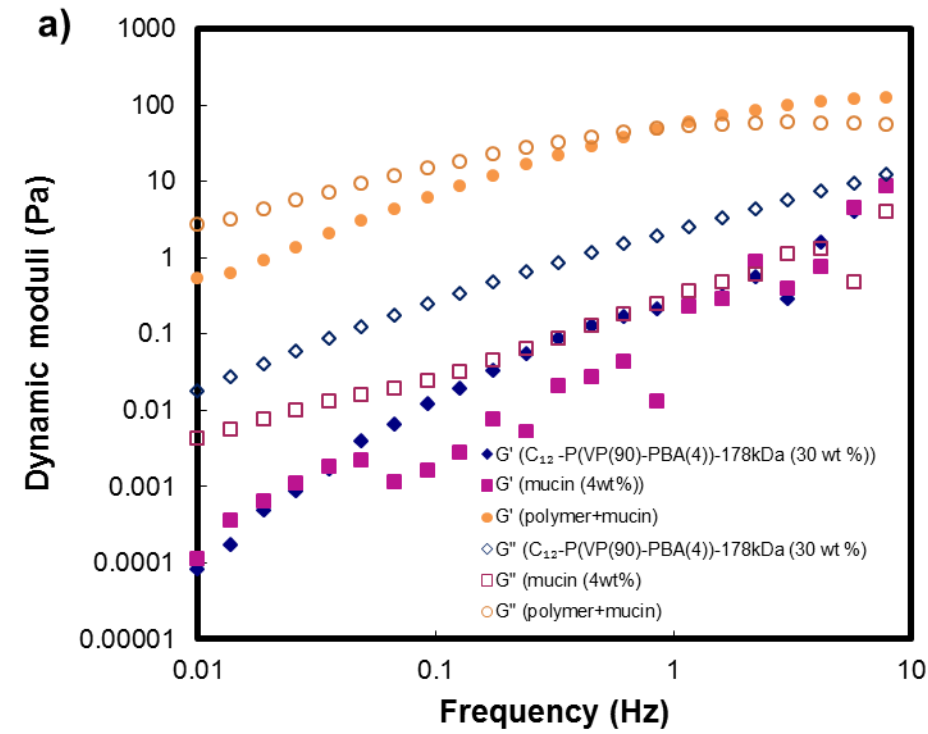
**Figure 3-7-**Viscosity versus shear rate of dual C<sub>x</sub>-PBA grafted C12-P (VP-PBA) polymers with different PBA contents

Polymers with 5, 13 and 19 mole% PBA conjugated on their backbone all show effectively the same viscosity profile over the full range of shear rates tested, confirming the independence of PBA content and polymer solution viscosity in these dual-grafted polymers. Thus, the solution viscosity can be tuned by changing the hydrophobe properties relatively independently of the presence of PBA groups, offering potential to tune mucoadhesivity (via PBA content) largely

independently of polymer rheology. This independence is highly beneficial in the design of artificial tear solutions targeting different residence times at the ocular surface, as the adhesive interaction (influencing only residence time) can be decoupled from the rheological properties influencing both residence time and lubricity upon blinking (and thus patient comfort).

### 3.3.6 Mucoadhesion

The capacity of the dual  $C_x$ -PBA grafted polymers to exhibit mucoadhesive properties was measured using the method of rheological synergism, in which non-linear increases in elastic modulus (or any modulus) observed when the polymer and mucin are mixed in a single solution relative to the moduli of those two components measured alone in solution can be related to the magnitude of intermolecular interactions that can occur. Figure 3- 8 shows representative examples of such experiments for two dual  $C_x$ -PBA grafted polymers and one ungrafted polymer; data for other polymers tested is provided in Appendix C, Figure C 1.



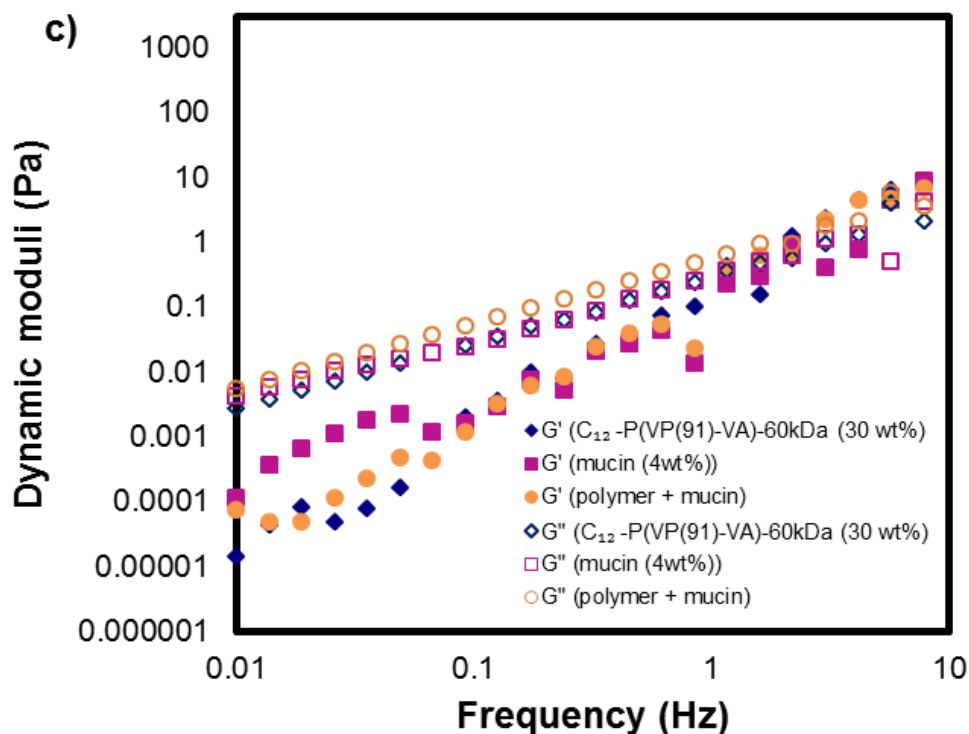


**Figure 3- 8**-Examples of dynamic oscillation responses of dual  $C_x$ -PBA grafted polymers for a) a polymer with low PBA content ( $C_{12}$ -P(VP(90)-PBA(4))-178kDa) and b) a polymer with high PBA content ( $C_{12}$ -P(VP(75)-PBA(19))-66kDa) and c) a polymer with no PBA conjugation ( $C_{12}$ -P(VP(75)-VA)-66kDa)

From the data for both  $G'$  and  $G''$ , a clear increase in both elastic and loss moduli can be observed when the polymer and mucin are mixed together relative to the polymer and mucin measured individually that exceeds the modulus value that would result by adding together the two individual component responses. As a result, some degree of rheological synergism is observed in these systems. Based on the magnitudes and shapes of both  $G'$  and  $G''$  responses as a function of frequency, the type and strength of mixture of polymer-mucin can be inferred. Polymers with higher molecular weights (Figure 3- 8 (a)) show much stronger frequency dependence of moduli, consistent with a more entangled network (i.e. physical cross-linking) in which polymers have sufficient time to reorient/untangle at lower shear (i.e. behave as a viscous

liquid) but not at higher shear (i.e. a more elastic response is observed). Alternately, the  $G'$  and  $G''$  profiles for the polymer lower molecular weights (Figure 3- 8 (b)) are less frequency-dependent, consistent with a more chemically cross-linked gel in which the interactions (bonds) are not shear-sensitive. Figure 3- 8 (c) confirms that PBA is the driving for the mucoadhesion observed for these polymers, as no mucoadhesive interaction is observed between the graft platform polymer and mucin prior to PBA grafting while strong mucoadhesion is observed following PBA grafting (Figure 3- 8 (b), representing the same graft platform polymer).

The  $\tan \delta$  data (representing the angular shift between the applied oscillatory force and the material response) confirms this interpretation (Figure 3- 9), with the significant observed decrease in  $\tan \delta$  in the polymer-mucin mixture indicative of the formation of a significantly more gel-like structure and thus intermolecular interactions between the dual grafted polymers and mucin.

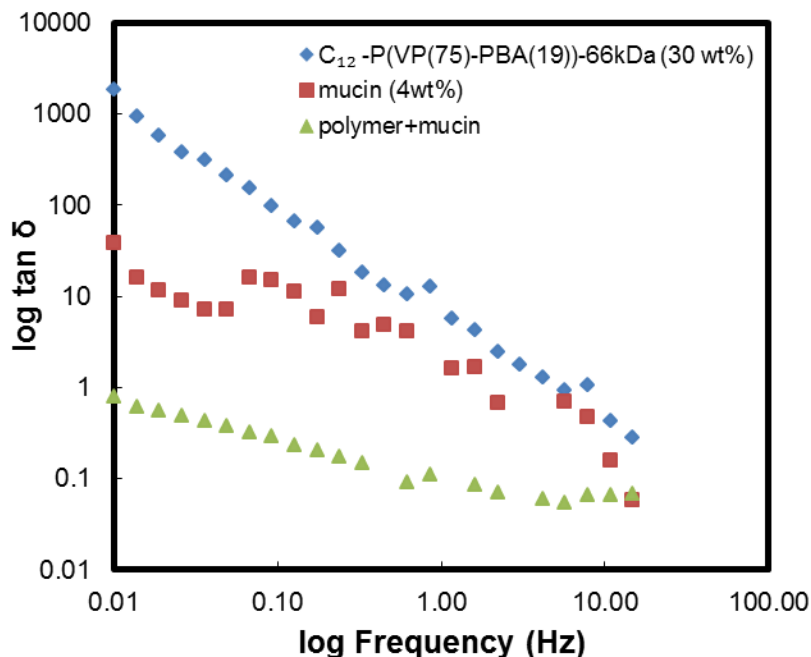


**Figure 3- 9** -  $\tan \delta$  versus frequency profile for high-PBA content  $C_{12}$ -P(VP(75)-PBA(19))-66kDa) dual  $C_x$ -PBA grafted polymer (30 wt%) in the absence and presence of mucin (4 wt%)

Calculation of the excess modulus ( $\Delta G$ , Eq. 3-1 and 3-2) and the relative synergism parameter ( $\Delta G/G$ , Eq. 3-3 and 3-4) can quantify the extent of mucoadhesion in different dual grafted polymer systems. Figure 3- 10 shows representative results for excess modulus (Figure 3- 10 (a)) and relative synergism (Figure 3- 10 (b)) as a function of frequency for  $C_{12}$ -P(VP(75)-PBA(18.8))-66kDa.

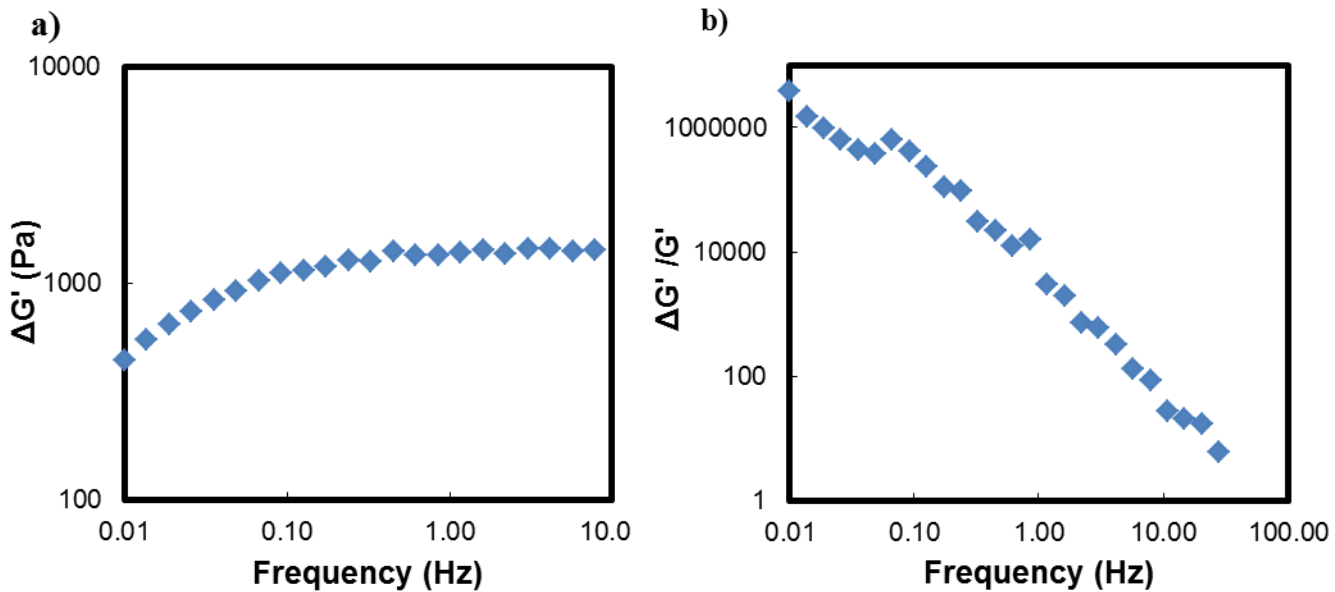
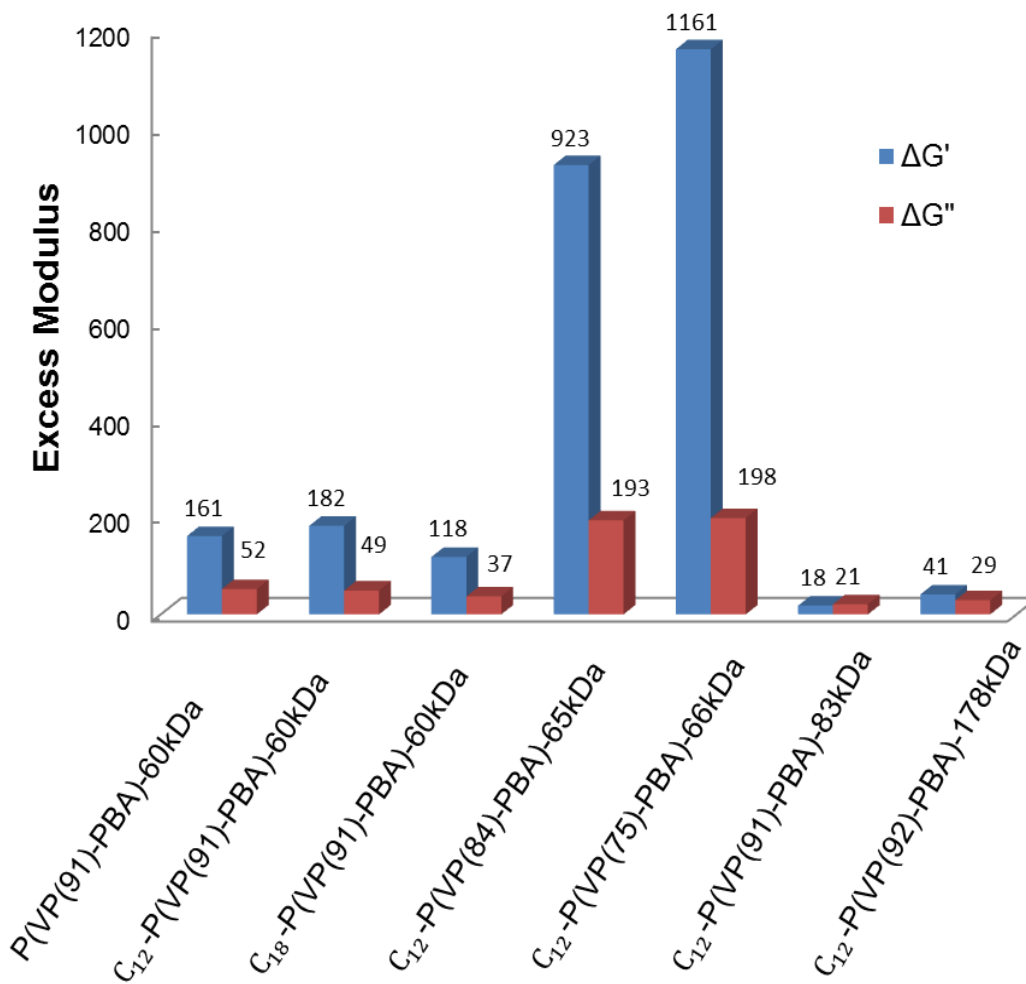


**Figure 3- 10** – Representative example of a) excess storage modulus and (b) relative synergism parameter or  $C_{12}$ -P(VP(75)-PBA(19))-66kDa measured as a function of frequency for dual  $C_x$ -PBA grafted polymers

Significant synergism is observed for all the polymers, with positive  $\Delta G'$  values and relative synergism values measured over the entire tested frequency range in each dual grafted  $C_x$ -PBA tested. Importantly, the magnitude of the synergism increases at lower frequencies relative to higher frequencies (Figure 3- 10 (b)), indicating the potential for improved retention of the polymer upon blinking (by viscosity build-up) without sacrificing the lubricity of the polymer at higher shear across all samples tested.

To facilitate comparisons of the degree of synergism between different samples, the mean modulus value was calculated as the geometric average of all 23 points of  $G'$  and  $G''$  obtained over the frequency range of 0.01-15 Hz [139], a range that typically represents a plateau modulus measurement in these materials. Figure 3- 11(a) shows the excess modulus and Figure 3- 11 (b) relative synergism parameter for each dual  $C_x$ -PBA polymer tested, with the raw data from which these parameters are calculated (i.e.  $G'$ ,  $G''$ , and  $\tan \delta$  for each individual polymer and mucin-polymer mixture) available in APPENDIX D Table D 1.

a)



b)

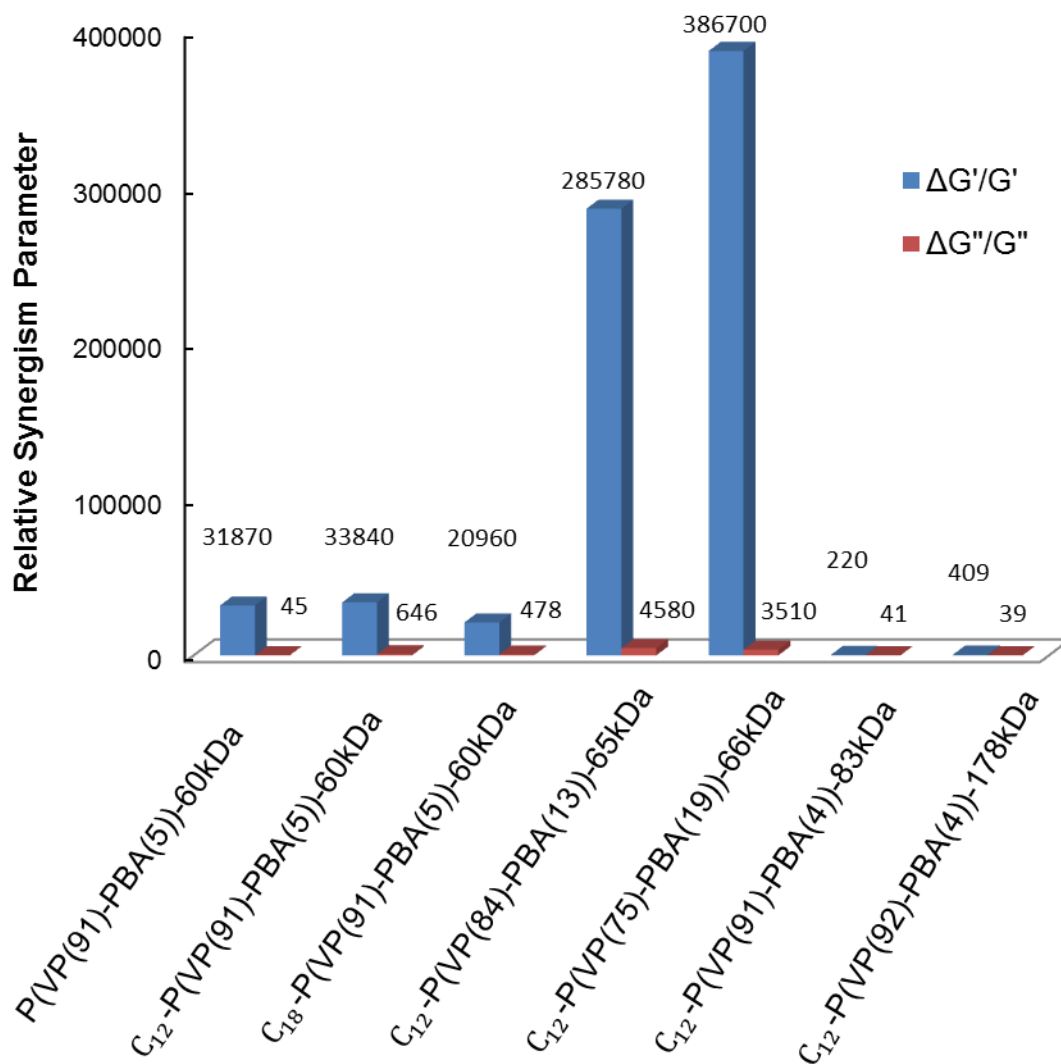


**Figure 3- 11** – Rheological synergism of polymer-mucin interactions: (a) excess modulus ( $\Delta G'$ , blue series, or  $\Delta G''$ , red series); (b) relative synergism parameter ( $\Delta G'/G'$ , blue series, or  $\Delta G''/G''$ , red series)

Two main conclusions can be drawn from this data. First, the excess elastic modulus is significantly higher than the excess loss modulus for all dual C<sub>x</sub>-PBA grafted polymers tested using the lower molecular weight (~60 kDa) graft platform (Figure 3- 11(a)), a trend duplicated in the relative synergism results (Fig. 3-9 (b)). This suggests that the presence of mucin

primarily contributes to enhancing the elastic modulus of the dual-grafted polymer solutions, consistent with covalent bond formation between PBA residues and mucin. This conclusion is further supported by the raw  $\tan \delta$  data given that the  $\tan \delta$  values are all less than one (the threshold for gel formation) once polymer and mucin is mixed (Table D 1). However, for the higher molecular weight graft platforms, the excess elastic and loss moduli are similar to each other and much smaller than analogous results for the lower molecular weight graft platform, a result we hypothesize is related to the increased potential of hydrophobic intramolecular interactions in higher molecular weight polymers that limits the accessibility of PBA groups for mucin-polymer interactions. This result suggests that the lower molecular weight graft platform is highly beneficial in terms of promoting mucoadhesion; when coupled with the higher degree of shear thinning achieved with this graft platform (Figure 3- 6) as well as the potential additional benefits of improved clearance following lachrymal drainage, using a lower molecular weight graft platform will be pursued for the design of artificial tear formulations.

Second, a very strong dependence of the PBA content of the polymer is observed on the mucoadhesion response. Increasing the PBA content of the dual-grafted polymers from 5 mole% to 13 mole% results in a nearly 5-fold increase in the excess elastic modulus, while a further increase to 19 mole% PBA yields a nearly 7-fold increase in excess elastic modulus (Figure 3- 11(a)). A similar and even more dramatic result is observed with the relative synergism parameter, which increases by nearly one order of magnitude when the PBA content is increased from 5 mole% to 13 mole% and over one order of magnitude upon a further increase in PBA concentration to 19 mole% (Figure 3- 11 (b)). Thus, there is a significant benefit to increasing the PBA content of the polymer, with the higher density of available functional groups able to more effectively form multiple bonds with *cis*-diol groups of mucin glycoproteins; alternately, it

is also possible that the increased PBA density increases the probability that each PBA residue is not only attached to the polymer backbone via a secondary amine (reducing the  $pK_a$  due to inductive effects) but also close geometrically to residual primary amine groups or other secondary amine bonds, providing further inductive effects to reduce the  $pK_a$  of the PBA groups thus increase the percentage of PBA residues in their stronger-binding, more mucoadhesive trigonal form at physiological pH (Figure 3- 1). The magnitude of rheological synergism reported for these polymers is significantly stronger than that reported in the literature even for other polymers recognized to be mucoadhesive; for example, excess elastic moduli of up to 1150 can be achieved with dual  $C_x$ -PBA grafted polymers while excess moduli of 140 have been reported for lightly cross-linked poly(acrylic acid) polymers commonly used as effective mucoadhesives[38].

### 3.4 Conclusion

Dual hydrophobe-boronic acid grafted copolymers based on a poly(vinylpyrrolidone-co-vinylformamide) graft platform polymer offer significant potential as artificial tear additives. The concentration of both grafts (4-formylphenylboronic acid and  $C_{12}$  or  $C_{18}$  alkyl halides) on the graft platform copolymers can be independently controlled, as can the molecular weight of the graft platform used. The dual  $C_x$ -PBA polymers have transparencies of  $>90\%$  in the visible wavelength range (a suitable result for a 1 cm path length evaluation when the tear film thickness is only 0.01 cm) and have similar refractive indices to the cornea even at high (15 wt%) polymer concentrations, suggesting these polymers may be used without any significant disruption or distortion of vision. Rheology results indicate that the presence of the PBA groups have no significant influence on the shear thinning properties of the polymers (facilitating independent tuning of mucoadhesion via PBA content and lubricity upon blinking via shear thinning),

although lower molecular weight polymers are preferable given their improved shear thinning performance (i.e. significantly lower infinite shear viscosity and similar low-shear viscosities to polymers prepared using the higher molecular weight graft platform). Mucoadhesion results via rheological synergism measurements indicated a similar advantage to the use of the low molecular weight graft platform, with significant mucoadhesion observed at even 5 mole% PBA for a ~60 kDa graft platform but minimal mucoadhesion observed for the ~85 kDa and ~180 kDa graft platforms with the same PBA content. Increasing the PBA content to ~19 mole% enhances this mucoadhesion by approximately one order of magnitude, mucoadhesion at least on par and in some cases significantly better than some of the best performing mucoadhesive polymers reported [38]. As such, the favourable optical, rheological, and mucoadhesive properties of dual C<sub>x</sub>-PBA grafted polymers make these polymers highly relevant to the design of artificial tear formulations with higher residence times (and thus higher drug bioavailabilities if they are used as drug carriers) without compromising the excellent lubricity that is essential for patient comfort.

## **4-Conclusions and Recommendations**

## 4.1 Part I

### 4.1.1 Conclusions

- POEGMA-co-AA hyperbranched polymers were synthesized using the Strathclyde methodology using 1-dodecanethiol as the chain transfer and ethylene glycol dimethacrylate as the cross-linker
- Optimization of the recipe was pursued to generate hyperbranched polymers with the maximum possible amount of EGDMA (cross-linking) and DDT (hydrophobes) while maintaining aqueous solubility
- The hydrophobic chain transfer agent imparts shear thinning properties to these polymers in a manner that is relatively independent of the cross-linker and chain transfer agent concentrations used in the polymer recipe, with reduced shear thinning only observed at extremely high (>6 mole%) cross-linker contents
- Hyperbranched polymers prepared with higher EGDMA contents can be dually effective as tear substitute materials by both increasing the molecular weight (increasing the viscosity) and decreasing the size of the hyperbranched units (lower light scattering)
- Single-pass filtration of samples eliminates less than 10% of the total sample mass (i.e. the larger microgel-like particles) while increasing transparency of a high concentration solution from less than 30% to more than 90% at 600 nm wavelength
- Dilution does not significantly reduce the viscosity of the polymers at low shear rates, making them ideal for highly diluting environment of the eye
- Mixing DDT-terminated hyperbranched polymers with hydrophobically modified linear PVP polymers results in polymer solutions with significantly higher infinite shear

viscosities than achieved with either component alone, potentially useful to enhance ocular retention time during blinking without changing molecular weight

- Mixing cyclodextrin functionalized, DDT-terminated hyperbranched polymers with hydrophobically modified linear polymers generates stiff gel materials at low shear rates due to inclusion complex formation between the hydrophobic groups of linear polymers and the hydrophobic cavity of cyclodextrin

#### 4.1.2 Recommendation

- Mixing PVP polymer that is not hydrophobically grafted (or hydrolyzed, so there is no charge) with CD grafted polymers is important to confirm that the interactions are due to the hydrophobes and not just interaction between PVP and POEGMA chain units
- Measuring the viscosity of different concentrations of polymer 35 solutions is important to confirm that the effect of dilution is consistent for all the polymers (given that P35 appears to be the optimized polymer)

## 4.2 Part II

### 4.2.1 Conclusion

- Dual functionalized water soluble polymers are made via copolymerization of NVP and NVF followed by basic hydrolysis of formamide groups to provide the platform needed for the subsequent grafting of hydrophobic alkyl groups and phenylboronic acid mucoadhesive groups.
- Polymer solutions have transparencies above >90% in the visible wavelength range and refractive indices close to the cornea even at high concentrations of 15 wt%

- Cytotoxicity studies using human corneal epithelial cells exposed to concentrations of dual grafted material suggested these materials exhibit no significant cytotoxicity
- PBA grafting has no significant effect on the shear thinning or rheological characteristics of these polymers
- The positive relative synergism seen for polymers confirms the mucoadhesion properties of these polymers, with lower degrees of mucoadhesion observed with higher molecular weight (~85 kDa and ~180 kDa) polymers compared to lower molecular weight polymers
- Increasing the PBA content to ~19 mole% enhances this mucoadhesion by approximately one order of magnitude

#### 4.2.2 Recommendation

- Grafting longer alkyl chain lengths and/or no alkyl chains on the high PBA (13 mole % and 19 mole %) content polymers to confirm the consistency of results shown for lower PBA content polymers
- Given the highly diluting nature of the tear film and low concentration of mucin in the eye, a dilution assay has to be done to ensure these polymers are able to maintain their mucoadhesive properties even at low concentrations
- *In vivo* assessment of the use of these polymers for dry eye treatment in rabbits should be done to confirm the biocompatibility of the polymers on the ocular surface
- Fluorescently labeling the polymers will be pursued to track retention time at the ocular surface via fluorescence analysis as a function of time
- Isothermal titration calorimetry will be used to measure the enthalpy/entropy of the binding interaction between the dual grafted polymers and mucin

**References:**

- [1] W. M. Saltzman, “Drug Delivery: Engineering Principles for Drug Therapy,” Oxford University Press, p. 384, 2001.
- [2] “Implantable Drug Delivery Devices—An Overview.” [Online]. Available: <http://www.mdtmag.com/articles/2013/07/implantable-drug-delivery-devices%E2%80%9494-overview>. [Accessed: 25-Oct-2014].
- [3] “The Eyes (Human Anatomy): Diagram, Optic Nerve, Iris, Cornea, Pupil, & More.” [Online]. Available: <http://www.webmd.com/eye-health/picture-of-the-eyes>. [Accessed: 25-Oct-2014].
- [4] A. K. Agrawal, M. Das, and S. Jain, “In situ gel systems as ‘ smart ’ carriers for sustained ocular drug delivery,” *J. Expert Opin. drug Deliv.*, pp. 383–402, 2012.
- [5] D. Achouri, K. Alhanout, P. Piccerelle, and V. Andrieu, “Recent advances in ocular drug delivery.,” *Drug Dev. Ind. Pharm.*, vol. 39, no. 11, pp. 1599–617, Nov. 2013.
- [6] S. Mishima, A. Gasset, J. Klyce, S. D., and J. L. Baum, “Determination of Tear Volume and Tear Flow,” *Invest. Ophthalmol. Vis. Sci.*, vol. 5, no. 3, pp. 264–276, Jun. 1966.
- [7] T. P. Johnston, C. S. Dias, H. Alur, and A. K. Mitra, “Mucoadhesive polymers in ophthalmic drug delivery,” in *Ophthalmic Drug Delivery Systems, Second Edition*, A. K. Mitra, Ed. 2003, pp. 409–35.
- [8] R. Gaudana, H. K. Ananthula, A. Parenky, and A. K. Mitra, “Ocular drug delivery.,” *AAPS J.*, vol. 12, no. 3, pp. 348–60, Sep. 2010.
- [9] D. Ghate and H. F. Edelhauser, “Ocular drug delivery.,” *Expert Opin. Drug Deliv.*, vol. 3, no. 2, pp. 275–87, Mar. 2006.
- [10] J. Greaves and C. Wilson, “Treatment of diseases of the eye with mucoadhesive delivery systems,” *Adv. Drug Deliv. Rev.*, pp. 349–383, 1993.
- [11] A. J. W. Huang, C. G. Tseng, and K. R. Kenyont, “Paracellular Permeability of Corneal and Conjunctival Epithelia,” *Invest. Ophthalmol. Vis. Sci.*, vol. 30, no. 4, pp. 648–9, 1989.
- [12] J. W. Shell, “Ophthalmic drug delivery systems.,” *Surv. Ophthalmol.*, vol. 29, no. 2, pp. 117–28, 1984.

- [13] H. Brewitt and F. Sistani, "Dry eye disease: the scale of the problem.," *Surv. Ophthalmol.*, vol. 45 Suppl 2, no. March, pp. S199–202, Mar. 2001.
- [14] M. B. Sintzel, S. F. Bernatchez, C. Tabatabay, and R. Gurny, "Biomaterials in ophthalmic drug delivery," *Eur. J. Pharm. Biopharm.*, vol. 42, no. 6, pp. 358–374, 1996.
- [15] J.-M. Korte, T. Kaila, and K. M. Saari, "Systemic bioavailability and cardiopulmonary effects of 0.5% timolol eyedrops.," *Graefes Arch. Clin. Exp. Ophthalmol.*, vol. 240, no. 6, pp. 430–5, Jun. 2002.
- [16] V. Pooniya and N. Pandey, "Systemic toxicity of topical cyclopentolate eyedrops in a child.," *Eye (The Sci. J. R. Coll. Ophthalmologists)*, vol. 26, no. 10, pp. 1391–2, Oct. 2012.
- [17] P. N. Dilly, "Structure and function of the tear film," *Adv. Exp. Med. Biol.* 350,, vol. 350, pp. 239–47, 1994.
- [18] E. Wolff, *Eugene Wolff's Anatomy of the Eye and Orbit*, 7th ed. Philadelphia: W. B. Saunders, 1976, p. 545.
- [19] S. Dikstein and B. Street, "Eyedrops having non-Newtonian rheological properties," US51066151992.
- [20] M. F. Saettone, M. Bucci, and P. Speiser, Eds., *Ophthalmic Drug Delivery*. New York, NY: Springer New York, 1987.
- [21] G. Meseguer, P. Buri, B. Plazonnet, A. Rozier, and R. Gurny, "Gamma scintigraphic comparison of eyedrops containing pilocarpine in healthy volunteers.," *J. Ocul. Pharmacol. Ther.*, vol. 12, no. 4, pp. 481–8, Jan. 1996.
- [22] R. Herrero-Vanrell, A. Fernandez-Carballido, G. Frutos, and R. Cadórniga, "Enhancement of the mydriatic response to tropicamide by bioadhesive polymers.," *J. Ocul. Pharmacol. Ther.*, vol. 16, no. 5, pp. 419–28, Oct. 2000.
- [23] A. Patel, "Ocular drug delivery systems: An overview," *World J. Pharmacol.*, vol. 2, no. 2, p. 47, 2013.
- [24] U. B. Kompella, R. S. Kadam, and V. H. L. Lee, "Recent advances in ophthalmic drug delivery.," *Ther. Deliv.*, vol. 1, no. 3, pp. 435–56, Sep. 2010.
- [25] F. Seattone, "Evaluation of ocular permeation chnacers: in vitro effects on corneal transport of four B-blockers, and in vitro/in vivo toxic activity," *Int. J. Pharm.*, vol. 142, pp. 103–113, 1996.

- [26] A. Ahuja, R. K. Khar, and J. Ali, "Mucoadhesive Drug Delivery Systems," *Drug Dev. Ind. Pharm.*, vol. 23, no. 5, pp. 489–515, 1997.
- [27] V. V Khutoryanskiy, "Advances in mucoadhesion and mucoadhesive polymers.," *Macromol. Biosci.*, vol. 11, no. 6, pp. 748–64, Jun. 2011.
- [28] N. a Peppas and J. J. Sahlin, "Hydrogels as mucoadhesive and bioadhesive materials: a review.," *Biomaterials*, vol. 17, no. 16, pp. 1553–61, Aug. 1996.
- [29] X. Yang, K. Forier, L. Steukers, S. Van Vlierberghe, P. Dubruel, K. Braeckmans, S. Glorieux, and H. J. Nauwynck, "Immobilization of pseudorabies virus in porcine tracheal respiratory mucus revealed by single particle tracking.," *PLoS One*, vol. 7, no. 12, p. e51054, Jan. 2012.
- [30] B. Govindarajan and I. K. Gipson, "Membrane-tethered mucins have multiple functions on the ocular surface," *Exp Eye Res.*, vol. 90, no. 6, pp. 655–663, 2010.
- [31] S. K. Lai, Y.-Y. Wang, and J. Hanes, "Mucus-penetrating nanoparticles for drug and gene delivery to mucosal tissues.," *Adv. Drug Deliv. Rev.*, vol. 61, no. 2, pp. 158–71, Feb. 2009.
- [32] J. W. Lee, J. H. Park, and J. R. Robinson, "Bioadhesive-based dosage forms: the next generation.," *J. Pharm. Sci.*, vol. 89, no. 7, pp. 850–66, Jul. 2000.
- [33] R. Gurny, J. M. Meyer, and N. a Peppas, "Bioadhesive intraoral release systems: design, testing and analysis.," *Biomaterials*, vol. 5, no. 6, pp. 336–40, Nov. 1984.
- [34] D. Duchene, F. Touchard, and N. A. Peppas, "Pharmaceutical and Medical Aspects of Bioadhesive Systems for Drug Administration," *Drug Dev. Ind. Pharm.*, vol. 14, no. 2&3, pp. 283–318, 1988.
- [35] R. M. Barrer, J. a. Barrie, and P. S.-L. Wong, "The diffusion and solution of gases in highly crosslinked copolymers," *Polymer (Guildf).*, vol. 9, pp. 609–627, Jan. 1968.
- [36] A. Ludwig, "The use of mucoadhesive polymers in ocular drug delivery.," *Adv. Drug Deliv. Rev.*, vol. 57, no. 11, pp. 1595–639, Nov. 2005.
- [37] H. Park and J. R. Robinson, "Phusico-chemical properties of water insoluble polymers important to mucin/epithelial adhesion," *J. Control. release*, vol. 2, pp. 47–57, 1985.

- [38] F. Madsen, K. Eberth, and J. D. Smart, "A rheological assessment of the nature of interactions between mucoadhesive polymers and a homogenised mucus gel," *Biomaterials*, vol. 19, pp. 1083–1092, 1998.
- [39] G. S. Asane, S. a Nirmal, K. B. Rasal, a a Naik, M. S. Mahadik, and Y. M. Rao, "Polymers for mucoadhesive drug delivery system: a current status.," *Drug Dev. Ind. Pharm.*, vol. 34, no. 11, pp. 1246–66, Nov. 2008.
- [40] C.-M. Lehr, F. G. J. Poelma, H. E. Junginger, and J. J. Tukker, "An estimate of turnover time of intestinal in the rat in situ loop," *Int. J. Pharm.*, vol. 70, pp. 235–240, 1991.
- [41] J. R. Robinson and G. M. Mlynek, "Bioadhesive and phase-change polymers for ocular drug delivery," *Adv. Drug Deliv. Rev.*, vol. 16, pp. 45–50, 1995.
- [42] C. Gilles, "Liquid aqueous ophthalmic composition undergoing liquid-gel phase transition," European Patent EP04240431991.
- [43] Bawa, "Gelling ophthalmic compositions containing xanthan gum," US Patent US 61745242001.
- [44] J. G. Souza, K. Dias, T. A. Pereira, D. S. Bernardi, and R. F. V Lopez, "Topical delivery of ocular therapeutics: carrier systems and physical methods.," *J. Pharm. Pharmacol.*, vol. 66, no. 4, pp. 507–30, Apr. 2014.
- [45] M. F. Saettone, M. T. Torracca, B. Giannaccini, and S. Burgalassi, "Evaluation of muco-adhesive properties and in vivo activity of ophthalmic vehicles based on hyaluronic acid," *Int. J. Pharm.*, vol. 51, pp. 203–212, 1989.
- [46] S. Wadhwa, R. Paliwal, S. R. Paliwal, and S. P. Vyas, "Hyaluronic acid modified chitosan nanoparticles for effective management of glaucoma: development, characterization, and evaluation.," *J. Drug Target.*, vol. 18, no. 4, pp. 292–302, May 2010.
- [47] L. K. Widjaja, M. Bora, P. N. P. H. Chan, V. Lipik, T. T. L. Wong, and S. S. Venkatraman, "Hyaluronic acid-based nanocomposite hydrogels for ocular drug delivery applications.," *J. Biomed. Mater. Res. A*, vol. 102, no. 9, pp. 3056–65, Sep. 2014.
- [48] K. Kyyronen and A. Urrri, "Improved Ocular : Systemic Absorption Ratio of Timolol by Viscous Vehicle and Phenylephrine," *Invest. Ophthalmol. Vis. Sci.*, vol. 31, no. 9, pp. 1827–1833, 1990.

- [49] I. Henriksen, K. L. Green, J. D. Smart, G. Smista, and J. Karlsen, "International journal of pharmaceutics Bioadhesion of hydrated chitosans : an in vitro and in vivo study," *Int. J. Pharm.*, vol. 145, pp. 231–240, 1996.
- [50] P. He, S. S. Davis, and L. Illum, "In vitro evaluation of the mucoadhesive properties of chitosan microspheres," *Int. J. Pharm.*, vol. 166, pp. 75–88, 1998.
- [51] I. Genta, B. Conti, P. Perugini, F. Pavanetto, A. Spadaro, and G. Puglisi, "Bioadhesive Microspheres for Ophthalmic Administration of Acyclovir," *J. Pharm. Pharmacol.*, vol. 49, no. 8, pp. 737–742, 1997.
- [52] J. D. Smart, I. W. Kellaway, and H. E. C. Worthington, "An in-vitro investigation of mucosa-adhesive materials for use in controlled drug delivery," *J. Pharm. Pharmacol.*, vol. 36, no. 5, pp. 295–299, 1984.
- [53] C. A. Le Boursais, F. Chevanne, B. Turlin, L. Acar, H. Zia, P. A. Sado, T. E. Needham, and R. Leverage, "Effect of cyclosporine A formulations on bovine corneal absorption: ex-vivo study," *J. Microencapsul.*, vol. 14, no. 4, pp. 457–467, 1997.
- [54] D. Miller, *Ophthalmology: The Essentials*. Boston: Houghton Mifflin Professional Publishers, 1979.
- [55] T. Hoare and R. Pelton, "Charge-Switching, Amphoteric Glucose-Responsive Microgels with Physiological Swelling Activity," *Biomacromolecules*, vol. 9, no. 2, pp. 733–740, 2008.
- [56] T. Hoare and R. Pelton, "Engineering Glucose Swelling Responses in Poly (N - isopropylacrylamide)-Based Microgels," *Macromolecules*, vol. 40, no. 3, pp. 670–678, 2007.
- [57] H. Otsuka, E. Uchimura, H. Koshino, T. Okano, K. Kataoka, and T. Uni, "Anomalous Binding Profile of Phenylboronic Acid with N-Acetylneuraminic Acid ( Neu5Ac ) in Aqueous Solution with Varying pH," *J. Am. Chem. Soc.*, vol. 125, no. 9, pp. 3493–3502, 2003.
- [58] A. Matsumoto, H. Cabral, N. Sato, K. Kataoka, and Y. Miyahara, "Assessment of tumor metastasis by the direct determination of cell-membrane sialic acid expression," *Angew. Chem. Int. Ed. Engl.*, vol. 49, no. 32, pp. 5494–7, Jul. 2010.
- [59] A. E. Ivanov, L. Nilsson, I. Y. Galaev, and B. Mattiasson, "Boronate-containing polymers form affinity complexes with mucin and enable tight and reversible

- occlusion of mucosal lumen by poly(vinyl alcohol) gel.," *Int. J. Pharm.*, vol. 358, no. 1–2, pp. 36–43, Jun. 2008.
- [60] N. System, L. Zhu, S. H. Shabbir, M. Gray, V. M. Lynch, S. Sorey, and E. V. Anslyn, "A Structural Investigation of the N - B Interaction in an o-(N, N-Dialkylaminomethyl)arylboronate System," *J. Am. Chem. Soc.*, vol. 128, no. 31, pp. 1222–1232, 2006.
- [61] W. Chen, C. Lu, and R. Pelton, "Polyvinylamine Boronate Adhesion to Cellulose Hydrogel," *Biomacromolecules*, vol. 7, no. 3, pp. 701–702, 2006.
- [62] W. Chen, V. Leung, H. Kroener, and R. Pelton, "Polyvinylamine-phenylboronic acid adhesion to cellulose hydrogel.," *Langmuir*, vol. 25, no. 12, pp. 6863–8, Jun. 2009.
- [63] S. Soundararajan, M. Badawi, C. Montano Kohlrust, and J. H. Hageman, "Boronic Acids for Affinity Chromatography : Spectral Methods for Determinations of Ionization and Diol-Binding Constants," *Anal. Biochem.*, vol. 178, pp. 125–134, 1989.
- [64] C. R. Yates and W. Hayes, "Synthesis and applications of hyperbranched polymers," *Eur. Polym. J.*, vol. 40, no. 7, pp. 1257–1281, Jul. 2004.
- [65] G. L. Drisko, L. Cao, M. C. Kimling, S. Harrisson, V. Luca, and R. A. Caruso, "Pore size and volume effects on the incorporation of polymer into macro- and mesoporous zirconium titanium oxide membranes.," *ACS Appl. Mater. Interfaces*, vol. 1, no. 12, pp. 2893–901, Dec. 2009.
- [66] B. Voit, "New developments in hyperbranched polymers," *J. Polym. Sci. Part A Polym. Chem.*, vol. 38, no. 14, pp. 2505–2525, Jul. 2000.
- [67] H. Jin, W. Huang, X. Zhu, Y. Zhou, and D. Yan, "Biocompatible or biodegradable hyperbranched polymers: from self-assembly to cytomimetic applications.," *Chem. Soc. Rev.*, vol. 41, no. 18, pp. 5986–97, Sep. 2012.
- [68] R. H. Kienkle, P. A. Van Der Meulen, and F. E. Petke, "The Polyhydric Alcohol-Polybasic Acid Reaction. IV. Glyceryl Phthalate from Phthalic Acid," *J. Am. Chem. Soc.*, vol. 61, no. 9, pp. 2268–2271, 1939.
- [69] L. J. Mathias and T. W. Carothers, "Hyperbranched Poly(siloxysilanes)," *J. Am. Chem. Soc.*, vol. 113, pp. 4043–4044, 1991.

- [70] J. F. Miravet and J. M. J. Fre, "New Hyperbranched Poly(siloxysilanes): Variation of the Branching Pattern and End-Functionalization," *Macromolecules*, vol. 31, no. 11, pp. 3461–3468, 1998.
- [71] J. M. Fréchet, M. Henmi, I. Gitsov, S. Aoshima, M. R. Leduc, and R. B. Grubbs, "Self-condensing vinyl polymerization: an approach to dendritic materials.," *Science*, vol. 269, no. 5227, pp. 1080–3, Aug. 1995.
- [72] N. M. B. Smeets, "Amphiphilic Hyperbranched Polymers from the copolymerization of a vinyl and divinyl monomer: The Potential of Catalytic Chain Transfer Polymerization," *Eur. Polym. J.*, vol. 49, no. 9, pp. 2528–2544, 2013.
- [73] N. O'Brien, a. McKee, D. C. Sherrington, a. T. Slark, and a. Titterton, "Facile, versatile and cost effective route to branched vinyl polymers," *Polymer (Guildf.)*, vol. 41, no. 15, pp. 6027–6031, Jul. 2000.
- [74] M. Antonietti, C. Rosenauer, and W. Germany, "Properties of Fractal Divinylbenzene Microgels," *Macromolecules*, vol. 24, no. 11, pp. 3434–3442, 1991.
- [75] R. C. Nagarwal, S. Kant, P. N. Singh, P. Maiti, and J. K. Pandit, "Polymeric nanoparticulate system: a potential approach for ocular drug delivery.," *J. Control. Release*, vol. 136, no. 1, pp. 2–13, May 2009.
- [76] H.-Y. Zhou, J.-L. Hao, S. Wang, Y. Zheng, and W.-S. Zhang, "Nanoparticles in the ocular drug delivery.," *Int. J. Ophthalmol.*, vol. 6, no. 3, pp. 390–6, Jan. 2013.
- [77] S. Liu, L. Jones, and F. X. Gu, "Nanomaterials for ocular drug delivery.," *Macromol. Biosci.*, vol. 12, no. 5, pp. 608–20, May 2012.
- [78] Y. Tong, S. Chang, C. Liu, and W. W. Kao, "Eye drop delivery of nano-polymeric micelle formulated genes with cornea-specific promoters," *J. Gene Med.*, vol. 9, no. 11, pp. 956–966, 2007.
- [79] A. Zimmer and J. Kreuter, "Microspheres and nanoparticles used in ocular delivery systems," *Adv. Drug Deliv. Rev.*, vol. 16, pp. 61–73, 1995.
- [80] E. Gavini, P. Chetoni, M. Cossu, M. G. Alvarez, M. F. Saettone, and P. Giunchedi, "PLGA microspheres for the ocular delivery of a peptide drug, vancomycin using emulsification/spray-drying as the preparation method: in vitro/in vivo studies.," *Eur. J. Pharm. Biopharm.*, vol. 57, no. 2, pp. 207–12, Mar. 2004.

- [81] A. M. De Campos, A. Sánchez, R. Gref, P. Calvo, and M. J. Alonso, "The effect of a PEG versus a chitosan coating on the interaction of drug colloidal carriers with the ocular mucosa.," *Eur. J. Pharm. Sci.*, vol. 20, no. 1, pp. 73–81, Sep. 2003.
- [82] C. Losa, L. Marchal-Heussler, F. Orallo, J. L. Vila Jato, and M. J. Alonso, "Design of new formulations for topical ocular administration: polymeric nanocapsules containing metipranolol.," *Pharm. Res.*, vol. 10, no. 1, pp. 80–7, Jan. 1993.
- [83] P. Calvo, A. Sanchez, J. Martinez, M. I. Lopez, M. Calonge, J. C. Pastor, and M. J. Alonso, "Polyester nanocapsules as new topical ocular delivery systems for cyclosporin A.," *Pharm. Res.*, vol. 13, no. 2, pp. 311–5, Feb. 1996.
- [84] R. Mainardes, M. Urban, P. Cinto, N. Khalil, M. Chaud, R. Evangelista, and M. Daflon Gremiao, "Colloidal Carriers for Ophthalmic Drug Delivery," *Curr. Drug Targets*, vol. 6, no. 3, pp. 363–371, May 2005.
- [85] R. Wood, "Ocular disposition of poly-hexyl-2-cyano[3-14C]acrylate nanoparticles in the albino rabbit," *Int. J. Pharm.*, vol. 23, no. 2, pp. 175–183, Feb. 1985.
- [86] A. Zimmer, J. Kreuter, and J. R. Robinson, "Studies on the transport pathway of PBCA nanoparticles in ocular tissues.," *J. Microencapsul.*, vol. 8, no. 4, pp. 497–504.
- [87] Y. Kadam, U. Yerramilli, and A. Bahadur, "Solubilization of poorly water-soluble drug carbamezapine in pluronic micelles: effect of molecular characteristics, temperature and added salt on the solubilizing capacity.," *Colloids Surf. B. Biointerfaces*, vol. 72, no. 1, pp. 141–7, Aug. 2009.
- [88] I. Pepić, N. Jalsenjak, and I. Jalsenjak, "Micellar solutions of triblock copolymer surfactants with pilocarpine.," *Int. J. Pharm.*, vol. 272, no. 1–2, pp. 57–64, Mar. 2004.
- [89] A. H. El-Kamel, "In vitro and in vivo evaluation of Pluronic F127-based ocular delivery system for timolol maleate.," *Int. J. Pharm.*, vol. 241, no. 1, pp. 47–55, Jul. 2002.
- [90] Z. Wang, Y. Itoh, Y. Hosaka, I. Kobayashi, Y. Nakano, I. Maeda, F. Umeda, J. Yamakawa, M. Kawase, and K. Yag, "Novel transdermal drug delivery system with polyhydroxyalkanoate and starburst polyamidoamine dendrimer.," *J. Biosci. Bioeng.*, vol. 95, no. 5, pp. 541–3, Jan. 2003.
- [91] Z. Wang, Y. Itoh, Y. Hosaka, I. Kobayashi, Y. Nakano, I. Maeda, F. Umeda, J. Yamakawa, M. Nishimine, T. Suenobu, S. Fukuzumi, M. Kawase, and K. Yagi,

- “Mechanism of enhancement effect of dendrimer on transdermal drug permeation through polyhydroxyalkanoate matrix.” *J. Biosci. Bioeng.*, vol. 96, no. 6, pp. 537–40, Jan. 2003.
- [92] Y. Diebold, M. Jarrín, V. Sáez, E. L. S. Carvalho, M. Orea, M. Calonge, B. Seijo, and M. J. Alonso, “Ocular drug delivery by liposome-chitosan nanoparticle complexes (LCS-NP).” *Biomaterials*, vol. 28, no. 8, pp. 1553–64, Mar. 2007.
- [93] N. Li, C. Zhuang, M. Wang, X. Sun, S. Nie, and W. Pan, “Liposome coated with low molecular weight chitosan and its potential use in ocular drug delivery.” *Int. J. Pharm.*, vol. 379, no. 1, pp. 131–8, Sep. 2009.
- [94] E. R. Gillies and J. M. J. Fréchet, “Dendrimers and dendritic polymers in drug delivery.” *Drug Discov. Today*, vol. 10, no. 1, pp. 35–43, Jan. 2005.
- [95] T. F. Vandamme and L. Brobeck, “Poly(amidoamine) dendrimers as ophthalmic vehicles for ocular delivery of pilocarpine nitrate and tropicamide.” *J. Control. Release*, vol. 102, no. 1, pp. 23–38, Jan. 2005.
- [96] S. Shaunak, S. Thomas, E. Gianasi, A. Godwin, E. Jones, I. Teo, K. Mireskandari, P. Luthert, R. Duncan, S. Patterson, P. Khaw, and S. Brocchini, “Polyvalent dendrimer glucosamine conjugates prevent scar tissue formation.” *Nat. Biotechnol.*, vol. 22, no. 8, pp. 977–84, Aug. 2004.
- [97] R. Iezzi, B. R. Guru, I. V Glybina, M. K. Mishra, A. Kennedy, and R. M. Kannan, “Dendrimer-based targeted intravitreal therapy for sustained attenuation of neuroinflammation in retinal degeneration.” *Biomaterials*, vol. 33, no. 3, pp. 979–88, Jan. 2012.
- [98] G. Spataro, F. Malecaze, C.-O. Turrin, V. Soler, C. Duhayon, P.-P. Elena, J.-P. Majoral, and A.-M. Caminade, “Designing dendrimers for ocular drug delivery.” *Eur. J. Med. Chem.*, vol. 45, no. 1, pp. 326–34, Jan. 2010.
- [99] C. Durairaj, R. S. Kadam, J. W. Chandler, S. L. Hutcherson, and U. B. Kompella, “Nanosized dendritic polyguanidilyated translocators for enhanced solubility, permeability, and delivery of gatifloxacin.” *Invest. Ophthalmol. Vis. Sci.*, vol. 51, no. 11, pp. 5804–16, Nov. 2010.
- [100] D. N. Schulz, J. J. Kaladas, J. J. Maurer, J. Beck, S. J. Pace, and W. W. Schulz, “Copolymers of acrylamide and surfactant macromonomers : synthesis and solution properties,” vol. 28, pp. 2110–2115, 1987.

- [101] L. M. Landoll, "Nonionic Polymer Surfactants," *J. Polym. Sci. Polym. Chem. Ed.*, vol. 20, pp. 443–455, 1982.
- [102] K. C. Taylor and H. A. Nasr-el-din, "Water-soluble hydrophobically associating polymers for improved oil recovery : A literature review," *J. Pet. Sci. Eng.*, vol. 19, pp. 265–280, 1998.
- [103] R. Tanaka, "Viscometric and Spectroscopic Studies on the Solution Behaviour of Hydrophobically Modified Cellulosic Polymers," *Carbohydr. Polym.*, vol. 12, pp. 443–459, 1990.
- [104] D. N. Schulz and J. Bock, "Synthesis and Fluid Properties of Associating Polymer Systems," *J. Macromol. Sci. Part A - Chem.*, vol. 28, no. 11–12, pp. 1235–1243, Nov. 1991.
- [105] C. L. McCormick, T. Nonaka, and C. B. Johnson, "aqueous solution behaviour of associative acrylamide / N-alkylacrylamide copolymers," *J. Polym.*, vol. 29, pp. 731–739, 1988.
- [106] J. Desbrières, C. Martinez, and M. Rinaudo, "Hydrophobic derivatives of chitosan: Characterization and rheological behaviour," *Int. J. Biol. Macromol.*, vol. 19, no. 1, pp. 21–28, Jul. 1996.
- [107] L. G. Butler, "Enzyme Immobilization Cellulose by Adsorption on Hydrophobic Derivatives and Other Hydrophilic Materials'," *Arch. Biochem. Biophys.*, vol. 171, pp. 645–650, 1975.
- [108] M. K. Arici, D. S. Arici, A. Topalkara, and C. Güler, "Adverse effects of topical antiglaucoma drugs on the ocular surface.," *Clin. Experiment. Ophthalmol.*, vol. 28, no. 2, pp. 113–7, Apr. 2000.
- [109] Y. Sakurai, K. Kataoka, F. Application, P. Data, and P. E. M. Nutter, "Physical trapping type polymeric micelle drug preparation," US 5449513 A1995.
- [110] M. Guvendiren, H. D. Lu, and J. a. Burdick, "Shear-thinning hydrogels for biomedical applications," *Soft Matter*, vol. 8, no. 2, p. 260, 2012.
- [111] T. Hoare, D. Zurakowski, R. Langer, and D. S. Kohane, "Rheological blends for drug delivery. I. Characterization in vitro.," *J. Biomed. Mater. Res. A*, vol. 92, no. 2, pp. 575–85, Feb. 2010.
- [112] P. Sheikholeslami, "Highly Shear-Thinning Mucoadhesive Hydrogels for Ophthalmic Applications," McMaster University, 2012.

- [113] M. Luzon, C. Boyer, C. Peinado, T. Corrales, M. Whittaker, L. E. I. Tao, and T. P. Davis, "Water-Soluble, Thermoresponsive, Hyperbranched Copolymers Based on PEG-Methacrylates: Synthesis, Characterization, and LCST Behavior," *J. Polym. Sci. Part A Polym. Chem.*, vol. 48, pp. 2783–2792, 2010.
- [114] M. Chisholm, N. Hudson, N. Kirtley, F. Vilela, and D. C. Sherrington, "Application of the 'Strathclyde Route' to Branched Vinyl Polymers in Suspension Polymerization: Architectural, Thermal, and Rheological Characterization of the Derived Branched Products," *Macromolecules*, vol. 42, no. 20, pp. 7745–7752, Oct. 2009.
- [115] P. Besenius, S. Slavin, F. Vilela, and D. C. Sherrington, "Synthesis and characterization of water-soluble densely branched glycopolymers," *React. Funct. Polym.*, vol. 68, no. 11, pp. 1524–1533, Nov. 2008.
- [116] R. Baudry and D. C. Sherrington, "Synthesis of Highly Branched Poly(methyl methacrylate)s Using the 'Strathclyde Methodology' in Aqueous Emulsion," *Macromolecules*, vol. 39, no. 4, pp. 1455–1460, Feb. 2006.
- [117] C. de Las Heras Alarcon, S. Pennadam, and C. Alexander, "Stimuli responsive polymers for biomedical applications," *Chem. Soc. Rev.*, vol. 34, no. 3, pp. 276–85, Mar. 2005.
- [118] T. Loftsson and M. E. Brewster, "Pharmaceutical Applications of Cyclodextrins . 1. Drug Solubilization and Stabilization," *J. Pharm. Sci.*, vol. 85, no. 10, pp. 1017–1025, 1996.
- [119] P. Jara, L. Barrientos, B. Herrera, and I. Sobrados, "Inclusion Compounds of  $\alpha$ -Cyclodextrin with Alkylthiols," *J. Chil. Chem. Soc.*, vol. 53, no. 2, pp. 1474–1476, 2008.
- [120] P. Jara, X. Canete, V. Lavayen, and N. Yutronic, "Inclusion Compounds of  $\alpha$  and  $\gamma$ -Cyclodextrin with n-alkylamine (n=12, 18)," *J. Chil. Chem. Soc.*, vol. 49, no. 3, pp. 241–243, Sep. 2004.
- [121] R. Challa, A. Ahuja, J. Ali, and R. K. Khar, "Cyclodextrins in Drug Delivery: An Updated Review," *AAPS PharmSciTech*, vol. 6, no. 2, pp. 329–357, 2005.
- [122] R. Mateen and T. Hoare, "Carboxymethyl and hydrazide functionalized  $\beta$ -cyclodextrin derivatives: a systematic investigation of complexation behaviours with the model hydrophobic drug dexamethasone," *Int. J. Pharm.*, vol. 472, no. 1–2, pp. 315–26, Sep. 2014.

- [123] Y. Dong, A. O. Saeed, W. Hassan, C. Keigher, Y. Zheng, H. Tai, A. Pandit, and W. Wang, “‘One-step’ Preparation of Thiol-Ene Clickable PEG-Based Thermoresponsive Hyperbranched Copolymer for In Situ Crosslinking Hybrid Hydrogel,” *Macromol. Rapid Commun.*, pp. 120–126, Dec. 2011.
- [124] H. C. Hulst and H. C. van de Hulst, *Light Scattering by Small Particles*. Courier Dover Publications, 1957, p. 470.
- [125] J. C. Lang, “Ocular drug delivery conventional ocular formulations,” *Adv. Drug Deliv. Rev.*, vol. 16, no. 1, pp. 39–43, Aug. 1995.
- [126] A. Urtti and L. Salminen, “Minimizing systemic absorption of topically administered ophthalmic drugs,” *Surv. Ophthalmol.*, vol. 37, no. 6, pp. 435–56.
- [127] A. Kumari, P. K. Sharma, V. K. Garg, and G. Garg, “Ocular inserts - Advancement in therapy of eye diseases,” *J. Adv. Pharm. Technol. Res.*, vol. 1, no. 3, pp. 291–6, Jul. 2010.
- [128] P. C. Nicolson and J. Vogt, “Soft contact lens polymers: an evolution,” *Biomaterials*, vol. 22, no. 24, pp. 3273–3283, Dec. 2001.
- [129] M. F. Saettone, D. Monti, M. T. Torracca, P. Chetoni, and B. Giannaccini, “Muco-Adhesive Liquid Ophthalmic Vehicles - Evaluation of Macromolecular Ionic Complexes of Pilocarpine,” *Drug Dev. Ind. Pharm.*, vol. 15, no. 14–16, pp. 2475–2489, Jan. 1989.
- [130] J. W. Wallace, “Cellulose derivatives and natural products utilized in pharmaceuticals,” in *Encyclopedia of Pharmaceutical Technology*, J. Swarbrick and J. C. Boylan, Eds. New York: Marcel Dekker, 1991, pp. 319–337.
- [131] H. Park and J. R. Robinson, “Mechanisms of Mucoadhesion of Poly(acrylic Acid) Hydrogels,” *Pharm. Res.*, vol. 4, no. 6, pp. 457–464, Dec. 1987.
- [132] R. D. Schoenwald and J. J. Boltralik, “A bioavailability comparison in rabbits of two steroids formulated as high-viscosity gels and reference aqueous preparations,” *Invest. Ophthalmol. Vis. Sci.*, vol. 18, no. 1, pp. 61–6, Jan. 1979.
- [133] N. A. Peppas and P. A. Buri, “Surface, interfacial and molecular aspects of polymer bioadhesion on soft tissues,” *J. Control. release*, vol. 2, pp. 257–275, 1985.
- [134] I. È. Kirsh and Y. E. Kirsh, *Water Soluble Poly-N-Vinylamides: Synthesis and Physicochemical Properties*. John Wiley & Sons, 1998, p. 233.

- [135] L. Gu, S. Zhu, and A. N. Hrymak, "Acidic and basic hydrolysis of poly(N-vinylformamide)," *J. Appl. Polym. Sci.*, vol. 86, no. 13, pp. 3412–3419, Dec. 2002.
- [136] R. J. Badesso, A. F. Nordquist, R. K. Pinschmidt, and D. J. Sagl, *Hydrophilic Polymers*, vol. 248. Washington, DC: American Chemical Society, 1996, pp. 489–504.
- [137] R. F. Borch, M. D. Bernstein, and H. Dupont Durst, "Cyanohydrinoborate anion as a selective reducing agent," *J. Am. Chem. Soc.*, vol. 93, no. 12, pp. 2897–2940, 1971.
- [138] S. Ligorio Fialho and A. Da Silva-Cunha, "New vehicle based on a microemulsion for topical ocular administration of dexamethasone," *Clin. Experiment. Ophthalmol.*, vol. 32, no. 6, pp. 626–632, 2004.
- [139] S. A. Mortazavi, B. G. Carpenter, and J. D. Smart, "An investigation of the rheological behaviour of the mucoadhesive / mucosal interface," *Int. J. Pharm.*, vol. 83, pp. 221–225, 1992.

## 5 Appendices

### APPENDIX A

**Table A 1**– Recipes of hyperbranched polymers prepared via copolymerization of OEGMA and AA using EGDMA as the cross-linker and DDT as the chain transfer agent; see Figure 2-1 for a graphical representation of the gelation data

| Sample code | OEGMA [mol%] | AA<br>[mol%] | EGDMA<br>[mol%] | DDT<br>[mol%] | [DDT/EGDMA] | Gel<br>[Y/N] |
|-------------|--------------|--------------|-----------------|---------------|-------------|--------------|
| <b>P1</b>   | 78.2         | 20.3         | 0.19            | 1.23          | 6.36        | N            |
| <b>P2</b>   | 78.1         | 20.3         | 0.33            | 1.23          | 3.76        | N            |
| <b>P3</b>   | 75.5         | 19.6         | 3.67            | 1.23          | 0.33        | N            |
| <b>P4</b>   | 75.3         | 19.6         | 3.85            | 1.23          | 0.32        | N            |
| <b>P5</b>   | 74.5         | 19.4         | 4.84            | 1.23          | 0.25        | N            |
| <b>P6</b>   | 73.7         | 19.2         | 5.78            | 1.23          | 0.21        | N            |
| <b>P7</b>   | 72.9         | 19           | 6.2             | 1.23          | 0.2         | N            |
| <b>P8</b>   | 63.2         | 16.5         | 7.67            | 1.23          | 0.15        | Y            |
| <b>P9</b>   | 71.2         | 18.5         | 8.99            | 1.23          | 0.13        | Y            |
| <b>P10</b>  | 78           | 20           | 0.15            | 1.45          | 9.66        | N            |
| <b>P11</b>  | 77.9         | 20           | 0.28            | 1.45          | 5.10        | N            |
| <b>P12</b>  | 76.4         | 19.9         | 2.13            | 1.45          | 0.68        | N            |
| <b>P13</b>  | 75.8         | 19.7         | 2.42            | 1.45          | 0.59        | N            |
| <b>P14</b>  | 75.6         | 19.7         | 2.65            | 1.45          | 0.55        | N            |
| <b>P15</b>  | 75.8         | 19.7         | 2.91            | 1.45          | 0.49        | N            |
| <b>P16</b>  | 75.7         | 19.7         | 3.12            | 1.45          | 0.46        | N            |
| <b>P17</b>  | 75.5         | 19.4         | 3.37            | 1.45          | 0.43        | N            |

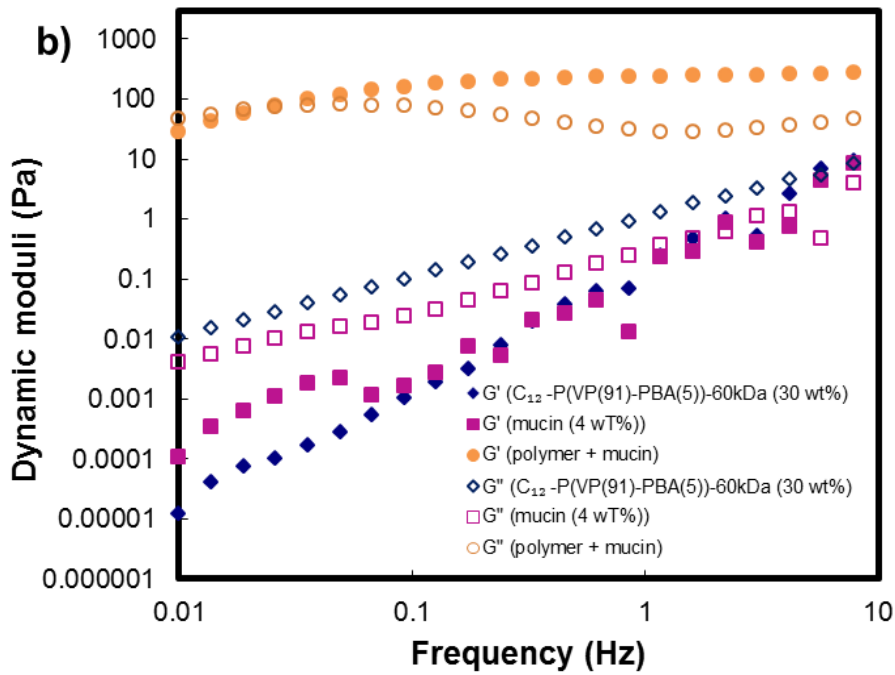
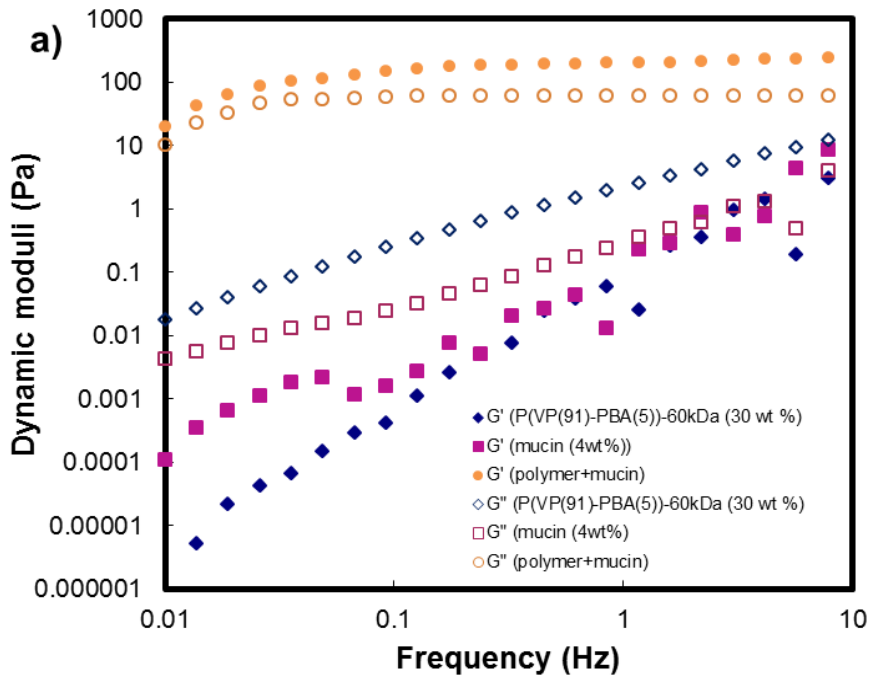
---

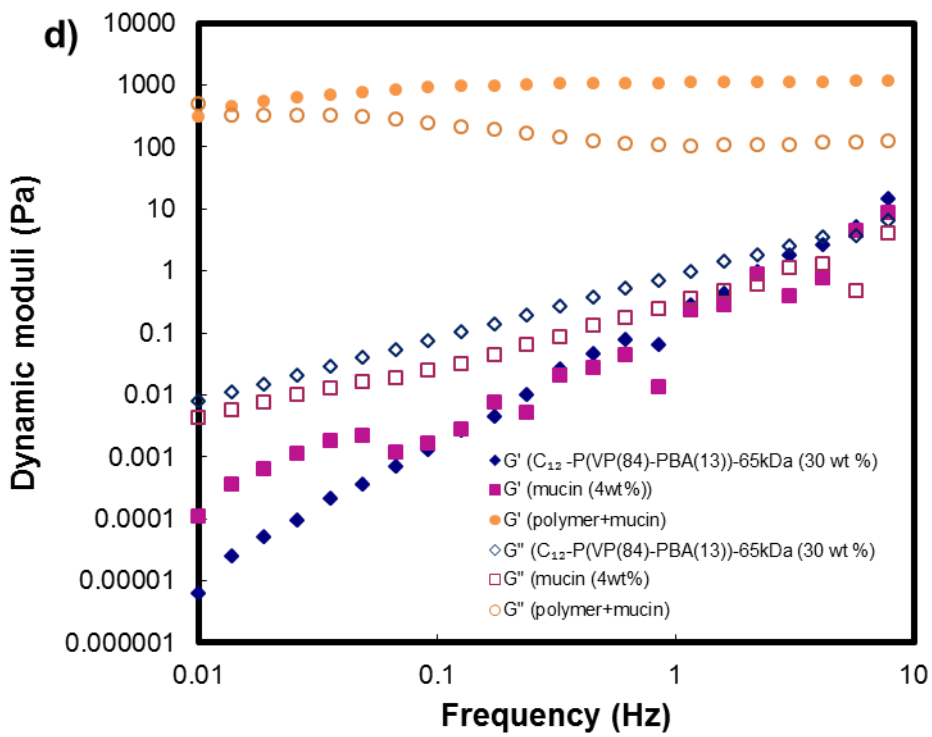
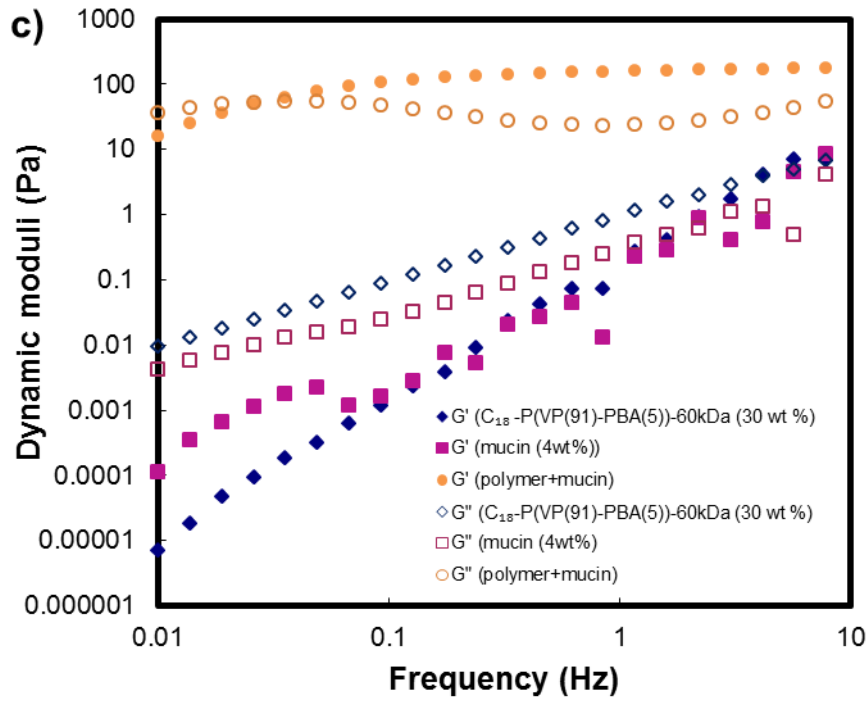
|            |      |      |       |      |       |   |
|------------|------|------|-------|------|-------|---|
| <b>P18</b> | 74.9 | 19.4 | 4.37  | 1.45 | 0.33  | N |
| <b>P19</b> | 73.8 | 19.2 | 5.45  | 1.45 | 0.26  | N |
| <b>P20</b> | 73   | 19   | 6.45  | 1.45 | 0.22  | N |
| <b>P21</b> | 72.5 | 18.9 | 7.08  | 1.45 | 0.20  | Y |
| <b>P22</b> | 71.1 | 18.5 | 8.85  | 1.45 | 0.16  | Y |
| <b>P23</b> | 70.4 | 18.3 | 9.8   | 1.45 | 0.15  | Y |
| <b>P24</b> | 73.4 | 19.1 | 5.99  | 1.2  | 4.99  | N |
| <b>P25</b> | 73.6 | 19.2 | 5.99  | 1.22 | 4.90  | N |
| <b>P26</b> | 73.5 | 19.1 | 1.3   | 5.98 | 4.6   | N |
| <b>P27</b> | 73.6 | 19.2 | 1.4   | 5.76 | 4.11  | N |
| <b>P28</b> | 74.5 | 19.4 | 1.42  | 4.59 | 3.23  | N |
| <b>P29</b> | 73.7 | 19.2 | 1.99  | 5    | 2.51  | N |
| <b>P30</b> | 75.4 | 19.6 | 2.48  | 2.47 | 0.99  | N |
| <b>P31</b> | 61.9 | 16.1 | 14.68 | 7.2  | 0.49  | N |
| <b>P32</b> | 62.2 | 16.2 | 14.86 | 6.57 | 0.44  | N |
| <b>P33</b> | 59.6 | 15.5 | 17.22 | 7.60 | 0.44  | N |
| <b>P34</b> | 65.2 | 16.9 | 12.68 | 4.99 | 0.39  | N |
| <b>P35</b> | 65.3 | 17   | 10.47 | 3.72 | 0.35  | N |
| <b>P36</b> | 68   | 17.7 | 6.97  | 1.99 | 0.28  | N |
| <b>P37</b> | 72.2 | 18.8 | 7.76  | 1.78 | 0.23  | N |
| <b>P38</b> | 67.3 | 17.5 | 10.91 | 1.89 | 0.17  | N |
| <b>P39</b> | 71.7 | 18.7 | 13.04 | 2.11 | 0.16  | N |
| <b>P40</b> | 72.2 | 18.8 | 13.07 | 1.84 | 0.14  | Y |
| <b>P41</b> | 65.2 | 17   | 15.79 | 2.05 | 0.13  | Y |
| <b>P42</b> | 65   | 16.9 | 16.51 | 1.5  | 0.09  | Y |
| <b>P43</b> | 62   | 16.1 | 20.12 | 1.69 | 0.084 | Y |
| <b>P44</b> | 59.4 | 15.5 | 23.21 | 1.90 | 0.081 | Y |
| <b>P45</b> | 51.3 | 13.4 | 33.18 | 2.08 | 0.063 | Y |
| <b>P46</b> | 47.6 | 12.4 | 37.63 | 2.33 | 0.062 | Y |

---



APPENDIX C





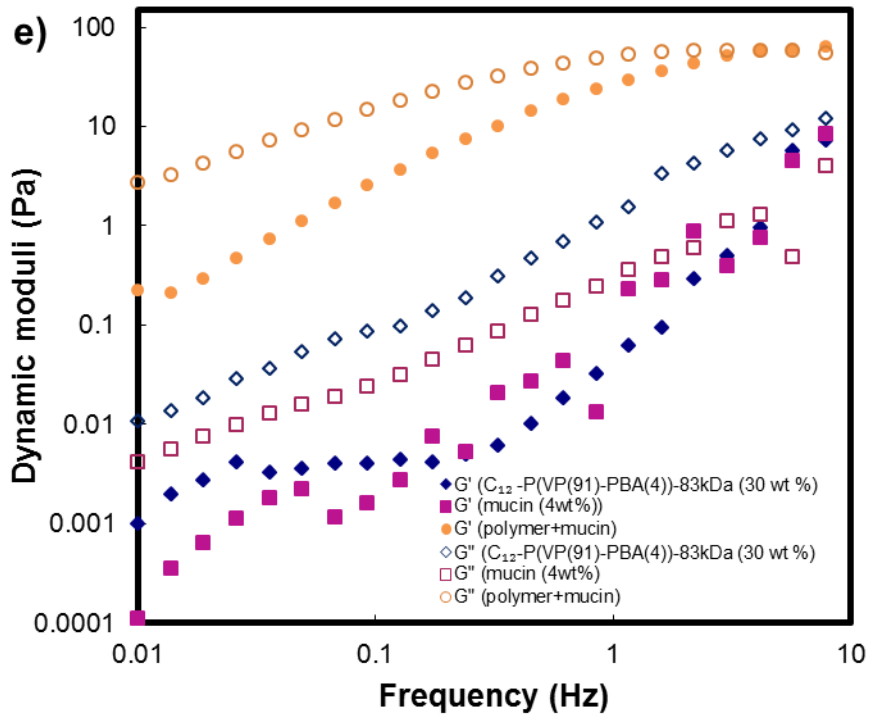


**Figure C 1-** Dynamic oscillation responses of dual  $C_x$ -PBA grafted polymers for a) P(VP(90)-PBA(5))-60kDa (30wt%), b)  $C_{12}$ -P(VP(91)-PBA(5))-60kDa (30 wt %), c)  $C_{18}$ -P(VP(91)-PBA(5))-60kDa (30 wt %), d)  $C_{12}$ -P(VP(84)-PBA(13))-65kDa (30 wt %), e)  $C_{12}$ -P(VP(91)-PBA(4))-83kDa (30 wt %),

## APPENDIX D

**Table D 1-** Viscoelastic parameters for dual C<sub>x</sub>-PBA grafted polymers and polymer–mucus mixtures (dynamic mean parameters obtained from frequency sweeps from 10 to 0.1 Hz)

| Sample code                                      | G'     | G''    | tanδ   | G'/G'' |
|--|--------|--------|--------|--------|
| Mucin (4wt%)                                     | 3.08   | 0.64   | 7.95   | 1.68   |
| P(VP(91)-PBA(5))-60kDa (30wt%)                   | 3.73   | 1.19   | 94.4   | 0.77   |
| Polymer + mucin                                  | 168.02 | 54.18  | 0.36   | 2.9    |
| C <sub>12</sub> -P(VP(91)-PBA(5))-60kDa (30wt%)  | 3.81   | 2.21   | 112.81 | 0.44   |
| Polymer + mucin                                  | 188.96 | 51.92  | 0.44   | 4.4    |
| C <sub>18</sub> -P(VP(91)-PBA(5))-60kDa (30wt%)  | 2.65   | 1.43   | 140    | 0.4    |
| Polymer + mucin                                  | 123.47 | 39.13  | 0.496  | 3.7    |
| C <sub>12</sub> -P(VP(84)-PBA(13))-65kDa (30wt%) | 2.80   | 1.47   | 113    | 0.5    |
| Polymer + mucin                                  | 857.8  | 194.87 | 0.29   | 6.50   |
| C <sub>12</sub> -P(VP(78)-PBA(19))-66kDa (30wt%) | 5.93   | 2.93   | 199    | 0.43   |
| Polymer + mucin                                  | 1166.9 | 201.16 | 0.23   | 10.4   |
| C <sub>12</sub> -P(VP(90)-PBA(4))-83kDa (30wt%)  | 1.31   | 2.88   | 19.00  | 0.17   |
| Polymer + mucin                                  | 22.40  | 24.04  | 2.64   | 0.65   |
| C <sub>12</sub> -P(VP(90)-PBA(4))-178kDa (30wt%) | 2.24   | 3.11   | 33.1   | 0.25   |
| Polymer + mucin                                  | 46.48  | 32.40  | 1.93   | 1.01   |

